Supporting Information

Carbon Dots as Photocatalysts for Organic Synthesis: Metal Free Methylene-oxygen-bond Photocleavage

Simone Cailotto,[a‡] Matteo Negrato,[a‡] Salvatore Daniele,[a] Rafael Luque,[a,b] Maurizio Selva,[a] Emanuele Amadio,[a] Alvise Perosa[a]**

[a] Department of Molecular Sciences and Nanosystems, Università Ca' Foscari Venezia, Via Torino 155, 30172 Mestre–Venezia, Italy.
[b] Departamento de Química Organica, Universidad de Córdoba, Edif. Marie Curie, Ctra Nnal IV-A Km 396, E-14014 Córdoba, Spain.

Abstract: We report for the first time that irradiation of four different citric acid-derived carbon dots (CDs), in the absence of any other redox mediators, promotes an organic reaction. In this proof-of-concept study methylene-oxygen bond reductive photocleavage in N-methyl-4-picolinium esters is demonstrated. The experimental results indicate that photocleavage reactivity correlates with the redox energy levels, expressed in the Fermi scale, of CDs and esters measured by cyclic voltammetry and UV-Vis. A photo-fragmentation mechanism is proposed. This study offers a new possibility to employ inexpensive and readily available CDs to promote photo-organic reactions.

Table of contents

General information

All chemicals and dry solvents have been purchased from commercial sources and - unless otherwise specified - used as received without further purification. ^{1}H, ^{13}C, DOSY NMR spectra were recorded on a Bruker UltraShield 300'54 (^{1}H: 300 MHz; ^{13}C: 75.5 MHz;) and a Bruker Magnet System 400'54 Ascend (^{1}H: 400 MHz; ^{13}C: 100.6 MHz) spectrometers. For ^{1}H and $^{13}C\{^{1}H\}$ NMR the chemical shifts (δ) have been reported in parts per million (ppm) relative to TMS using the residual non-deuterated solvent as an internal reference. For the photocleavage experiments, a LED UV lamp with a fixed wavelength of 365 nm, 400 mA, 25 mV was used.
For electrochemical measurements, DMF was employed as solvent and was freshly distilled; tetrabutylammonium perchlorate (TBAP), purified by crystallization, was employed as supporting electrolyte; Milli-Q water was used, when necessary, to investigate the effect of water on the potential window available or to dissolve CDs. All voltammetric measurements were performed using a CHI 820 potentiostat (CH Instrument, USA), along with the CHI instrument software, version 8.15. A three-electrode cell, comprising a glassy carbon disc electrode (GCE, φ=3mm diameter) working electrode, a platinum spiral as counter electrode and an Ag/AgCl/KCl (saturated) as reference electrode. The latter was separated from the main solution by a porous septum in order to avoid contamination of DMF solutions with chloride ions leaching from the reference electrode. The potentials are also quoted against the ferrocenium/ferrocene (Fc^{+}/Fc) redox couple, which was employed as an internal reference system.

Experimental Procedures.

Synthesis of a-CDs, g-CDs and a-N-CDs, g-N-CDs and their photoreduction properties of methyl viologen[1]

The four different sets of CDs were synthetized as already reported,[1] using two different preparation methods – hydrothermal and pyrolytic, that yield amorphous and graphitic CDs, respectively – and two sets of reagents – citric acid and citric acid coupled with diethylenetriamine as dopant. In brief, the nanomaterials were obtained as follow:

1. amorphous non-doped CDs (**a-CDs**) were hydrothermally synthesized by heating an aqueous solution of citric acid in a sealed autoclave for 24 h at 180 °C. The mixture was then neutralized to pH 7 with aqueous NaOH and evaporated to dryness leading to a dark yellow luminescent oil (25%$_{wt}$ yield) which was used without any further purifications.

2. graphitic non-doped CDs (**g-CDs**) were synthetized by pyrolysis heating neat citric acid under air at 220 °C for 48 h. The resulting solid was then neutralized to pH 7 with aqueous NaOH, and the crude mixture dialyzed (cutoff Mn: 1.0 kDa) for 24 h against fresh water. The inner solution was evaporated to dryness leading to a dark-black solid (20%$_{wt}$ yield).

3. amorphous nitrogen-doped CDs (**a-N-CDs**) were hydrothermally synthesized by heating an aqueous solution of citric acid and diethylenetriamine in a sealed autoclave for 6 h at 180 °C. The mixture was then evaporated to dryness leading to a brown solid (72%$_{wt}$ yield) which was used without any further purifications.

4. graphitic nitrogen-doped CDs (**g-N-CDs**) was synthetized by pyrolysis heating a suspension of citric acid and diethylenetriamine under air at 220 °C for 48 h. The solid was then neutralized to pH 7 with aqueous NaOH, and the crude mixture dialyzed (*cutoff* Mn: 1.0 kDa) for 24 h against fresh water. The inner solution evaporated to dryness leading to a dark-brown solid (18%$_{wt}$ yield).

Extensive HR-TEM, FT-IT, UV-vis, XPS, PL/PLE, ESI-MS, $^{1}H/^{13}C\{^{1}H\}$ NMR and DOSY analyses [1] indicated that the hydrothermal method produced amorphous nano-aggregates containing low molecular weight compounds while pyrolysis formed small (2-5 nm) graphitic structures. Moreover, the addition of a dopant amine resulted in the formation of luminescent fluorophores and of larger nano-aggregates/oligomers. In the photoreduction of methyl viologen, purely carbonaceous – *i.e.* non-nitrogen-doped CDs – worked best

when the structure was graphitic rather than amorphous (**g-CDs** > **a-CDs**); while for nitrogen-doped CDs the graphitic particles were far less active compared to their amorphous counterpart (**a-N-CDs** > **g-N-CDs**). Overall the observed photocatalytic reaction rates followed the order **a-N-CDs** ≥ **g-CDs** > **a-CDs** ≥ **g-N-CDs**. Further details related to both synthesis/characterization of the nanoparticles and their photocatalytic activity with methyl viologen can be found in ref. 1.

Synthesis of N-methyl-4-picolinium compounds.

1a,1b,1d,1e were synthesized using the procedure described by Sundarajaan *et al*. [2] which consists of four synthetic steps as illustrated in scheme S1:

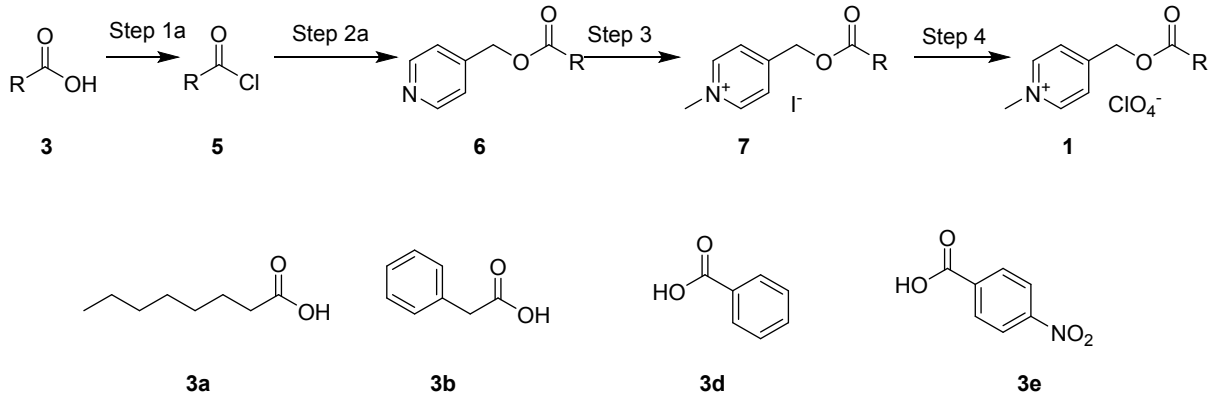

Scheme S1. General synthetic pathway for **1a,b,d,e**.

1c was synthesized following a modified four steps procedure (Scheme S2). L-Phenyl-alanine was first protected with a tertbutoxy-carbonyl group to obtain the product **3c**. Then the coupling reaction between **3c** and carbinol in presence of dicyclohexylcarbodiimide (DCC) as coupling agent yielded the intermediate **6c** which was further used to synthetize the desired product using the same procedures (step 3 and 4) above discussed for **1a,b,d,e**.

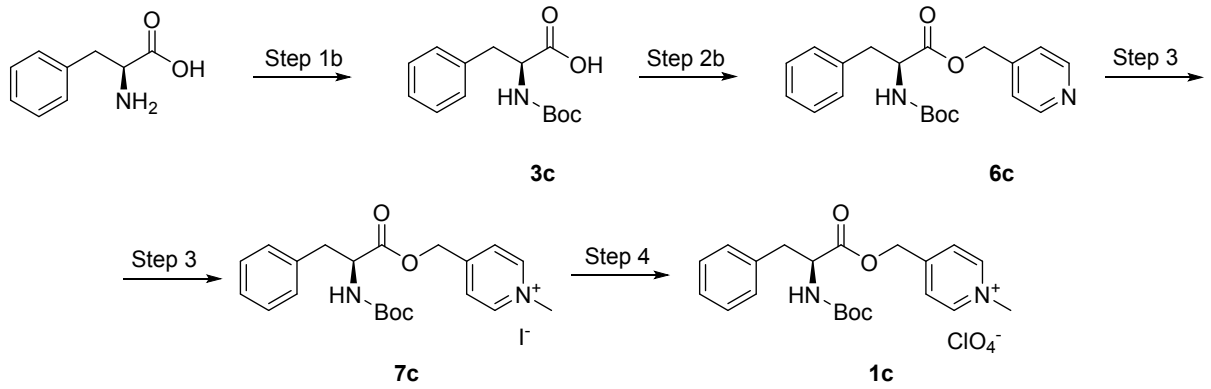

Scheme S2. Synthetic pathway for **1c**.

Step 1a

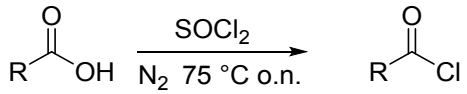

3 **5**

Acyl chloride **5a,b,d,e** were synthesized using the procedure of Douglas *et al*.[3] Carboxylic acid **3a-e** (30.99 mmol) was introduced into a three-necked flask equipped with a condenser, sodium bicarbonate and calcium chloride trap, rubber septum and tail. Then thionyl chloride (137.84 mmol) was added and the mixture was refluxed overnight at 75°C. Then the unreacted thionyl chloride was removed from the system by vacuum evaporation.

Acyl chloride **5a** was prepared from octanoic acid. The product was obtained in 89% yield as a white solid ^{1}H NMR (400 MHz, Chloroform-*d*) δ= 2.91 (t, *J* = 6.7 Hz, 2H), 1.88 – 1.63 (m, 2H), 1.39 – 1.29 (m, 8H), 0.92 (t, *J* = 8.6 Hz, 3H). ^{13}C NMR (101 MHz, Chloroform-*d*) δ= 173.77, 47.10, 31.51, 28.72, 28.38, 25.06, 22.52, 13.99.

Acyl chloride **5b** was prepared from phenylacetic acid. The product was obtained in 79% yield as a yellow oil. ^{1}H NMR (300 MHz, Chloroform-*d*) δ= 7.32-7.44 (m, 5H), 4.32(s, 2H). ^{13}C NMR (75 MHz, Chloroform-*d*) δ=172.33, 132.14, 129.71, 128.82, 127.98, 52.39.

Acyl chloride **5d** was prepared from benzoic acid. The product was obtained in 85% yield. ^{1}H NMR (300 MHz, Chloroform-*d*) δ= 8.14 (d, 2H), 7.71 (d, 1H), 7.63 – 7.44 (m, 2H). ^{13}C NMR (75 MHz, Chloroform-*d*) δ= 168.38, 135.36, 133.25, 131.41, 128.99.

Acyl chloride **5e** was prepared from p-nitro benzoic acid. The product was obtained in 86% yield as white solid. ^{1}H NMR (300 MHz, Chloroform-*d*) δ= 8.43 – 8.26 (m, 4H). ^{13}C NMR (75 MHz, Chloroform-*d*) δ= 167.41, 151.98, 138.38, 132.62, 124.43.

Step 1b

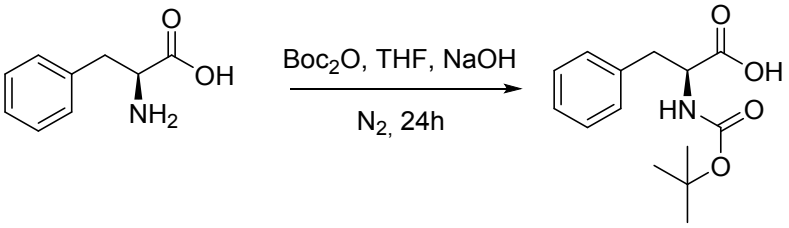

3c

The protected L-phenylalanine **3c** was synthesized following an already reported procedure[4]. Phenylalanine (4,95 g, 30 mmol) was placed in a 2 neck round bottomed flask with 63 mL of 1M NaOH water solution. The mixture was then cooled with an ice bath for 15 minutes, subsequently a 7.86 g Boc_2O dissolved in THF (84 mL, 36 mmol) were added and stirred for 10 min; the pH was adjusted to around 10.5. The reaction temperature was then slowly increased to room temperature, and the solution was stirred overnight. After 24 h, the solvent was removed by vacuum distillation, and the crude product was extracted with ethyl ether (200 mL). The resultant aqueous phase was cooled in the ice bath, acidified with 1 M HCl solution until pH=2 is reached. Then, the aqueous phase was further extracted three times with ethyl acetate (150 mL), washed with saturated NaCl solution (150 mL). and the organic layer was then dried and filtered. After complete distillation of the organic solvent, 7.72 white powder were obtained with a yield of 97 %.^{1}H NMR (300 MHz, Chloroform-*d*) δ= 7.25-7.37 (m, 5H), 4.38 (m, 1H), 2.93-3.33(m, 2H), 1.4(s, 9H). ^{13}C NMR (75 MHz, Chloroform-*d*) δ=174.49, 158.31, 137.59, 129.10, 80.65, 55.41, 37.42, 28.41.

Step 2a

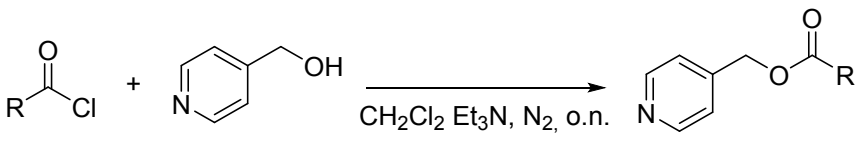

5 **6**

4-(Hydroxymethyl)pyridine (18.97 mmol), dichloromethane (20 ml) and triethylamine (32.92 mmol) were introduced into a three-necked flask equipped with a condenser, dropping funnel and gas inlet. A solution of the corresponding acyl chloride **5** (27,37 mmol) in dichloromethane was then added dropwise and the reaction mixture was left under stirring overnight at room temperature and under nitrogen. Subsequently, the ester product **6** was put into a separating funnel and washed with a solution of water and sodium bicarbonate (20ml), recovering the lower organic phase and repeating the operation three times. The organic phase was then dehydrated with sodium sulphate, filtered and the solvent was removed by rotary evaporation. The purified product was purified by column chromatography employing gradient elution with a mixture of hexane / ethyl acetate.

The product **6a** was obtained in 53% yield. ^{1}H NMR (400 MHz, Chloroform-*d*) δ= 8.61 (d, 1H), 7.26 (d, 1H), 5.14 (s, 1H), 2.41 (t, 1H), 1.72 – 1.63 (m, 1H), 1.41 – 1.21 (m, 5H), 0.89 (t, 2H). ^{13}C NMR (101 MHz, Chloroform-*d*) δ 173.29, 149.85, 145.24, 121.91, 64.01, 34.13, 31.62, 29.06, 24.90, 22.56, 14.03.
The product **6b** was obtained in 39% yield. ^{1}H NMR (400 MHz, Acetonitrile-d_3) δ= 8.55 (d, 2H), 7.30 – 7.40 (m, 7H), 5.2 (d, 2H), 3.78 (s, 2H). ^{13}C NMR (101 MHz, Acetonitrile-d_3) δ= 171.16, 150.13, 144.93, 133.64, 129.41, 128.84, 127.49, 121.87, 64.65, 41.41.
The product **6d** was obtained in 35% yield. ^{1}H NMR (400 MHz, Acetonitrile-d_3) δ= 8.66 (d, 2H), 8.13 (d, 2H), 7.61 (dd, 1H), 7.57 – 7.44 (m, 2H), 7.37 (d, 2H), 5.40 (s, 2H). ^{13}C NMR (101 MHz, Acetonitrile-d_3) δ= 165.89, 149.88, 145.54, 133.44, 129.83, 129.47, 128.71, 121.84, 64.59.
The product **6e** was obtained in 54% yield. ^{1}H NMR (400 MHz, Acetonitrile-d_3) δ= 8.62 (d, 1H), 8.39 – 8.25 (m, 2H), 7.45 (d, *J* = 4.4, 1.6, 0.7 Hz, 1H), 5.44 (s, 1H). ^{13}C NMR (101 MHz, Acetonitrile-d_3) δ= 164.36, 150.90, 150.00, 144.81, 135.25, 130.77, 123.75, 121.92, 65.37.

Step 2b

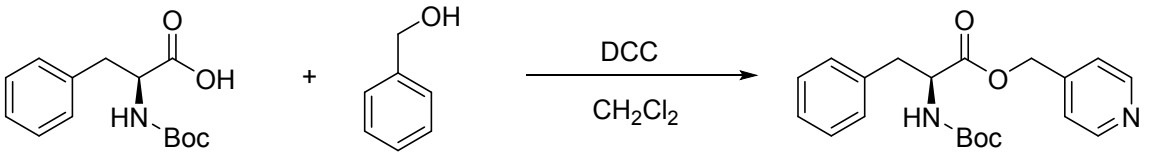

5c **6c**

For the synthesis of the product **6c** a different procedure was employed. Briefly, **5c** (3g, 11.3 mmol) and 4-(Hydroxymethyl)pyridine (1.3g 12.4 mmol) were dissolved in dichloromethane and then dicyclohexylcarbodiimide (2.4g, 12 mmol) were added to the solution. The mixture was stirred for 24h at room temperature. The product was recovered in 80% yield after purification as a white solid. ^{1}H NMR (400 MHz, Acetonitrile-d_3) δ= 8.55 (d, 2H), 7.25 (m, 5H), 5.67 (s, 1H), 5.16 (s, 2H), 4.44 (1H, m), 3.13-3.00 (m, 2H), 1.38 (m, 9H). ^{13}C NMR (101 MHz, Acetonitrile-d_3) δ= 171.73, 155.13, 149.99, 144.12, 129.23, 128.67, 127.17, 121.98, 80.15, 64.9, 54.62, 38.35, 28.28.

Step 3

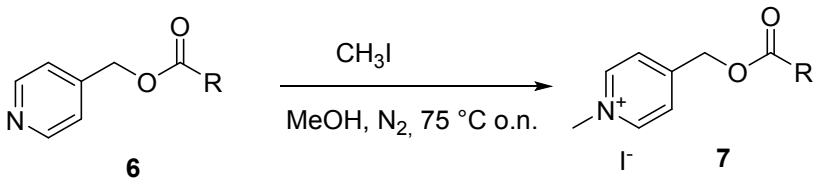

6 **7**

The corresponding ester **6** (7.38 mmol) and methanol (10 ml) were introduced into a three-necked darkened flask equipped with a condenser, rubber septum and tail. The system was put under nitrogen. The methyl iodide (11.29 mmol) was then added with a syringe and the reaction mixture was refluxed and left under stirring at 75 °C overnight. Subsequently, the unreacted methyl iodide and methanol were removed by vacuum evaporation leading to a solid. The product **7** was recrystallized in hot methanol. The solid was filtered and stored in the dark.
The product **7a** has been obtained in 53% yield. ^{1}H NMR (400 MHz, Chloroform-*d*) δ 9.25 (d, 2H), 8.01 (d, 2H), 5.40 (s, 2H), 4.71 (s, 3H), 2.50 (t, 2H), 1.76 – 1.59 (m, 3H), 1.39 – 1.25 (m, 6H), 0.91 (d, 4H). ^{13}C NMR (101 MHz, Acetonitrile-d_3) δ= 175.03, 156.48, 145.43, 125.48, 63.68, 49.23, 33.87, 31.57, 28.74, 24.71, 22.53, 13.80.
The product **7b** has been obtained with a yield of 61%. ^{1}H NMR (400 MHz, Acetonitrile-d_3) δ= 8.60 (d, 2H), 7.89 (d, 2H), 7.37 (d, 5H), 5.39 (s, 2H), 4.29 (s, 3H), 3.86 (s, 2H). ^{13}C NMR (101 MHz, Acetonitrile-d_3) δ= 170.8, 156.0, 145.5, 133.1, 129.5, 129.0, 127.7, 125.4, 63.5, 49.4, 41.
The product **7c** has been obtained with a yield of 86%. ^{1}H NMR (400 MHz, Acetonitrile-d_3) δ= 9.13 (d, 2H), 7.84 (d, 2H), 7.28 (m, 5H), 5.40 (m, 2H), 5.22 (m, 1H), 4.66 (s, 3H), 3.14 (m, 2H), 1.43 (s, 9H). ^{13}C NMR (101 MHz, Acetonitrile-d_3) δ= 171.6, 155.57, 145.36, 135.75, 129.1, 127.54, 80.48, 63.78, 54.95, 49.36, 38.11, 28.33.
The product **7d** has been obtained in 72% yield. ^{1}H NMR (400 MHz, Acetonitrile-d_3) δ= 8.67 (d, 2H), 8.16 (d, 2H), 8.07 (d, *J* = 6.3 Hz, 2H), 7.73 (dd, 1H), 7.65 – 7.55 (m, 2H), 5.64 (s, 2H), 4.33 (s, 3H). ^{13}C NMR (101 MHz, Acetonitrile-d_3) δ= 165.55, 152.93, 145.20, 133.87, 129.65, 129.14, 128.84, 125.26, 65.27, 48.00.

The product **7e** has been obtained with a yield of 40%. ^{1}H NMR (400 MHz, Acetonitrile-d_3) δ= 8.72 (d, 2H), 8.42 – 8.31 (m, 4H), 8.11 (d, J = 6.3 Hz, 2H), 5.69 (s, 2H), 4.35 (s, 3H). ^{13}C NMR (101 MHz, Acetonitrile-d3) δ= 164.07, 155.87, 151.12, 147.17 – 143.86 (m), 134.55, 130.99, 125.36, 123.85, 64.31, 48.05.

Step 4

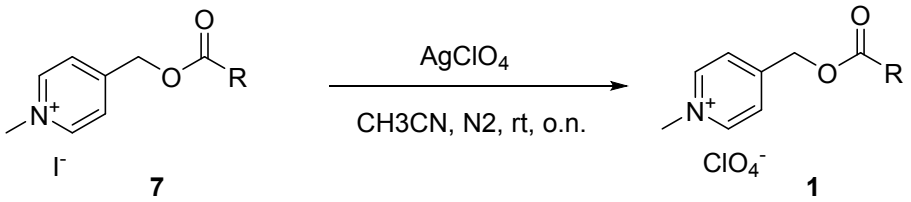

7 **1**

A solution of the corresponding ester **7** (3.19 mmol) in acetonitrile was added in a three-necked darkened flask with a tail and a plug. The silver perchlorate was then added in a stoichiometric amount. The system was placed under nitrogen and left under stirring at room temperature overnight. The reaction mixture was then filtered to remove the precipitated silver iodide and the filtrate was dried. The product **1** was then recrystallized with hot methanol.

The product **1a** was obtained in 72% yield. ^{1}H NMR (400 MHz, Acetonitrile-d_3) δ= 8.59 (d, 2H), 7.94 (d, 2H), 5.37 (s, 2H), 4.29 (s, 3H), 2.50 (t, *J* = 7.5 Hz, 2H), 1.74 – 1.61 (m, 2H), 1.40 – 1.29 (m, 4H), 0.92 (t, *J* = 7.0, 5.1 Hz, 3H). ^{13}C NMR (101 MHz, Acetonitrile-d_3) δ= 174.70, 155.32, 145.05, 125.11, 62.87, 47.92, 33.38, 31.41, 28.70, 24.50, 22.32, 13.34.

The product **1b** was obtained in 53% yield. ^{1}H NMR (400 MHz, Acetonitrile-d_3) δ= 8.60 (d, 2H), 7.89 (d, 2H), 7.37 (m, 5H), 5.39 (s, 2H), 4.29 (s, 3H), 3.86 (s, 2H). ^{13}C NMR (101 MHz, Acetonitrile-d_3) δ= 170.97, 156.5, 145.26, 133.99, 129.52, 128.61, 127.23, 125.05, 63.40, 57.18, 40.24

The product **1c** was obtained in 53% yield. ^{1}H NMR (400 MHz, Acetonitrile-d_3) δ= 8.56 (d, 2H), 7.85 (d, 2H), 7.29 (m, 5H), 5.40 (d, 2H), 4.51 (m, 1H), 4.28 (s, 3H), 3.08 (m, 2H), 1.41 (s, 9H). ^{13}C NMR (101 MHz, Acetonitrile-d_3) δ= 172.72, 155.40, 145.14, 136.86, 129.52, 127.46, 125.4, 81.17, 64.15, 55.44, 48.18, 37.11, 27.86

The product **1d** was obtained in 72% yield. ^{1}H NMR (400 MHz, Acetonitrile-d_3) δ= 8.62 (d, 2H), 8.16 (d, 2H), 8.06 (d, J = 6.3 Hz, 2H), 7.73 (d, 1H), 7.65 – 7.55 (m, 2H), 5.64 (s, 2H), 4.31 (s, 3H). ^{13}C NMR (101 MHz, Acetonitrile-d_3) δ= 165.55, 156.60, 145.57 – 144.63 (m), 133.88, 129.64, 129.14, 128.84, 125.26, 63.66, 47.95.

The product **1e** was obtained in 53% yield. ^{1}H NMR (400 MHz, Acetonitrile-d_3) δ= 8.69 – 8.62 (m, 2H), 8.42 – 8.30 (m, 4H), 8.09 (d, *J* = 6.3 Hz, 2H), 5.68 (d, *J* = 1.1 Hz, 2H), 4.33 (s, 3H). ^{13}C NMR (101 MHz, Acetonitrile-d_3) δ 164.07, 155.85, 151.10, 146.27 – 144.53 (m), 134.58, 130.99, 125.36, 123.84, 64.32, 48.78 – 47.05 (m).

Synthesis of 4-(hydroxymethyl)-1-methylpyridin-1-ium iodide (4)

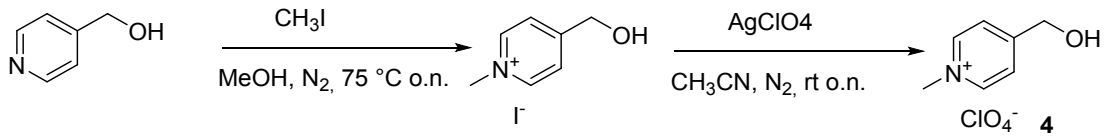

Scheme S3. Synthetic pathway for **4**.

4-(Hydroxymethyl)pyridine (9.52 mmol) and methanol (10 ml) were introduced into a three-necked darkened flask equipped with a condenser, rubber septum and tail. The system was put under nitrogen. The methyl iodide (23.80 mmol) was then added with a syringe and the reaction mixture was refluxed and left under stirring at 75 °C overnight. Subsequently, the unreacted methyl iodide and methanol were removed by vacuum evaporation leading to a yellow solid. The product was recrystallized in hot methanol. The solid was filtered and stored in the dark. The iodide product was obtained in 92% yield. ^{1}H NMR (300 MHz, Methanol-d_4) δ= 8.83 (d, 2H), 8.04 (d, J = 6.2 Hz, 2H), 4.83 (s, 2H), 4.40 (s, 3H). ^{13}C NMR (101 MHz, Methanol-d_4) δ= 164.11 – 161.70 (m), 144.66, 124.13, 61.38, 48.18.
In order to obtain the compound **4**, a solution of the iodide product (3.19 mmol) in acetonitrile was added in a three-necked darkened flask with a tail and a plug. The silver perchlorate was then added in a stoichiometric amount. The system was placed under nitrogen and left under stirring at room temperature overnight. The reaction mixture was then filtered to remove the precipitated silver iodide and the filtrate was dried. The product **4** then recrystallized with hot ethanol.

Synthesis of 1,4-dimethylpyridin-1-ium perchlorate (2)

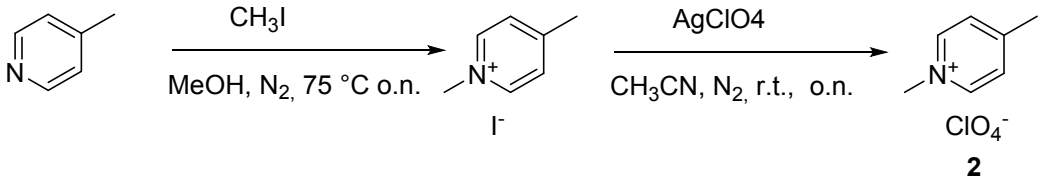

Scheme S4. Synthetic pathway for **2**.

The corresponding 4-methylpyridine (9.52 mmol) and methanol (10 ml) were introduced into a three-necked darkened flask equipped with a condenser, rubber septum and tail. The system was put under nitrogen. The methyl iodide (23.80 mmol) was then added with a syringe and the reaction mixture was refluxed and left under stirring at 75 °C overnight. Subsequently, the unreacted methyl iodide and methanol were removed by vacuum evaporation leading to a yellow solid. The product was recrystallized in hot methanol. The solid was filtered and stored in the dark. The iodide product was obtained in 89% yield. ^{1}H NMR (400 MHz, Chloroform-d) δ 9.17 (d, 2H), 7.89 (d, J = 6.2 Hz, 2H), 4.64 (s, 2H), 2.70 (s, 3H). ^{13}C NMR (101 MHz, Chloroform-d) δ 159.00, 146.27 – 143.18 (m), 128.76, 48.87, 22.47.
In order to obtain the compound **2**, a solution of the iodide product (3.19 mmol) in acetonitrile was added in a three-necked darkened flask with a tail and a plug. The silver perchlorate was then added in a stoichiometric amount. The system was placed under nitrogen and left under stirring at room temperature overnight. The reaction mixture was then filtered to remove the precipitated silver iodide and the filtrate was dried. The product **2** then recrystallized with hot ethanol (77% yield). ^{1}H NMR (400 MHz, Chloroform-d) δ 9.16 (d, 2H), 7.89 (d, J = 6.2 Hz, 2H), 4.63 (s, 2H), 2.71 (s, 3H). ^{13}C NMR (101 MHz, Chloroform-d) δ 159.05, 146.37 – 143.28 (m), 128.78, 48.96, 22.56.

Results and Discussion

Photocatalytic study

Photocleavage reactions were conducted in a Schlenk reactor with a total volume of 5 mL. For each test in a Schlenk reactor a solution of was prepared containing the corresponding protected acid (52.5 mg of 1a, 51.5 mg of 1b, 70.5 mg of 1c, 49 mg of 1d, 56 mg of 1e), dissolved in a 60% water, 40% acetonitrile mixture. Depending on the test, the CDs were added in variable quantities (from 2.5 mg to 250 mg), and the sacrificial donor EDTA in 0.1 M (60 mg) concentration when present. The pH of the solution was corrected to 7 using hydrochloric acid. The mixture thus prepared was then degassed with nitrogen using a suitable system. The Schlenk was then exposed

to the light of a UV lamp at 365 nm (Hangar s.r.l.; ATON LED-UV 365; 80 W/m2 of irradiance in the UV-A spectral range 315-400 nm) and NMR spectra were then recorded with sampling at different exposure times. For the reaction with $Ru(bpy)_3^{2+}$ a halogen lamp was employed

Photodeprotection of 1a

For the calculation of the conversions the signal of the terminal methyl group of the octanoic chain were chosen as internal standard since its chemical shift remains unchanged in both octanoic acid and **1a.** The signal **c** was used for evaluating the formation of the cleavage product **2**, while the signal **b** was used to monitor the formation of the hydrolysis product **4** as shown in Figure S1.

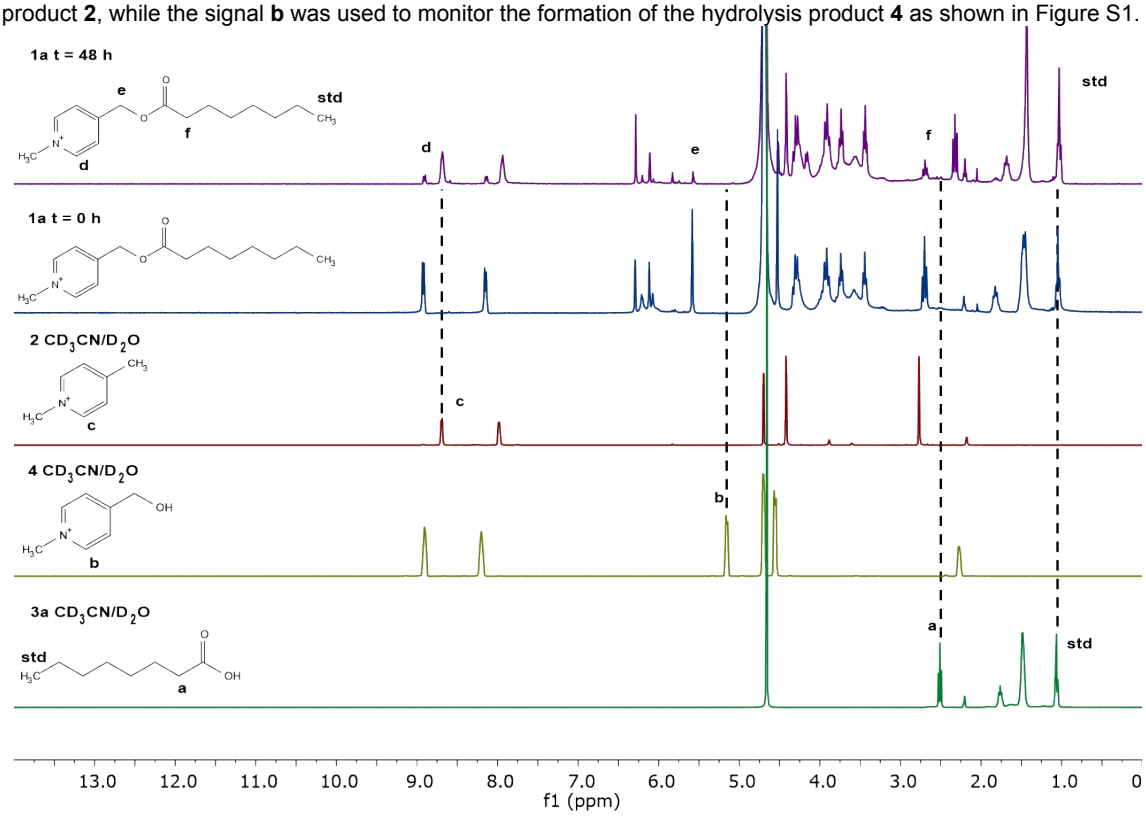

Figure S1. Typical 1HNMR spectra of the reaction of 1a at t= 0 and 48h compared with expected products in ACN-d3/D2O (6/4) at pD=7.

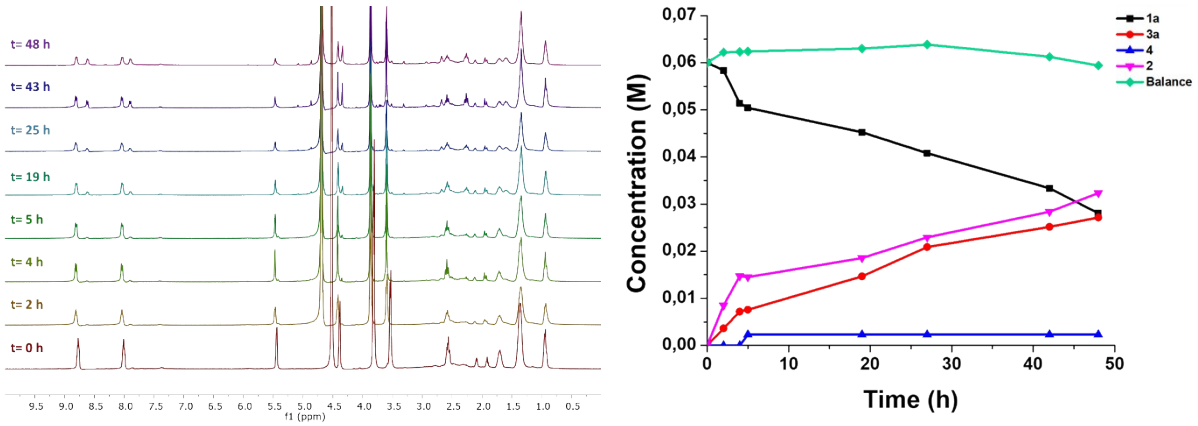

Figure S2. [1]HNMR evolution and concentration profiles of reagents and products in the photodeprotection reaction of: **1a** (0.06 M), **g-CDs** (20 mg/mL), EDTA (0.1 M) in ACN-d_3/D_2O (6/4) at pD = 7, hυ = 365 nm at R.T. under N_2.

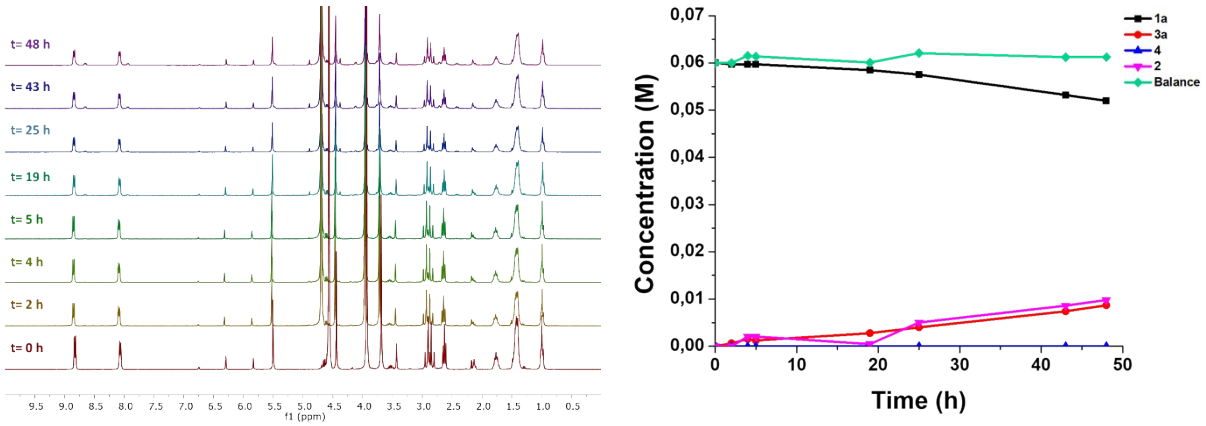

Figure S3. ^{1}HNMR evolution and concentration profiles of reagents and products in the photodeprotection reaction of: **1a** (0.06 M), **a-CDs** (20 mg/mL), EDTA (0.1 M) in ACN-d_3/D_2O (6/4) at pD = 7, hυ = 365 nm at R.T. under N_2.

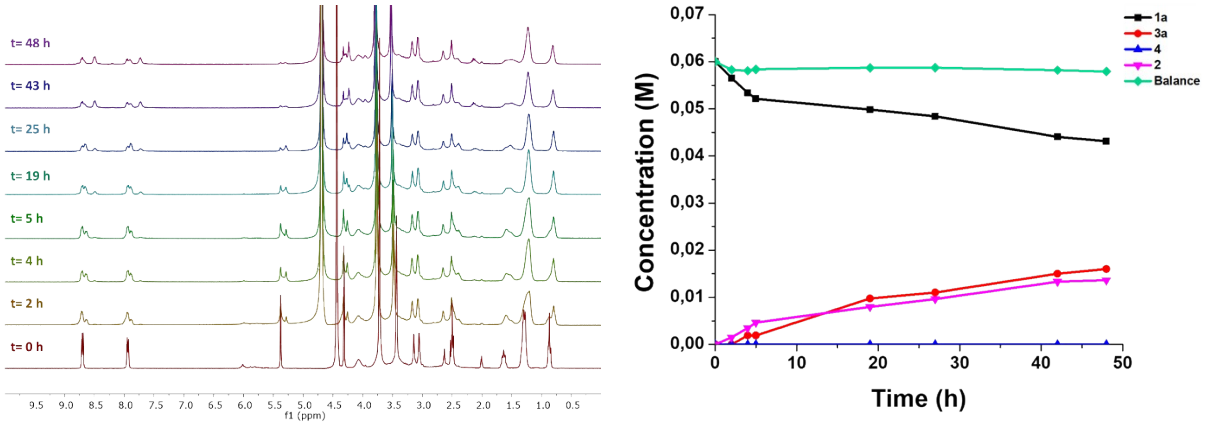

Figure S4. ^{1}HNMR evolution and concentration profiles of reagents and products in the photodeprotection reaction of: **1a** (0.06 M), **g-N-CDs** (20 mg/mL), EDTA (0.1 M) in ACN-d_3/D_2O (6/4) at pD = 7, hυ = 365 nm at R.T. under N_2.

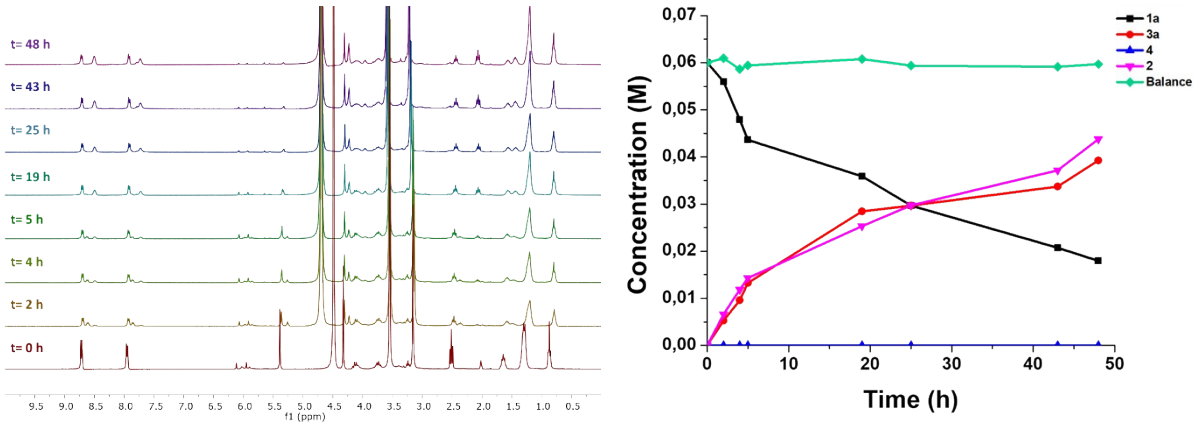

Figure S5. ^{1}HNMR evolution and concentration profiles of reagents and products in the photodeprotection reaction of: **1a** (0.06 M), **a-N-CDs** (20 mg/mL), EDTA (0.1 M) in ACN-d_3/D_2O (6/4) at pD = 7, hυ = 365 nm at R.T. under N_2.

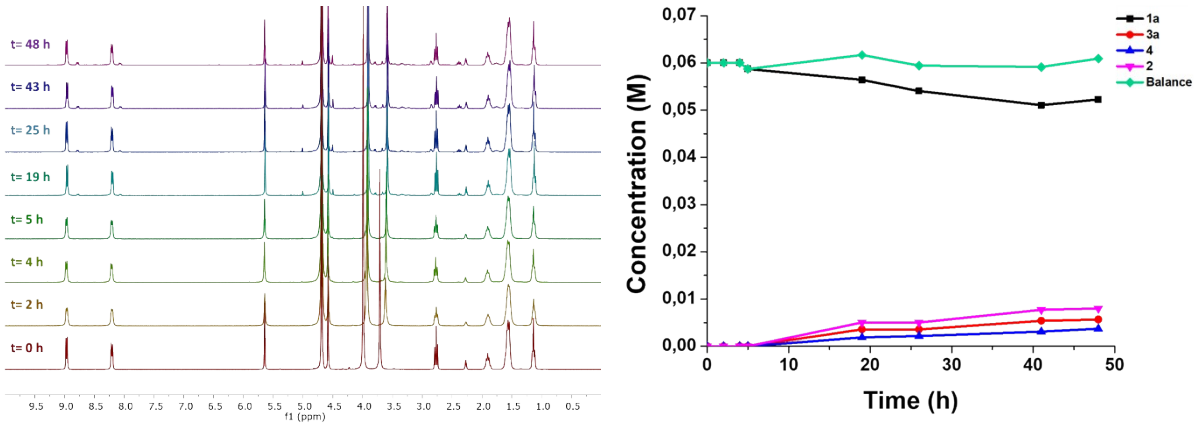

Figure S6. ^{1}HNMR evolution and concentration profiles of reagents and products in the photodeprotection reaction of: **1a** (0.06 M), EDTA (0.1 M) in ACN-d_3/D_2O (6/4) at pD = 7, hυ = 365 nm at R.T. under N_2.

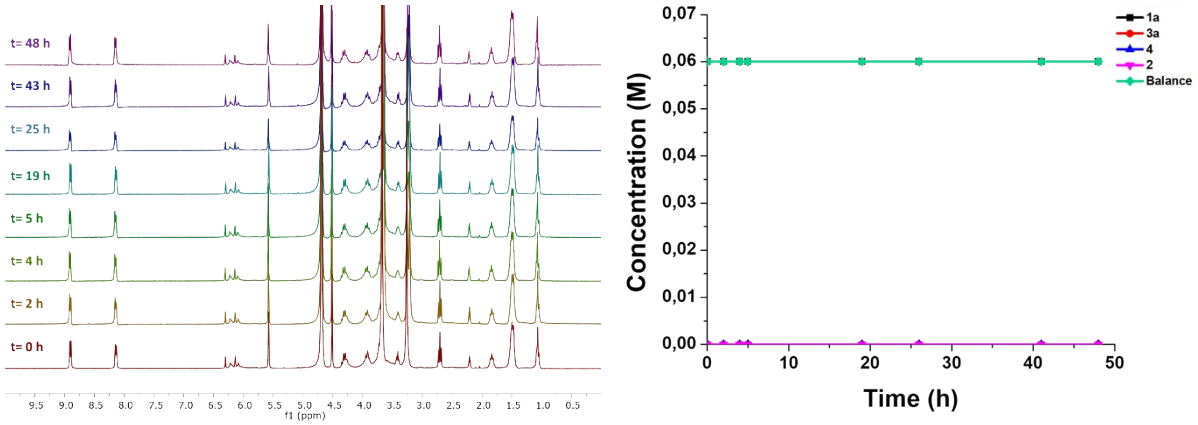

Figure S7. ^{1}HNMR evolution and concentration profiles of reagents and products in the photodeprotection reaction of: **1a** (0.06 M), **a-CDs** (20 mg/mL), EDTA (0.1 M) in ACN-d_3/D_2O (6/4) at pD = 7 at R.T. under N_2 .

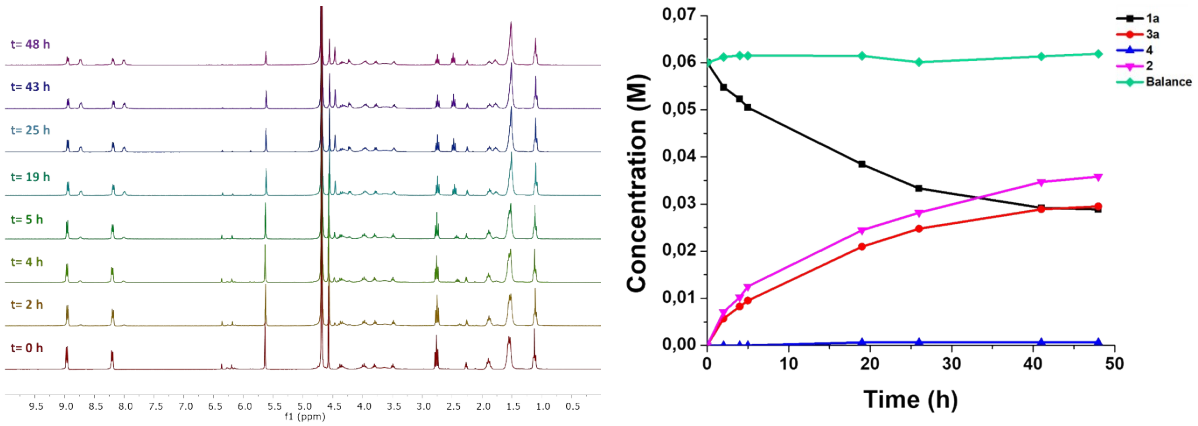

Figure S8. ^{1}HNMR evolution and concentration profiles of reagents and products in the photodeprotection reaction of: **1a** (0.06 M), **a-N-CDs** (20 mg/mL) in ACN-d_3/D_2O (6/4) at pD = 7, hυ = 365 nm at R.T. under N_2.

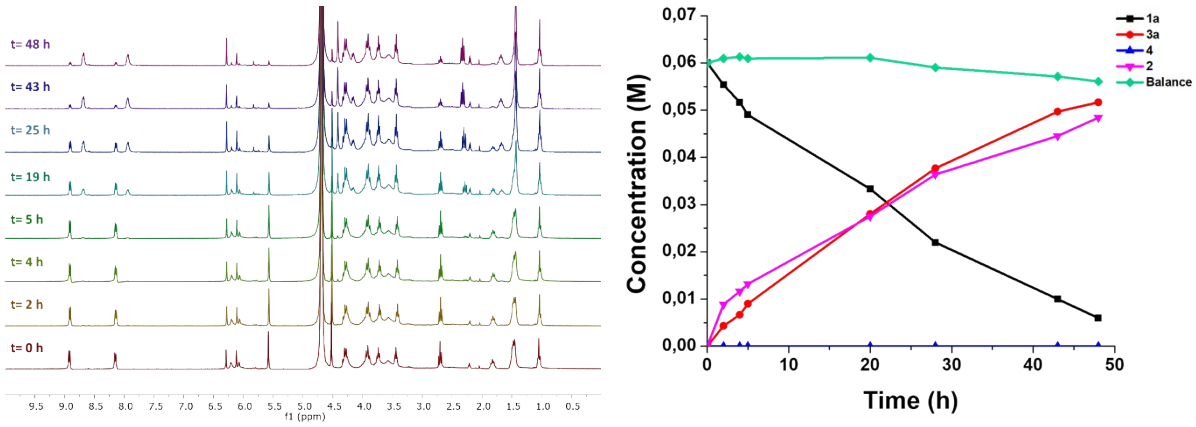

Figure S9. ^{1}HNMR evolution and concentration profiles of reagents and products in the photodeprotection reaction of: **1a** (0.06 M), **a-N-CDs** (100 mg/mL) in ACN-d_3/D_2O (6/4) at pD = 7, hυ = 365 nm at R.T. under N_2.

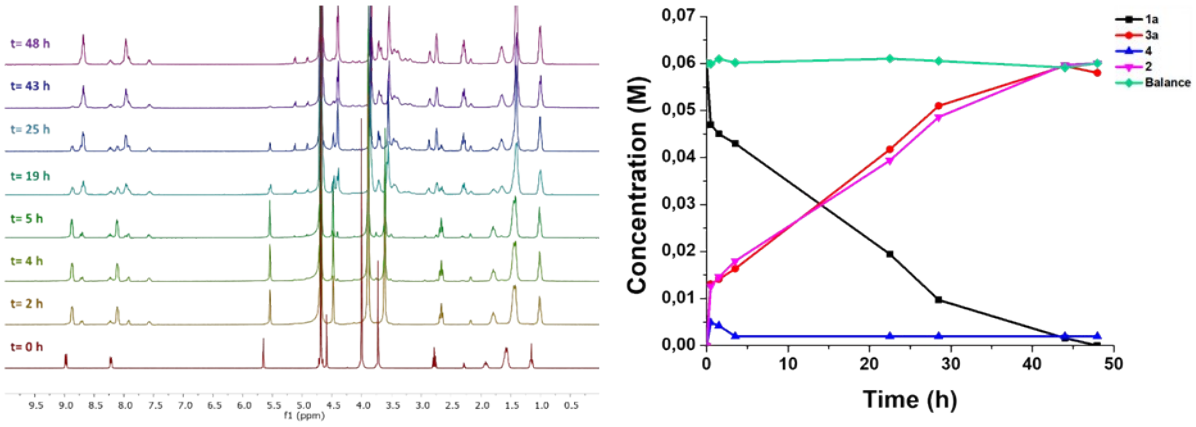

Figure S10. ^{1}HNMR evolution and concentration profiles of reagents and products in the photodeprotection reaction of: **1a** (0.06 M), $Ru(bpy)_3Cl_2$ 5 % mol, EDTA (0.1 M) in ACN-d_3/D_2O (6/4) at pD = 7, halogen lamp, 48 h at R.T. under N_2.

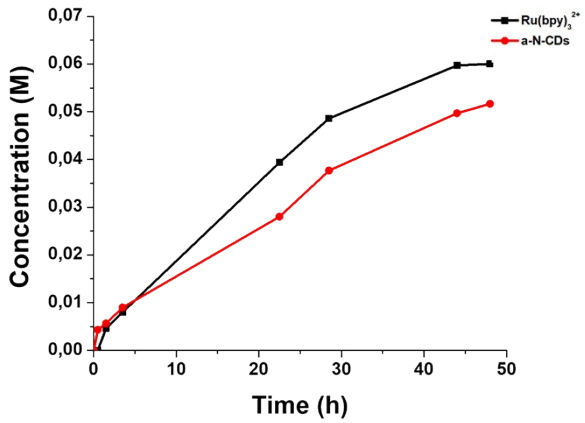

Figure S11. Comparison between the kinetics of the photo-deprotection reaction of **1a** with **a-N-CDs** and $Ru(bpy)_3^{2+}$.

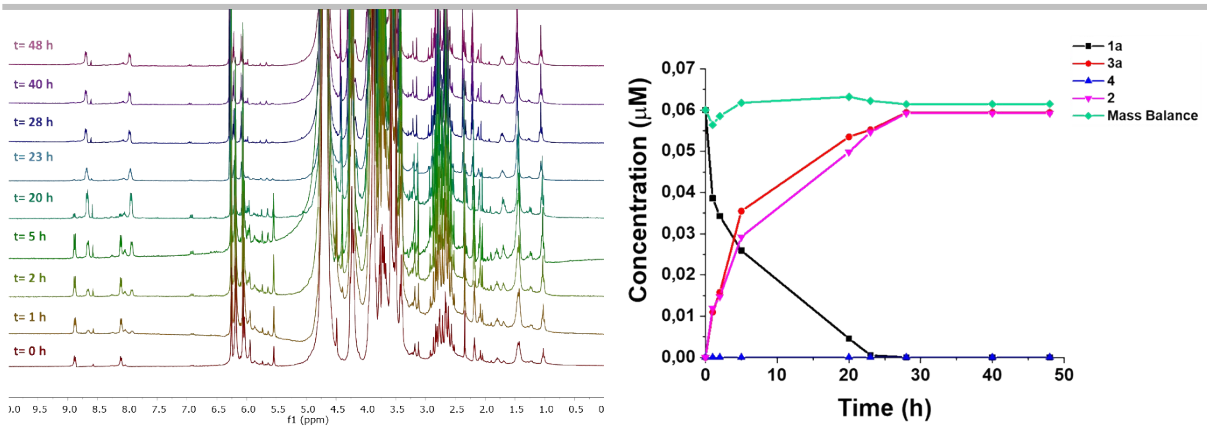

Figure S11. ^{1}HNMR evolution and concentration profiles of reagents and products in the photodeprotection reaction of: **1a** (0.06 M), **a-N-CDs** (100 mg/mL), EDTA (0.1 M) in ACN-d_3/D_2O (6/4) at pD = 7, h□□= 365 nm at R.T. under N_2.

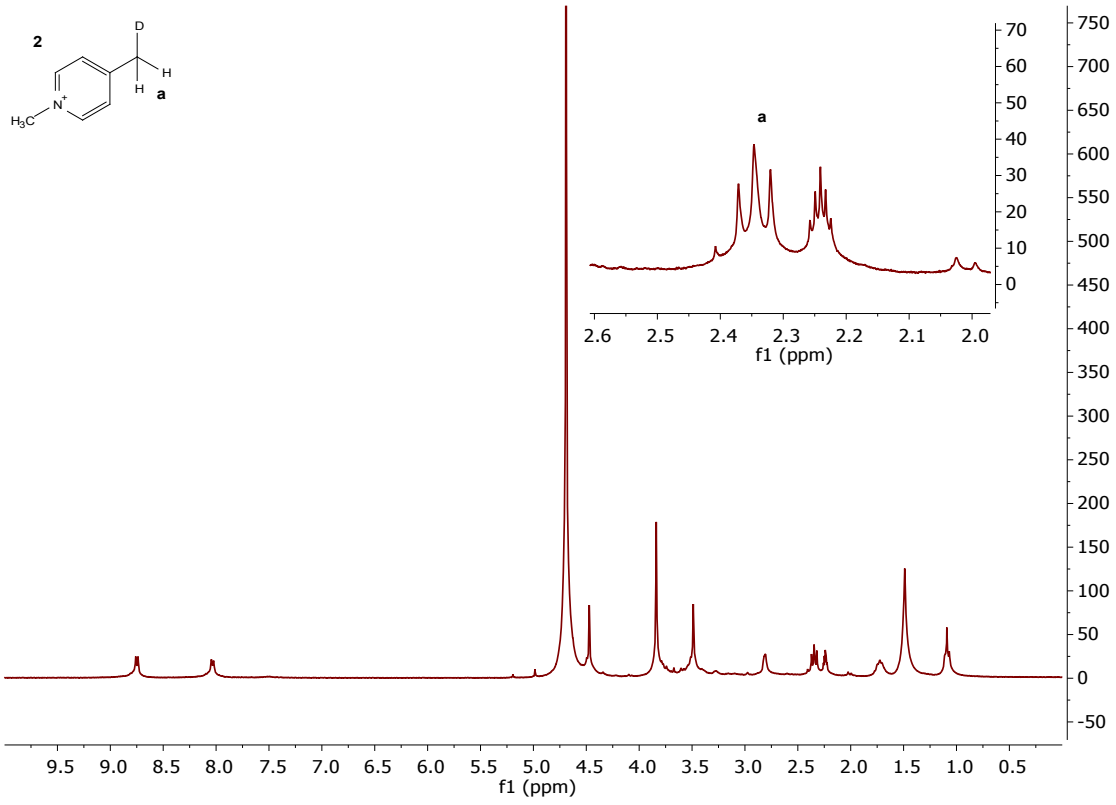

Figure S12. Typical ^{1}H NMR of photo-reaction **1a** with **a-N-CDs** after 48 hours of irradiation and evidence of the deuterated products in the inset.

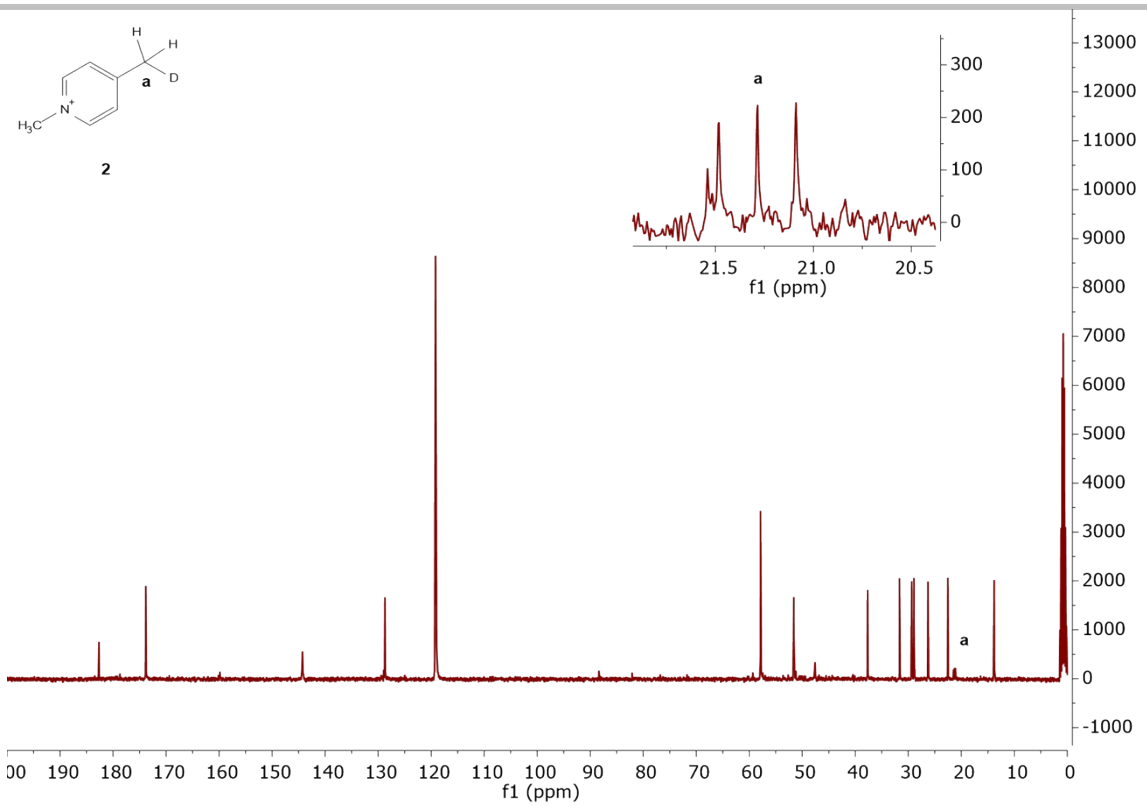

Figure S13. Typical ^{13}C {^{1}H} NMR of photo-reaction **1a** with **a-N-CDs** after 48 hours of irradiation and evidence of the deuterated products in the inset

Photodeprotection of 1b

For the calculation of the conversions of the reagent **1b** the intensity of the signals **a, b** and **c** were evaluated using the signal of the aromatic hydrogens of the benzylic group as internal standard since their chemical shift remain unchanged in both **1b** and **3b.** The signals **d** and **e** were used for evaluating the formation of the cleavage product **2**, while the signal **f** is characteristic of the formation of the hydrolysis product **4** as shown in Figure S14.

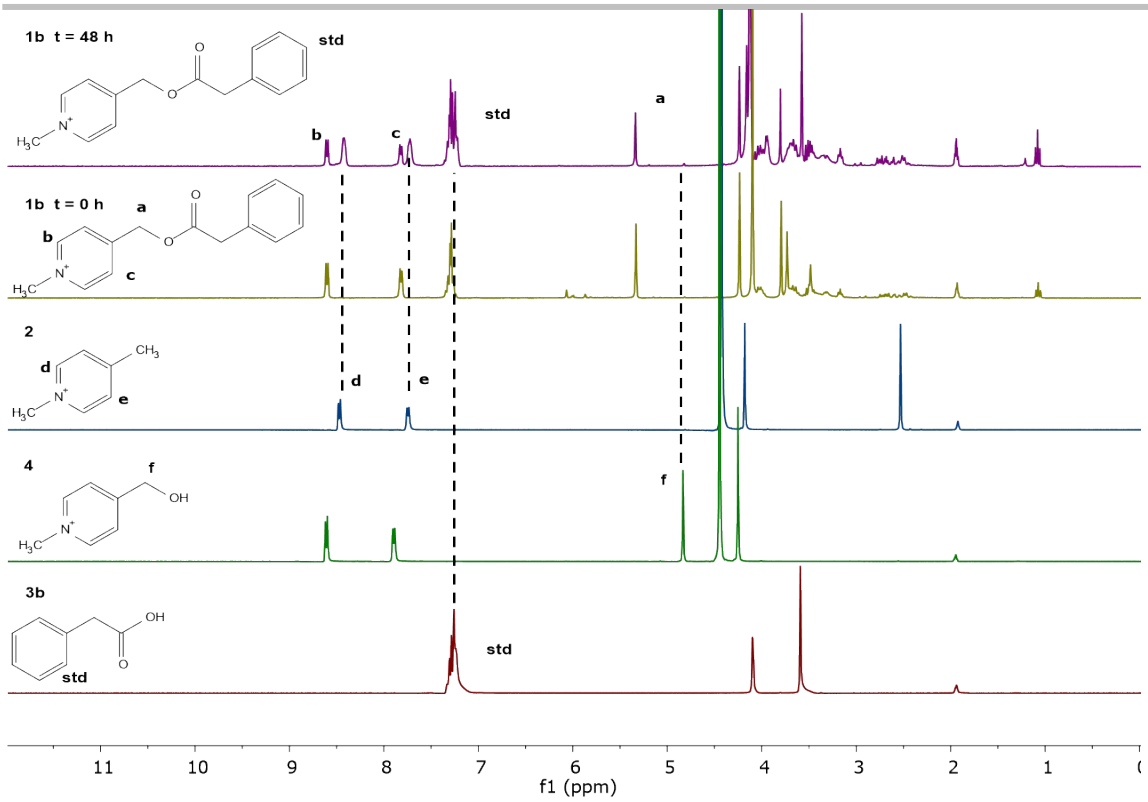

Figure S14. Typical ^{1}HNMR spectra of the reaction of **1b** at t= 0 and 48h compared with expected products in ACN-d_3/D_2O (6/4) at pD=7.

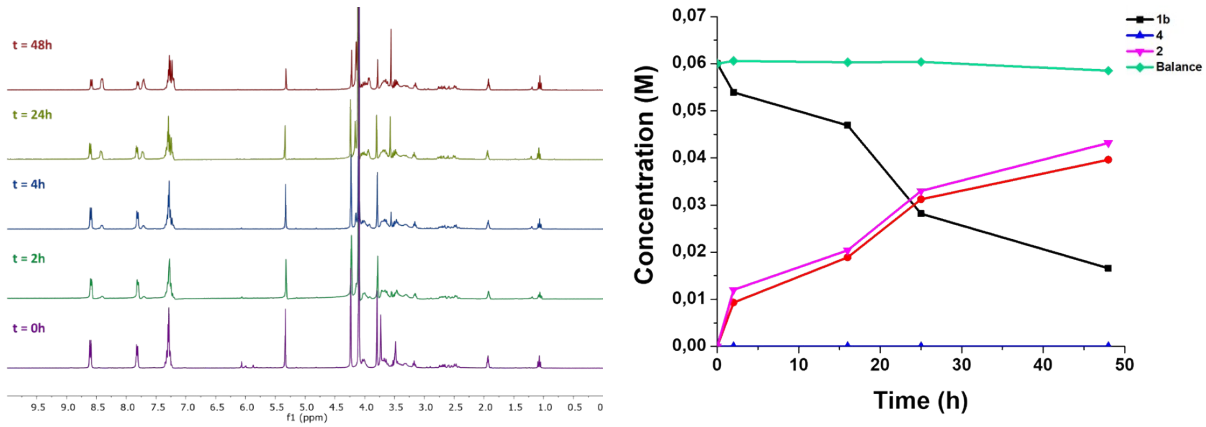

Figure S15. ^{1}HNMR evolution and concentration profiles of reagents and products in the photodeprotection reaction of: **1b** (0.06 M), **a-N-CDs** (20 mg/mL), EDTA (0.1 M) in ACN-d_3/D_2O (6/4) at pD = 7, hυ = 365 nm at R.T. under N_2.

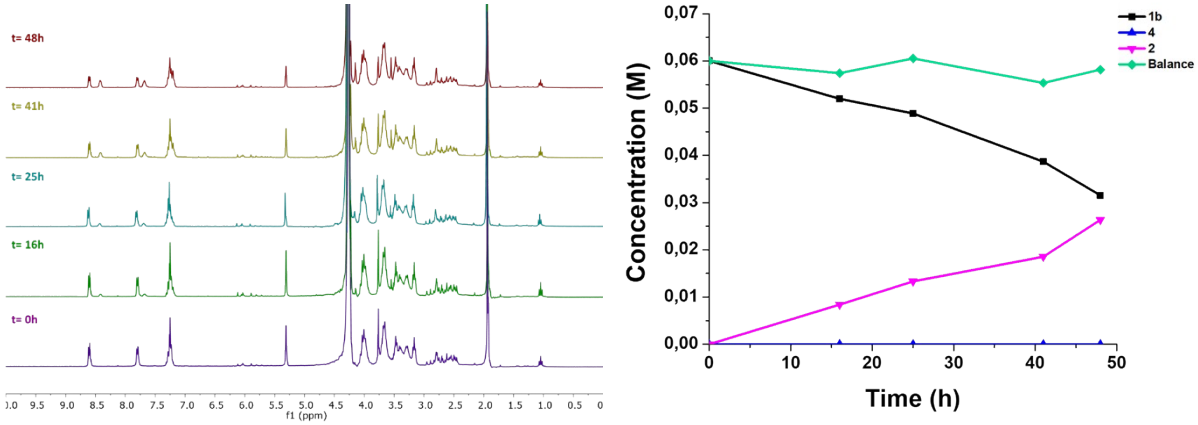

Figure S16. ^{1}HNMR evolution and concentration profiles of reagents and products in the photodeprotection reaction of: **1b** (0.06 M), **a-N-CDs** (100 mg/mL) in ACN-d_3/D_2O (6/4) at pD = 7, hυ = 365 nm at R.T. under N_2.

Photodeprotection of 1c

For the calculation of the conversions of the reagent **1c** the intensity of the signal **a** was evaluated using the signal of the aromatic hydrogens of the benzylic group as internal standard since their chemical shift remain unchanged in both **1b** and **3b.** The signal **b** was used for evaluating the formation of the cleavage product **2**, while the signal **c** is characteristic of the formation of the hydrolysis product **4** as shown in Figure S14.

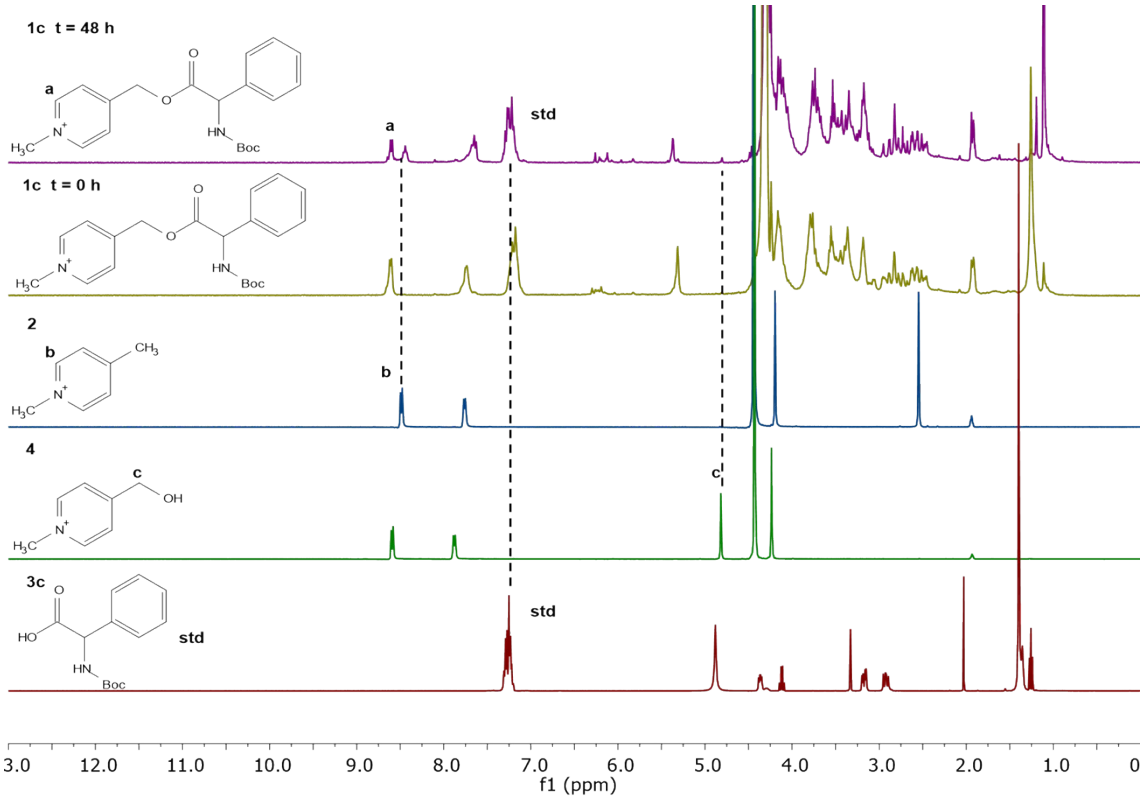

Figure S17. Typical ^{1}HNMR spectra of the reaction of **1c** at t= 0 and 48h compared with expected products in ACN-d_3/D_2O (6/4) at pD=7.

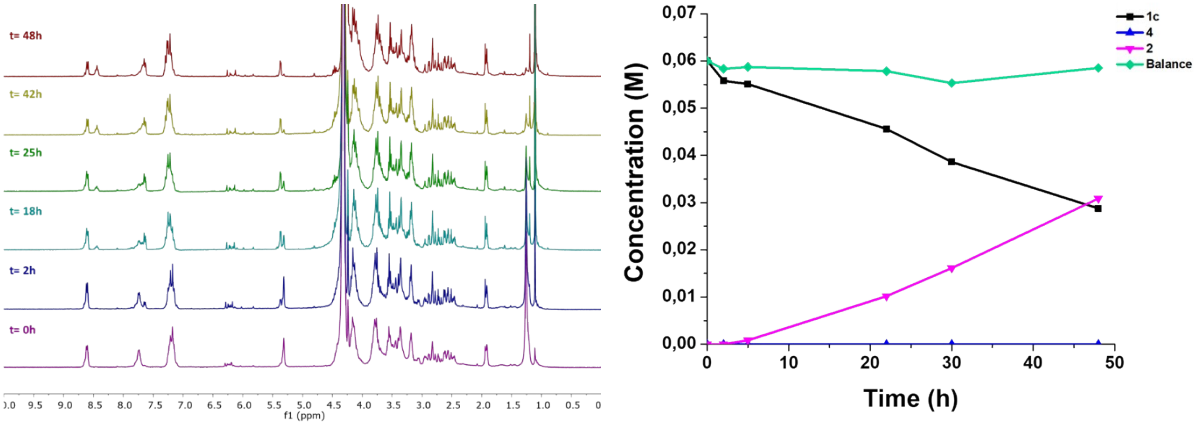

Figure S18. ^{1}HNMR evolution and concentration profiles of reagents and products in the photodeprotection reaction of: **1c** (0.06 M), **a-N-CDs** (20 mg/mL), EDTA (0.1 M) in ACN-d_3/D_2O (6/4) at pD = 7, hυ = 365 nm at R.T. under N_2.

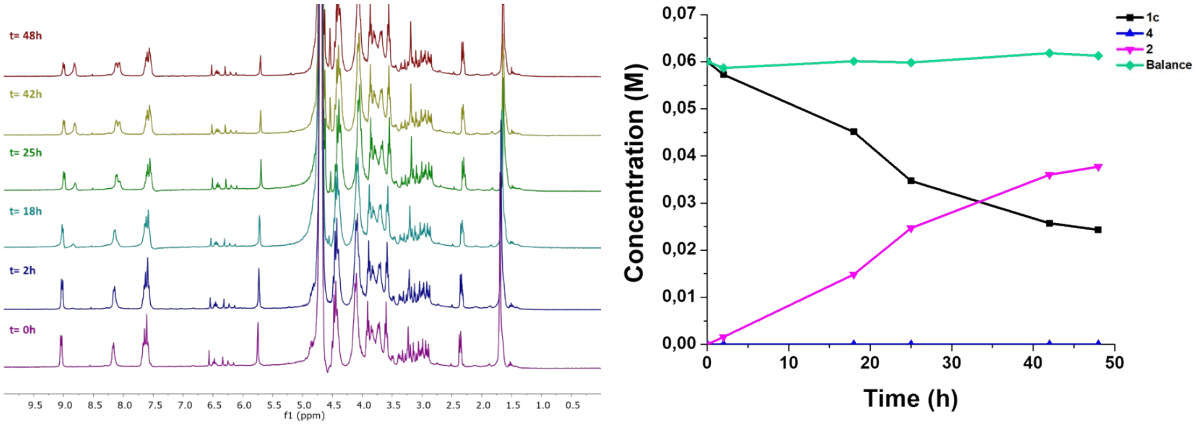

Figure S19. ^{1}HNMR evolution and concentration profiles of reagents and products in the photodeprotection reaction of: **1c** (0.06 M), **a-N-CDs** (100 mg/mL) in ACN-d_3/D_2O (6/4) at pD = 7, hυ = 365 nm at R.T. under N_2.

Photodeprotection of 1d

The formation of the hydrolysis product **4** can be followed by the singlet **a**. The formation of the cleavage product **2** can be followed by signals **b** and **d**. The conversion of the substrate **1d** can be evaluated with the singlet **c**. Each signals of the molecules are shown in the Figure S17. The terminal protons of ethyl acetate are used as internal standard **std** in concentration of 0.006 M. The formation of benzoic acid 1c results impossible to follow and it was evaluated by GC analysis.

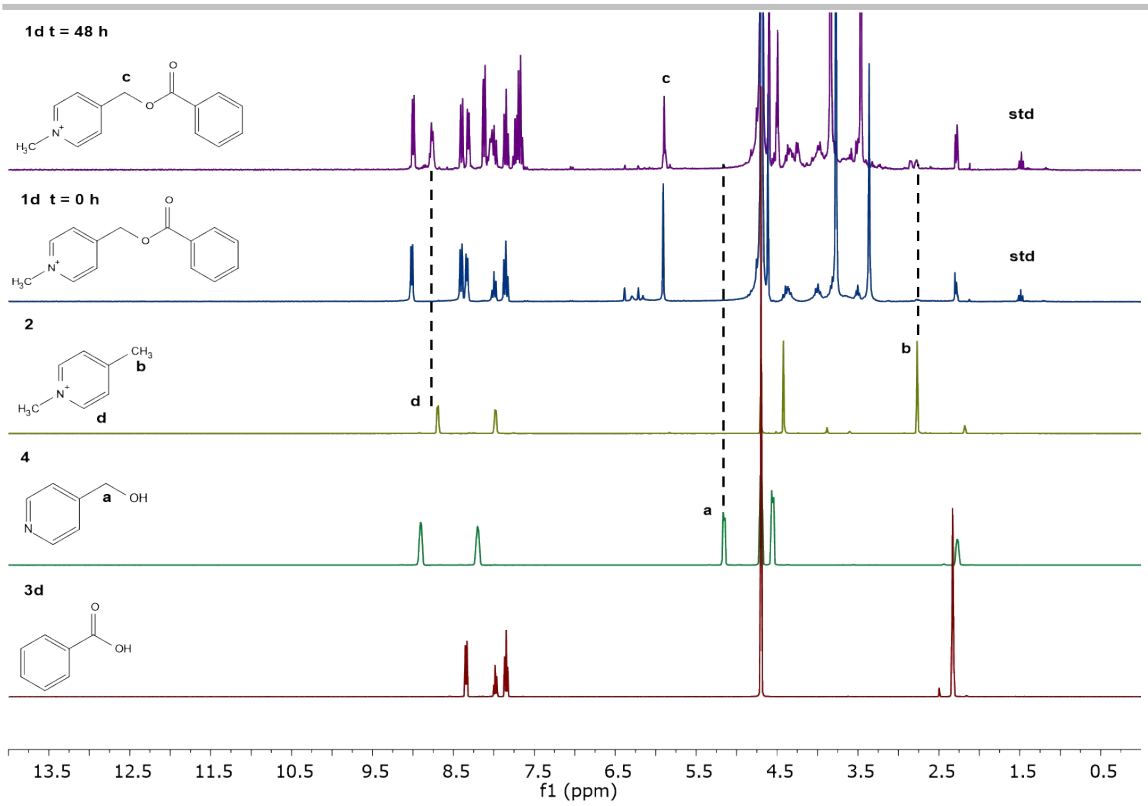

Figure S20. Typical ^{1}HNMR spectra of the reaction of **1d** at t= 0 and 48h compared with expected products in ACN-d_3/D_2O (6/4) at pD=7.

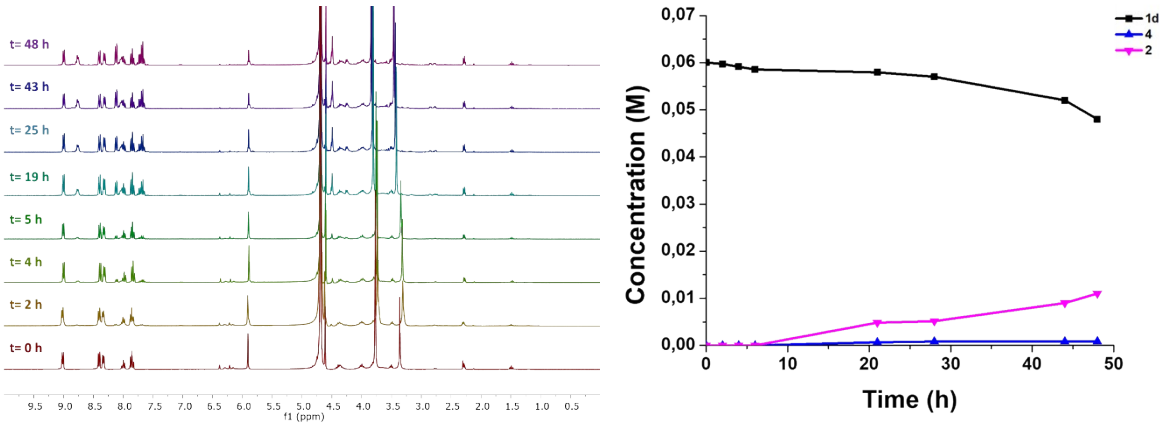

Figure S21. ^{1}HNMR evolution and concentration profiles of reagents and products in the photodeprotection reaction of: **1d** (0.06 M), **a-N-CDs** (20 mg/mL), EDTA (0.1 M) in ACN-d_3/D_2O (6/4) at pD = 7, hυ = 365 nm at R.T. under N_2.

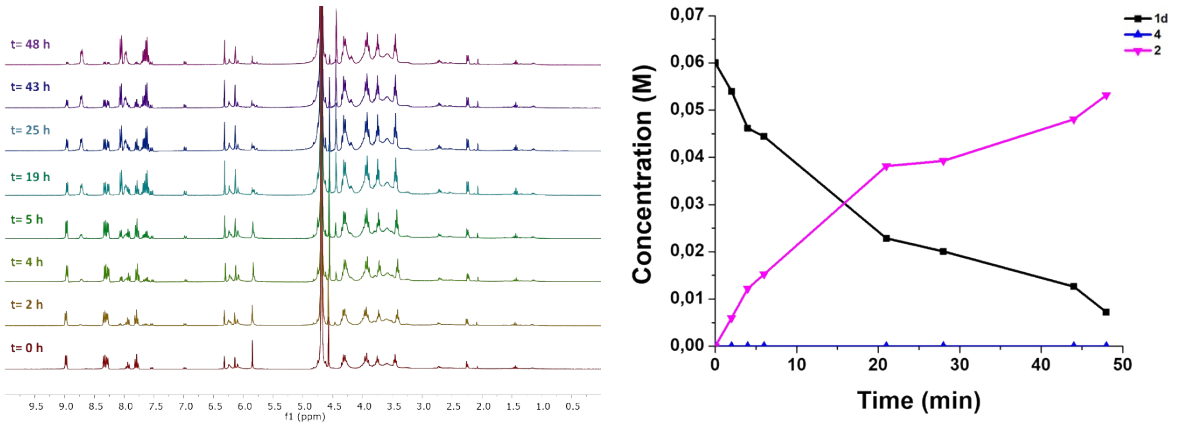

Figure S22. ^{1}HNMR evolution and concentration profiles of reagents and products in the photodeprotection reaction of: **1b** (0.06 M), **a-N-CDs** (100 mg/mL) in ACN-d_3/D_2O (6/4) at pD = 7, hυ = 365 nm at R.T. under N_2.

Photodeprotection of 1e

The formation of p-nitrobenzoic acid **3b** can be followed by using the doublet **a**. The formation of the hydrolysis product **4** can be followed by the singlet **b**. The formation of the cleavage product **2** can be followed by singlet **c**. The conversion of the substrate **1e** can be evaluated using doublet **d** or singlet **e**. Each signals of the molecules are shown in the Figure S20. The terminal protons of ethyl acetate are used as internal standard std in concentration of 0.006 M.

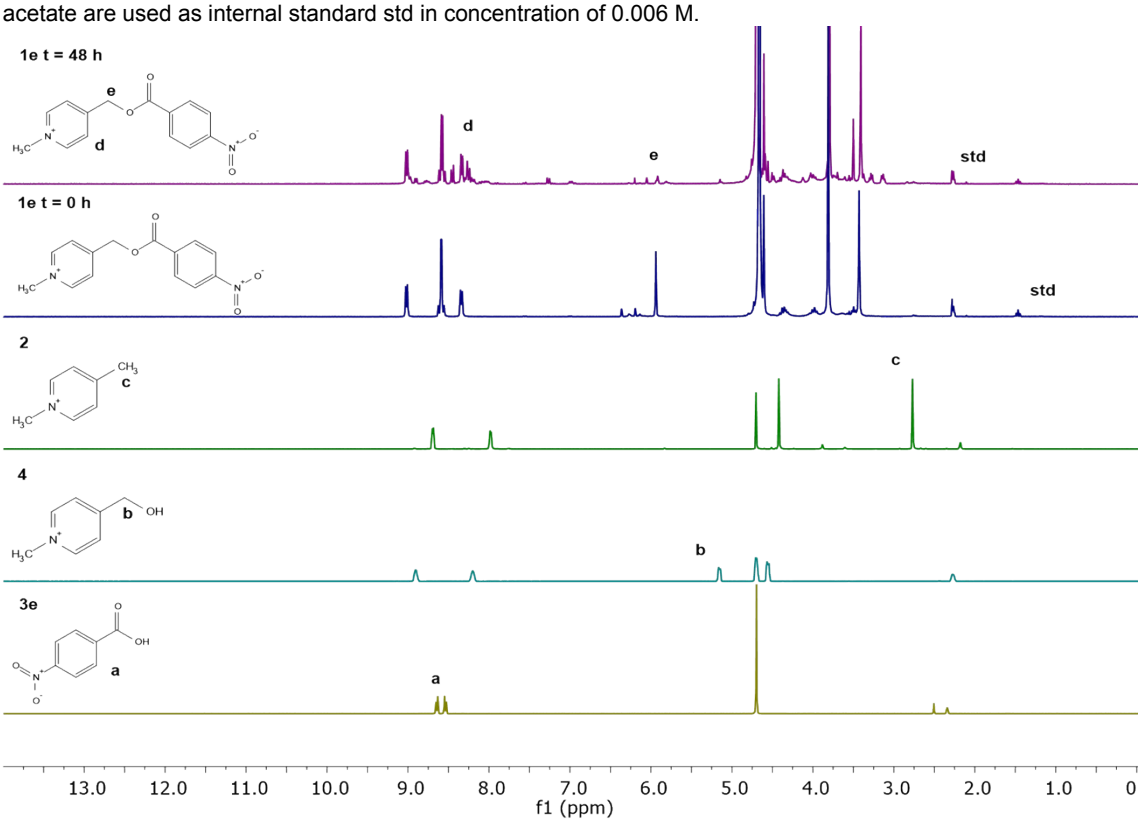

Figure S23. Typical ^{1}HNMR spectra of the reaction of **1e** at t= 0 and 48h compared with expected products in ACN-d_3/D_2O (6/4) at pD=7.

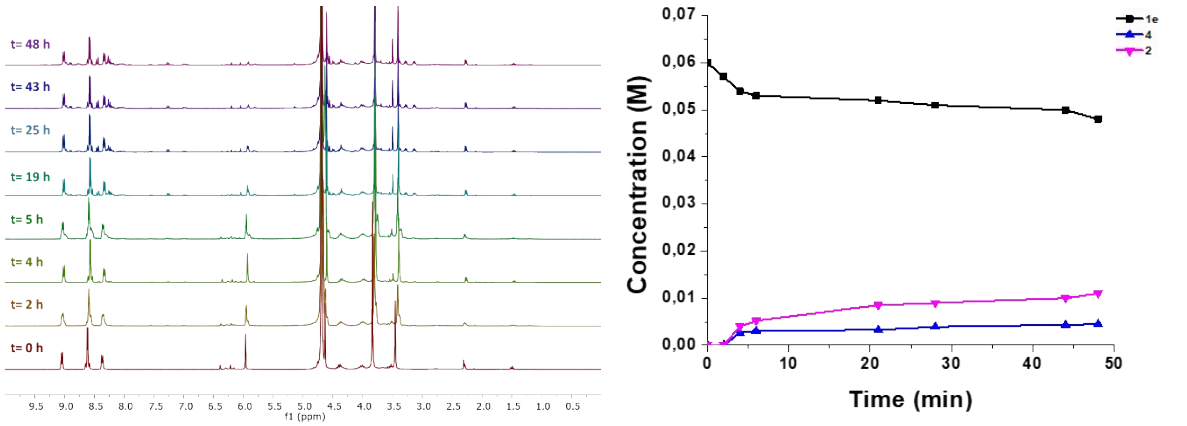

Figure S24. ^{1}HNMR evolution and concentration profiles of reagents and products in the photodeprotection reaction of: **1e** (0.06 M), **a-N-CDs** (20 mg/mL), EDTA (0.1 M) in ACN-d_3/D_2O (6/4) at pD = 7, hυ = 365 nm at R.T. under N_2.

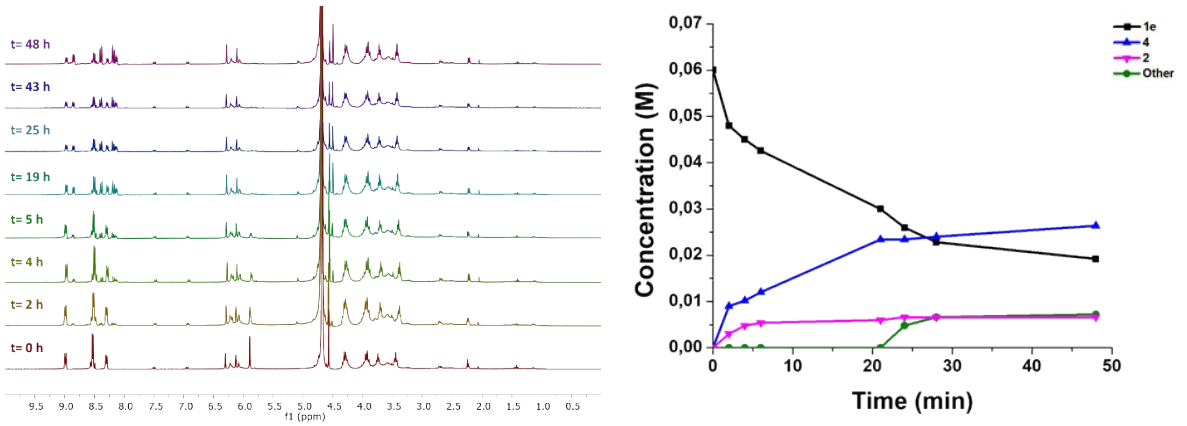

Figure S25. ^{1}HNMR evolution and concentration profiles of reagents and products in the photodeprotection reaction of: **1e** (0.06 M), **a-N-CDs** (100 mg/mL) in ACN-d_3/D_2O (6/4) at pD = 7, hυ = 365 nm at R.T. under N_2.

Cyclic voltammetry

The cyclic voltammetry of the CDs was carried out in DMF (with traces of water) for solubility reasons since CDs are not soluble in most common organic solvents (for example, not even in pure CH_3CN) and also to avoid the use of excessive water (as the special case of the reaction solvent) which significantly reduces the available redox potential window (see here below). The choice of DMF as solvent for CV of CDs finds also precedents in previous publications.[5]
All measurements were carried out in an electrochemical cell having a three-electrode configuration. It comprised a glassy carbon working electrode, a platinum coils as counter electrode, and an Ag/AgCl,KCl(saturated) reference electrode. The latter was separated from the main solution by a glass frit to avoid contamination from chloride ions and additional amounts of water (vide infra).
The DMF solutions containing CDs were prepared by adding to 5 mL of solvent 200 µL water containing a weighted amount of CDs (typically 25 mg). This procedure ensured full dispersion/solubilization of CDs in the medium. All measurements were performed under a nitrogen atmosphere.
Preliminarily, cyclic voltammetric measurements were performed in the background electrolyte - *i.e.*, DMF with 0.1 M tetrabutylammonium perchlorate (TBAP) - in order to establish the potential window available for the investigation of CDs and substrates. Figure S26 shows typical cyclic voltammograms (CVs) recorded at 100 mV/s, starting from 0.0 V vs. Ag/AgCl and scanning the potential in either the negative (left CV) or positive (right CV) direction up to the background discharge, which occurred at ca. -2.7 V (cathodic limit) and +1.8 V (anodic limit). Only minor features were recorded within the latter two limits due to impurities. The effect of trace water in the CV responses was also tested. As shown in Figure S27, by adding milli-Q water (i.e., 200 and 400 µL) into 5 mL of pure DMF, the peak at - 2.3 V, already present in the background, increased by increasing the water content. No process different from that due to the background discharge was instead observed in the anodic region. Overall, these results indicate that the potential window available to evaluate the CDs and substrates redox properties ranges from about -2.3 V to about 1.7 V.

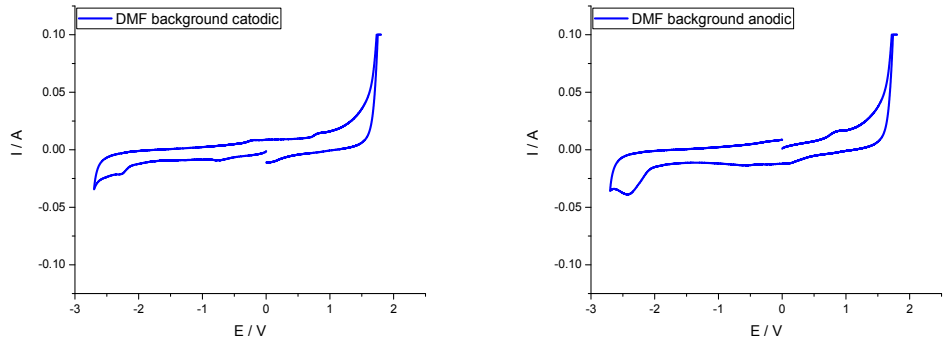

Figure S26. Cyclic voltammograms recorded at a GCE in pure DMF with 0.1 M TBAP, starting from 0 V vs . Ag/AgCl/KCl (saturated) towards the cathodic direction (left) and anodic direction (right). Scan rate 100 mV/s

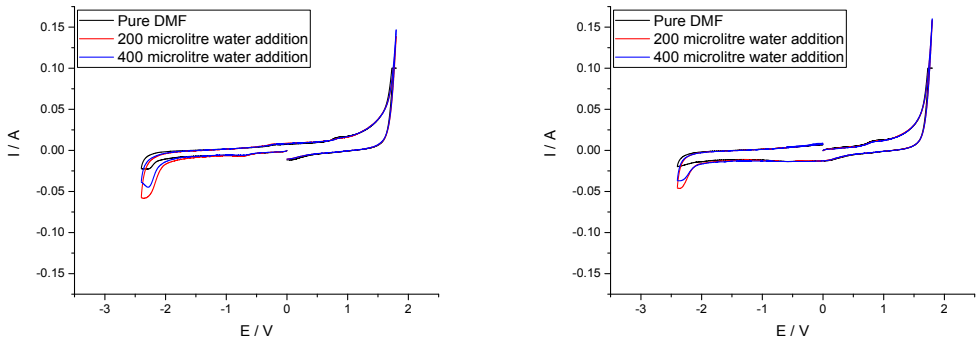

Figure S27. Cyclic voltammograms recorded at a GCE in 5 mL of pure DMF (black line)), containing 0.1 M TBAP and 200 µL (red line) and 400 µL (red line) milli-Q water. Scan rate 100mV/s, cathodic direction (left), anodic direction (right), Ag/AgCl/KCl saturated reference, platinum counter electrode.

The redox potential of the Ferrocenium / Ferrocene (Fc^+ / Fc) system was evaluated in a DMF solution containing 0.1 M TBAP and 200 µL milli-Q water. Figure S28 shows a series of CVs obtained at different scan rates in a DMF solution containing 5 mM Fc. The expected reversible anodic/cathodic pattern[6] is recorded; the halfway potential ($E_{1/2}$), evaluated as the half-sum of the anodic and cathodic peak potentials,[7] is equal to 0.492 (± 0.012) V vs. Ag/AgCl/KCl (saturated). Assuming that the diffusion coefficients of Fc and Fc^+ are equal, $E_{1/2}$ can be regarded as the formal potential (E^0) of the redox couple.[7]

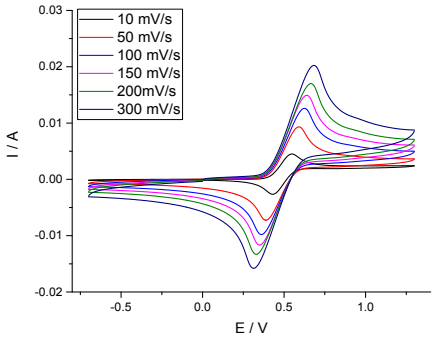

Figure S28. Cyclic voltammograms recorded at a GCE in 5 mM Fc in DMF solution containing 0.1 M TBAP. Scan rates as indicated in the figure. Ag/AgCl/KCl (saturated) reference electrode.

The scheme in Figure S29 shows how the potentials of CDs, substrates and $E_{1/2}$ of Fc^+/Fc are located against the Ag/AgCl/KCl (saturated), employed in all experimental measurements.

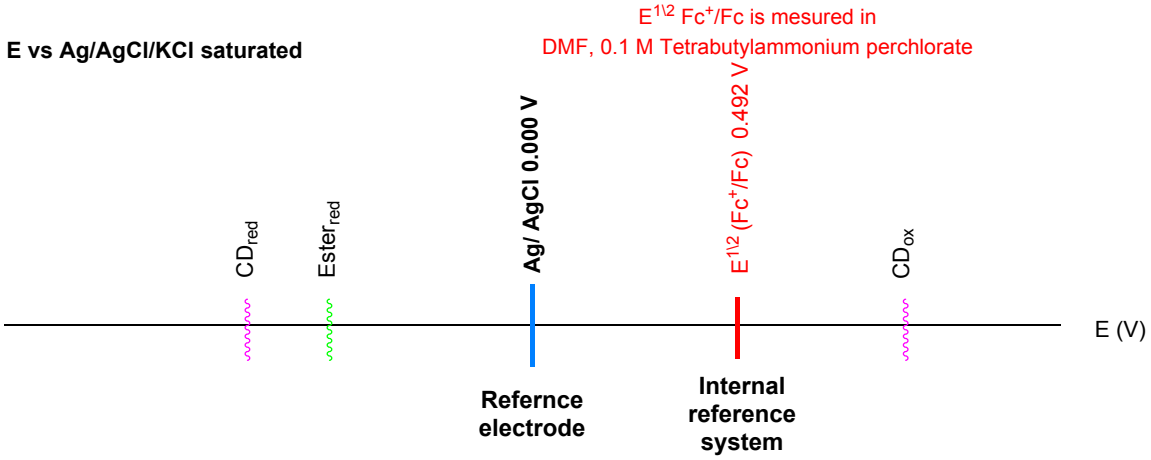

Figure S29. Scheme of the potentials characterizing the various redox systems considered in this work.

The voltammetric measurements of CDs were carried out in DMF solutions (5 mL), containing 25 mg/ml of CDs, 200 μl milli-Q water and 0.1 M TBAP. CVs of the **a,g-CDs** and **a,g-N-CDs** are shown In Figure S30. It is evident that both types of amorphous and graphitic CDs investigated provide irreversible processes in both the cathodic and anodic potentials. Therefore, their reduction and oxidation potentials were estimated by the onset potential.[8]

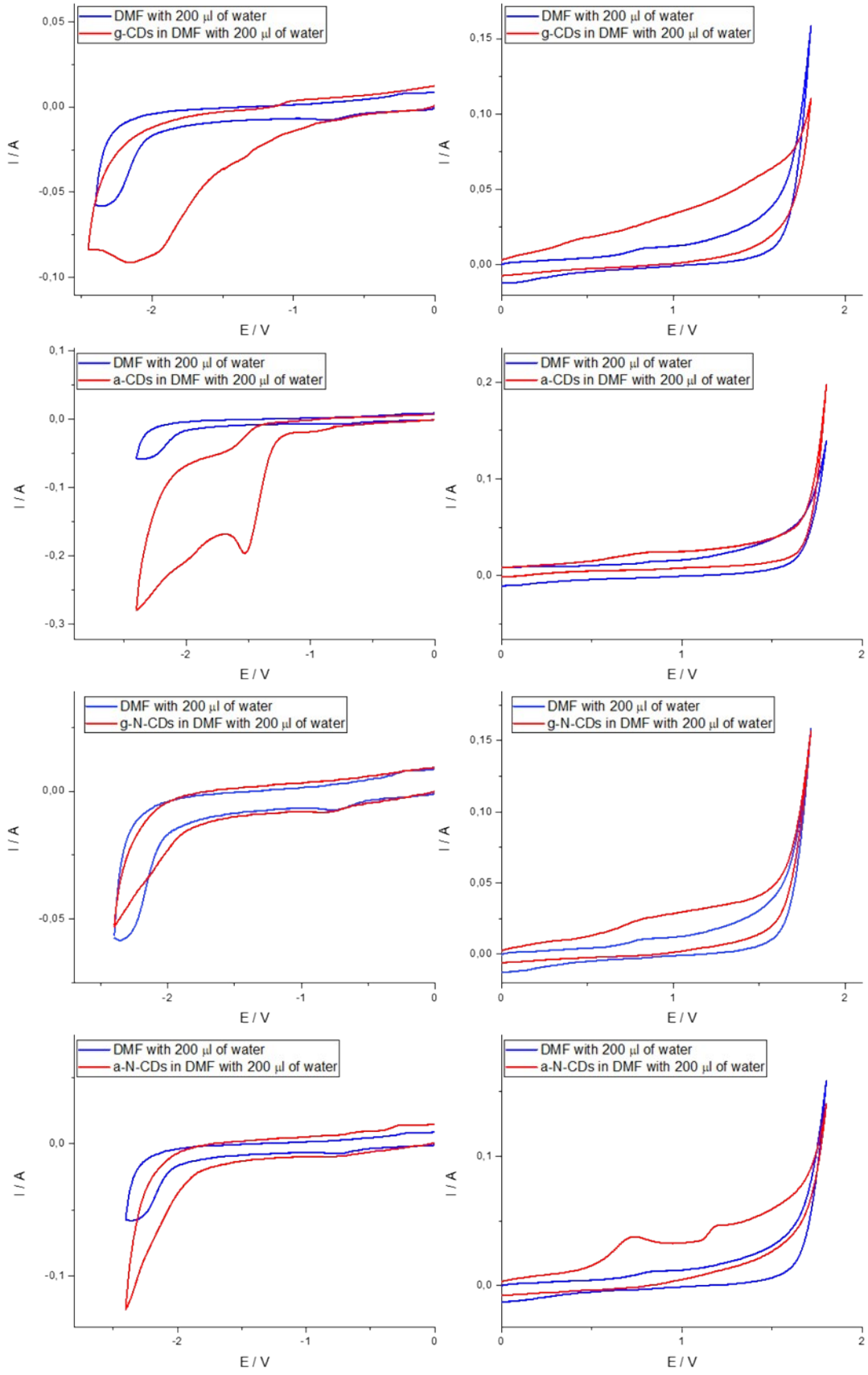

Figure S30. CVs recorded at the GCE in DMF containing 25 mg/mL of **a,g-CDs** and **a,g-N-CDs** and 200 µl miili-Q water and 0.1 M of TBAP. Scan rate 100mV/s. Initial scan direction: negative potentials (left), positive potentials (right). All potentials are quoted against an Ag/AgCl/KCl saturated. *Due to trace of oxygen.

Based on the onset potentials of the waves, the Fermi energy levels were evaluated by using the following equations: [6]

$$E_{oxidation} = -\left(5.1 + E_{onset,\, ox\ vs\ Fc+/Fc}\right)(eV) \qquad \text{Equation 1}$$

$$E_{reduction} = -\left(5.1 + E_{onset,\, red\ vs\ Fc+/Fc}\right)(eV) \qquad \text{Equation 2}$$

In principle, the energy of the reduction energy level can be approximated as the electron affinity and therefore the energy required to add an electron to a defined moiety into the CDs structure and this energy is correlated to the standard reduction potential. Conversely, the oxidation energy level is related to the ionization potentials and therefore to the minimum energy required to remove an electron from the CDs and this energy is correlated to the standard oxidation potential. Therefore, the energy difference between the highest oxidation energy level and the lowest reduction energy level are useful to understand the oxidative or reductive behaviors of the CDs. Tables S1 shows the **a-CDs**, **g-CDs**, **a-N-CDs**, **g-N-CDs** onset potentials - determined for either reduction or oxidation processes; for clarity they are referred against both Ag/AgCl and Fc/Fc^+ systems- and the corresponding orbital Fermi energy levels.

Table S1 Onset reduction potentials and Fermi energy levels for **a-CDs, g-CDs**, **a-N-CDs**, and **g-N-CDs**.

CDs	E_{onset} Vs. Ag/AgCl (V)[a]	E_{onset} Vs Fc/Fc^+ (V)[a]	Fermi energy (eV)
g-CDs	-1.40	-1.89	-3.2
	0.35	-0.14	-5.0
	0.69	0.20	-5.3
	1.27	0.77	-5.9
a-CDs	-1.83	-2.33	-2.8
	-1.30	-1.79	-3.3
	0.52	0.03	-5.1
g-N-CDs	-1.71	-2.21	-2.9
	0.08	-0.41	-4.7
	0.56	0.06	-5.2
a-N-CDs	-1.94	-2.43	-2.7
	0.53	0.03	-5.1
	1.12	0.62	-5.7

We report E_{onset} for the three systems. It was measured for the Ag/AgCl system and the E_{onset} was referenced to Fc+/Fc.
a) Uncertainty of E_{onset} is ± 0.01 V

Following, the onset reduction potentials and Fermi energy levels were also determined for substrates **1a-e** (Figure S31 and Table S2). The energy levels calculated with the equation 2 in these cases correspond to the LUMO.

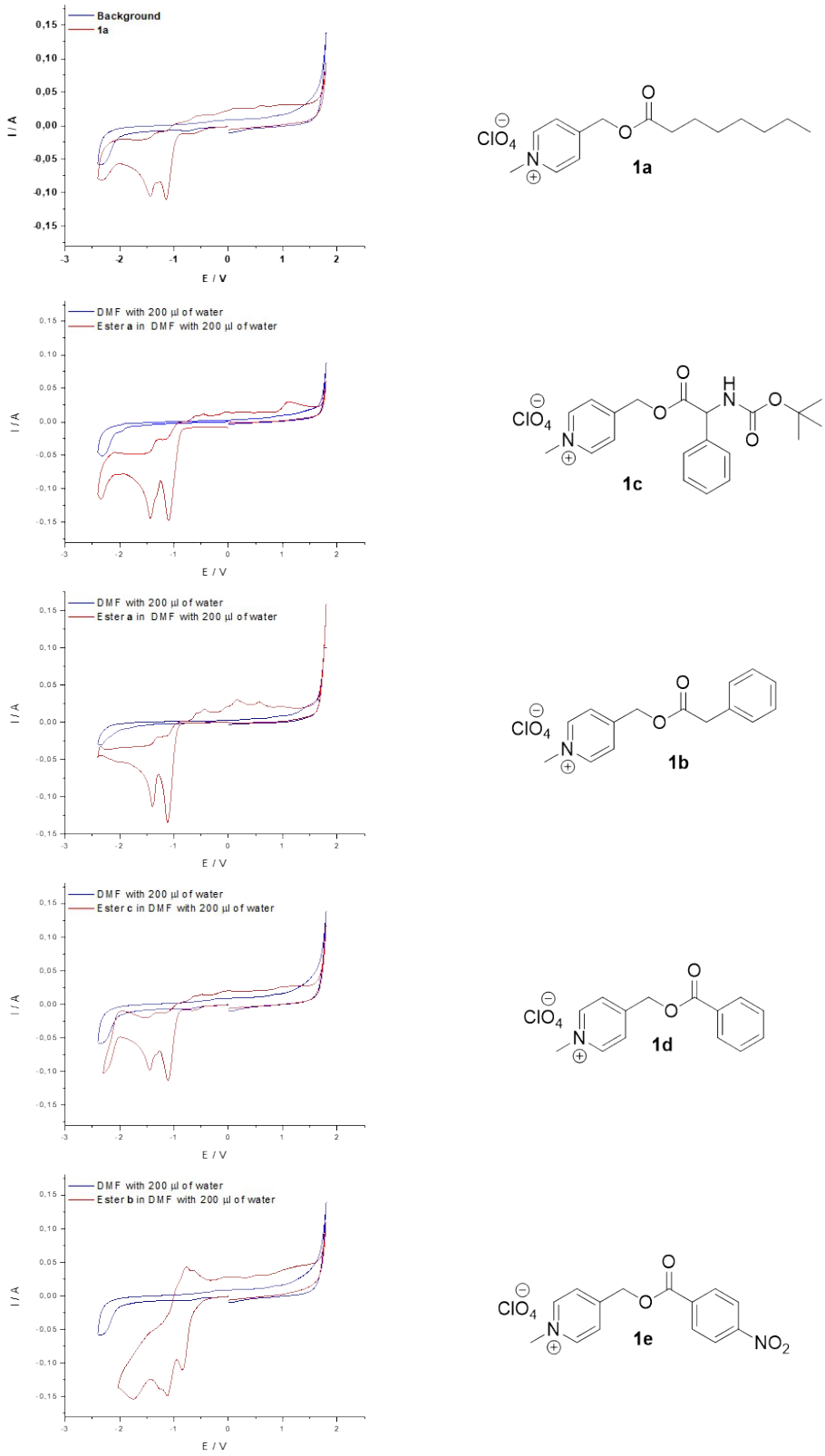

Figure S31. CVs recorded at the GCE in DMF containing 25 mg of **1a-e**, 200 µl miili-Q water and 0.1 M of TBAP. Scan rate 100mV/s. Initial scan direction towards negative potentials. All potentials are quoted against an Ag/AgCl/KCl saturated.

Table S2. Onset reduction potentials and Fermi energy levels calculated for **1a-e**.

Substrate	E_{onset} Ag/AgCl (V)[a]	E_{onset} Fc/Fc^+ (V)[a]	Fermi energy (eV)
1a	-0,97	-1,459	-3,6
	-1,35	-1,845	-3,3
1b	-0,94	-1,435	-3,7
	-1,32	-1,810	-3,3
1c	-0,89	-1,382	-3,7
	-1,36	-1,853	-3,2
1d	-0,93	-1,431	-3,7
	-1,38	-1,874	-3,2
1e	-0,65	-1,139	-4,0
	-0,99	-1,480	-3,6
	-1,46	-1,954	-3,1

We report E_{onset} for the three systems. It was measured for the Ag/AgCl system and the E_{onset} was referenced to Fc+/Fc. a) Uncertainty of E_{onset} is ± 0.01 V.

UV spectrum and optical band gap

The optical band gaps of the synthesized CDs were calculated from their absorption spectra (Figure S32).

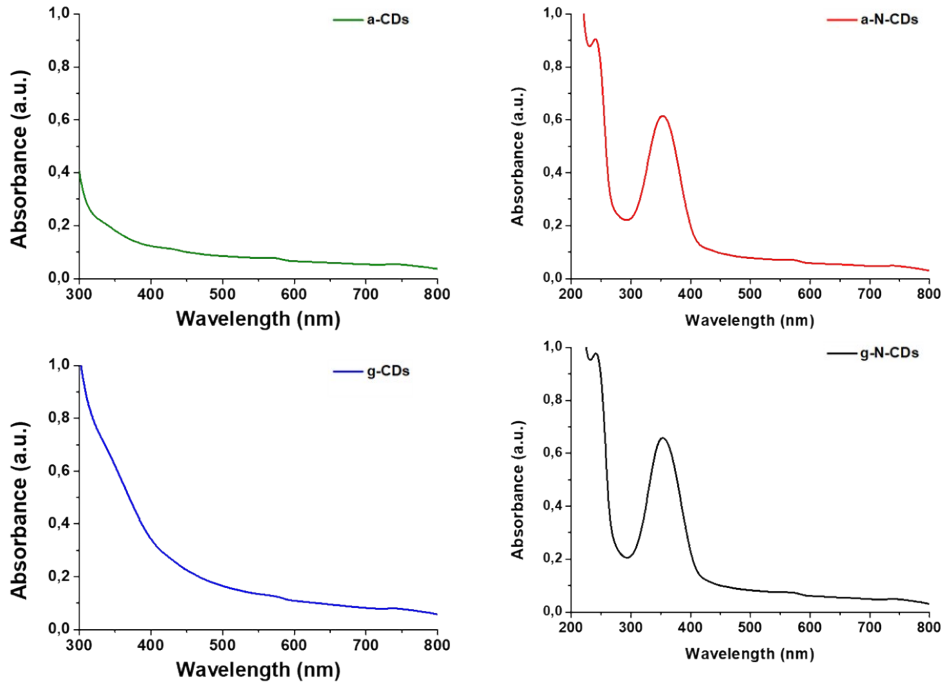

Figure S32.UV-Vis spectra of the CDs

The following equation was employed to calculate the optical band gap taking the onset wavelength of each spectra:

$$E = h * \frac{c}{\lambda}$$

Where:
E= optical band gap energy (eV)
h= Plank constant $4.13566751691 \cdot 10^{-15}$ eV·s
c= speed of light $3*10^{8}$ m\s
λ= absorption wavelength (m)

Table S3. Onset wavelength and optical band gap calculated for **a-CDs**, **g-CDs**, **a-N-CDs**, **g-N-CDs**.

CDs	Onset wavelength (nm)	Optical Band Gap (eV)
g-CDs	420	2.9
a-CDs	460	2.6
g-N-CDs	450	2.8
a-N-CDs	410	3.0

NMR Spectra of compounds 1a-e, 2 and 4

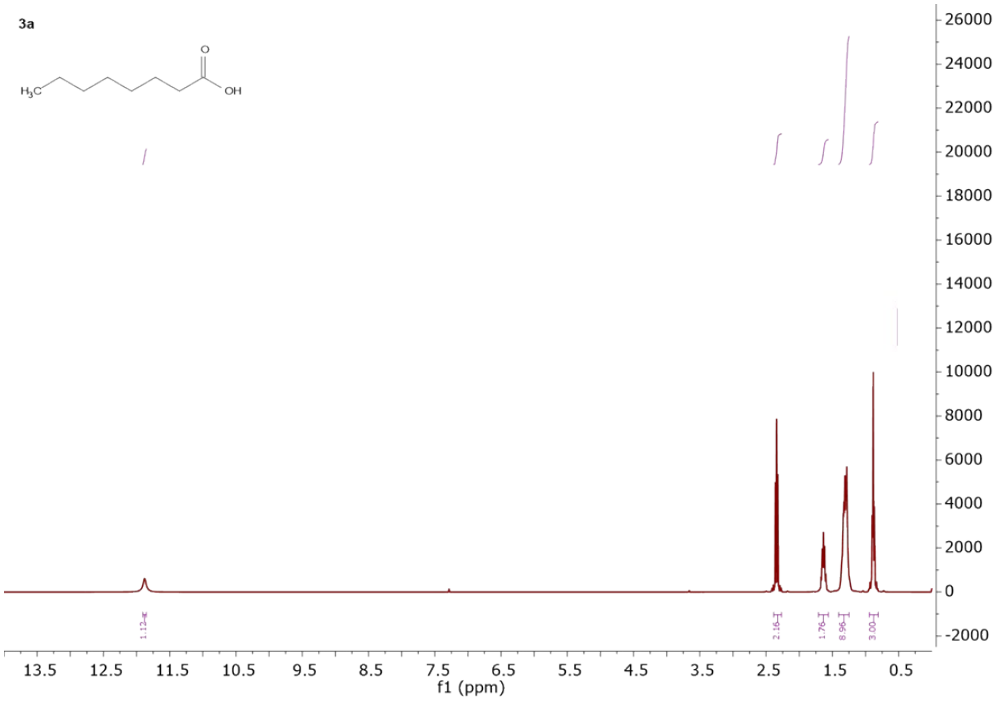

Figure S33. [1]HNMR spectra of compound **3a.**

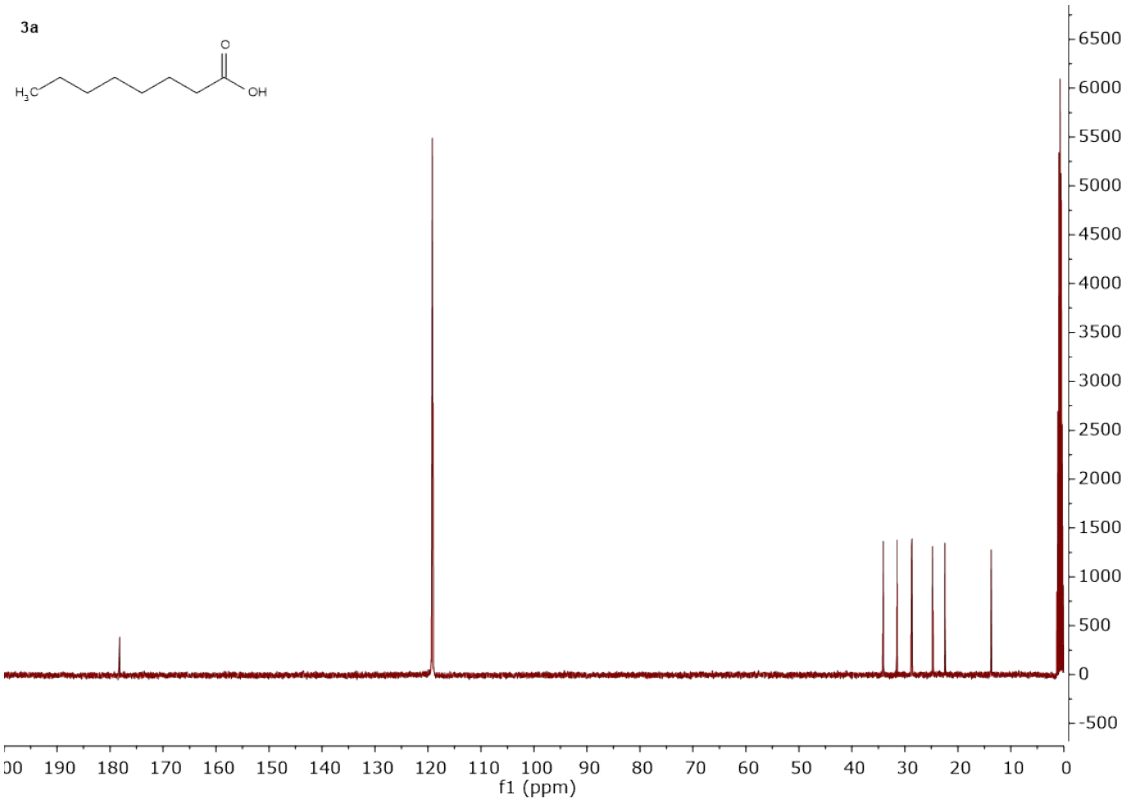

Figure S34. [13]C {[1]H} NMR spectra of compound **3a**.

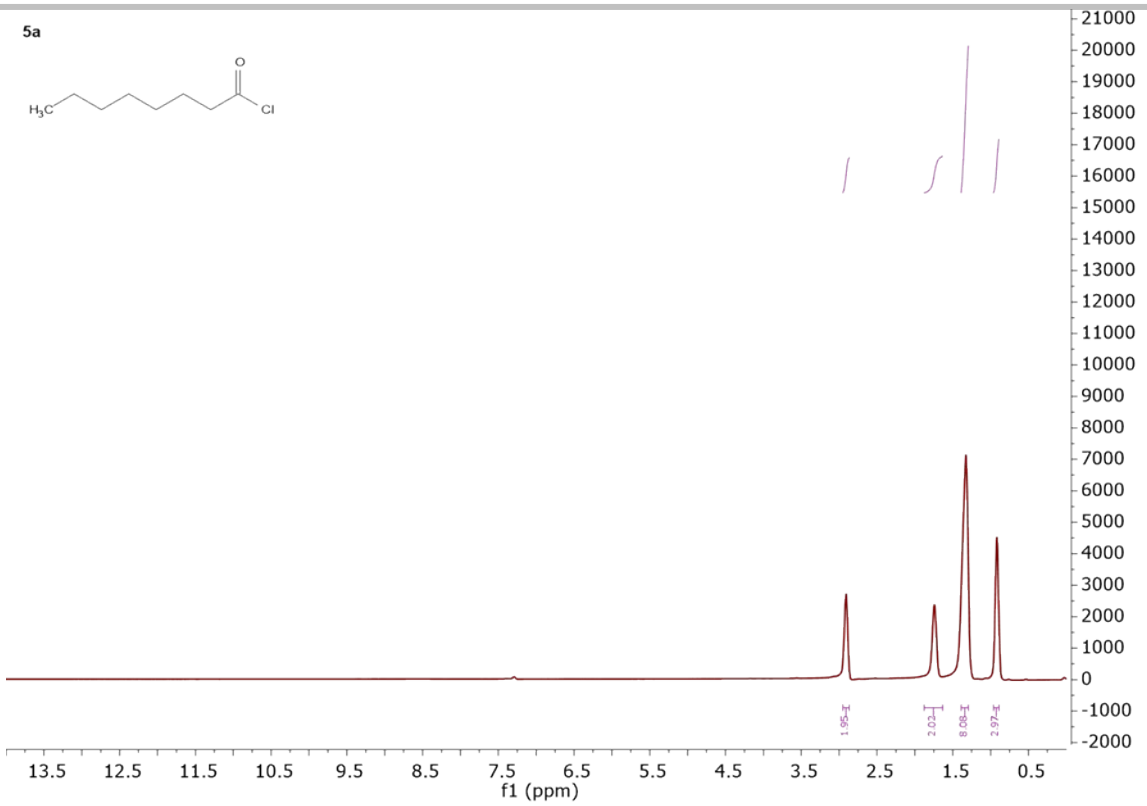

Figure S35. [1]HNMR spectra of compound **5a.**

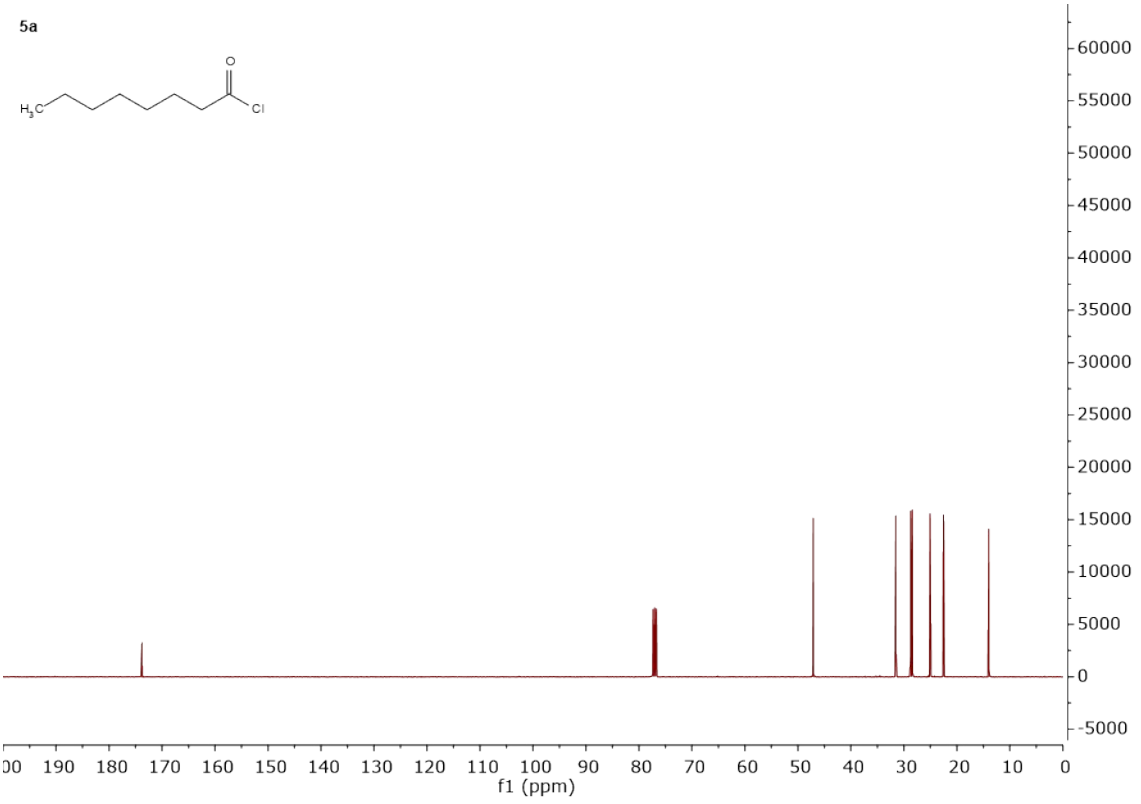

Figure S36. [13]C {[1]H} NMR spectra of compound **5a**.

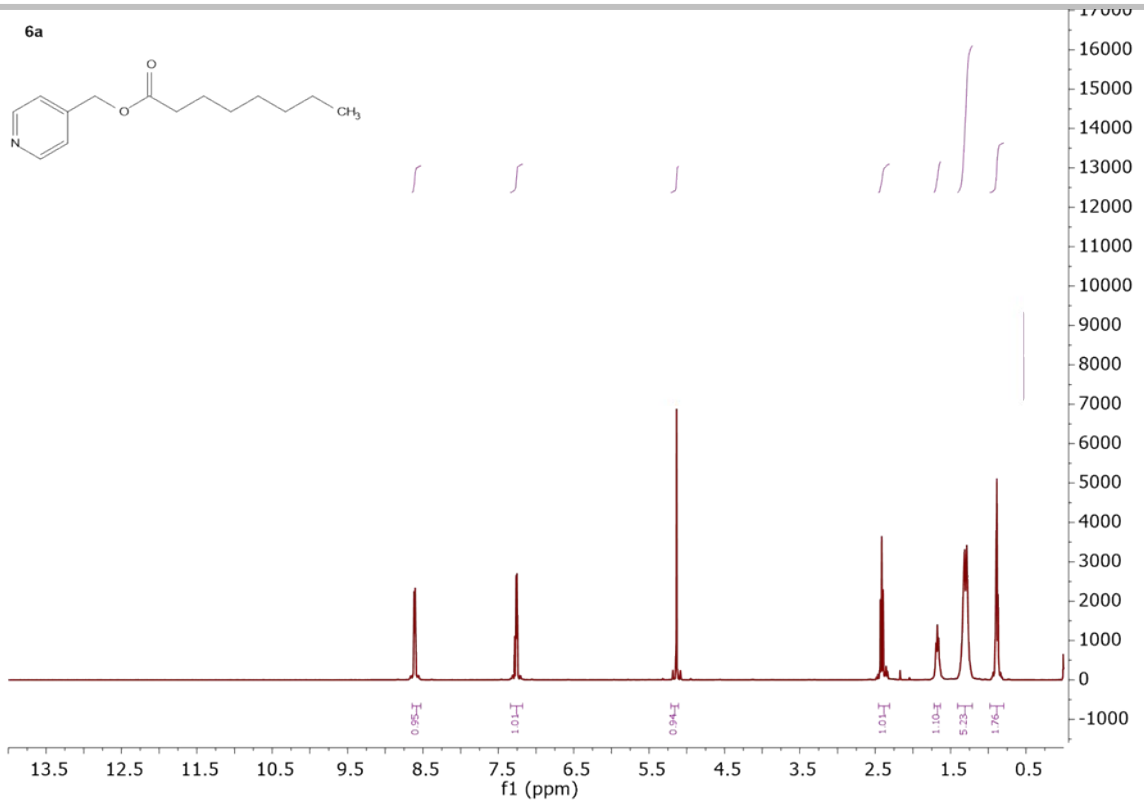

Figure S37. ^{1}HNMR spectra of compound **6a.**

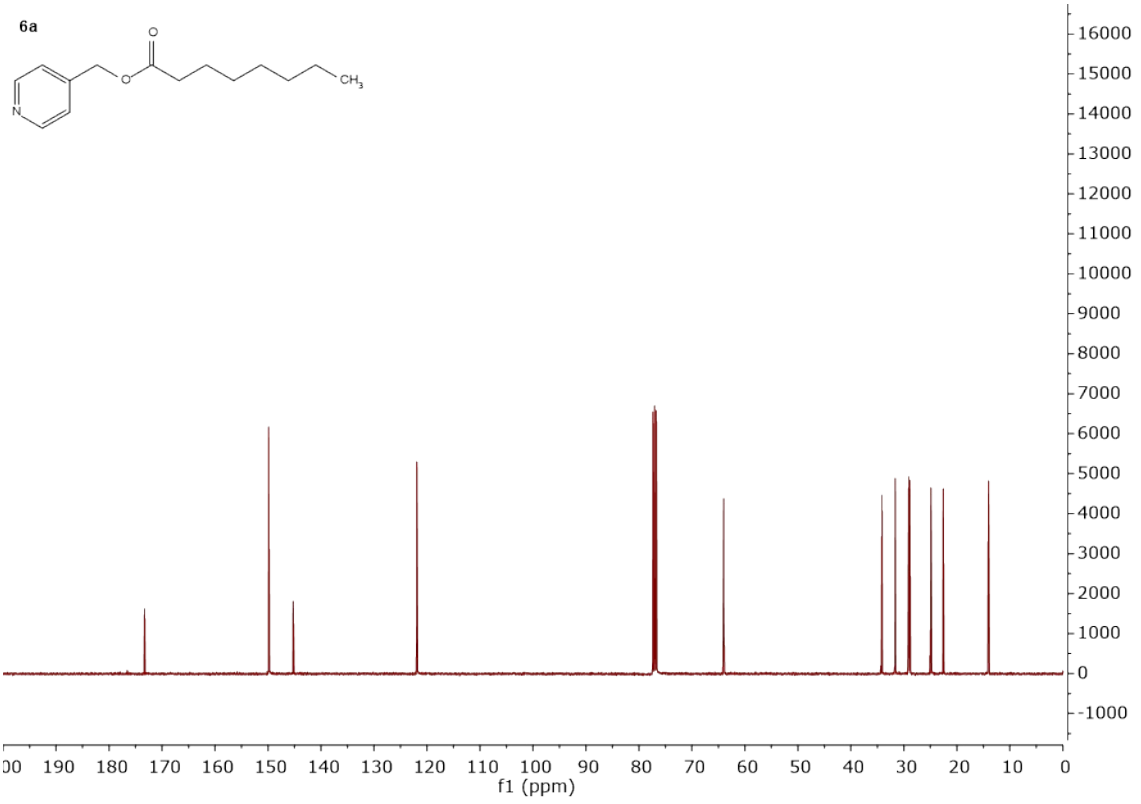

Figure S38. ^{13}C {^{1}H} NMR spectra of compound **6a**.

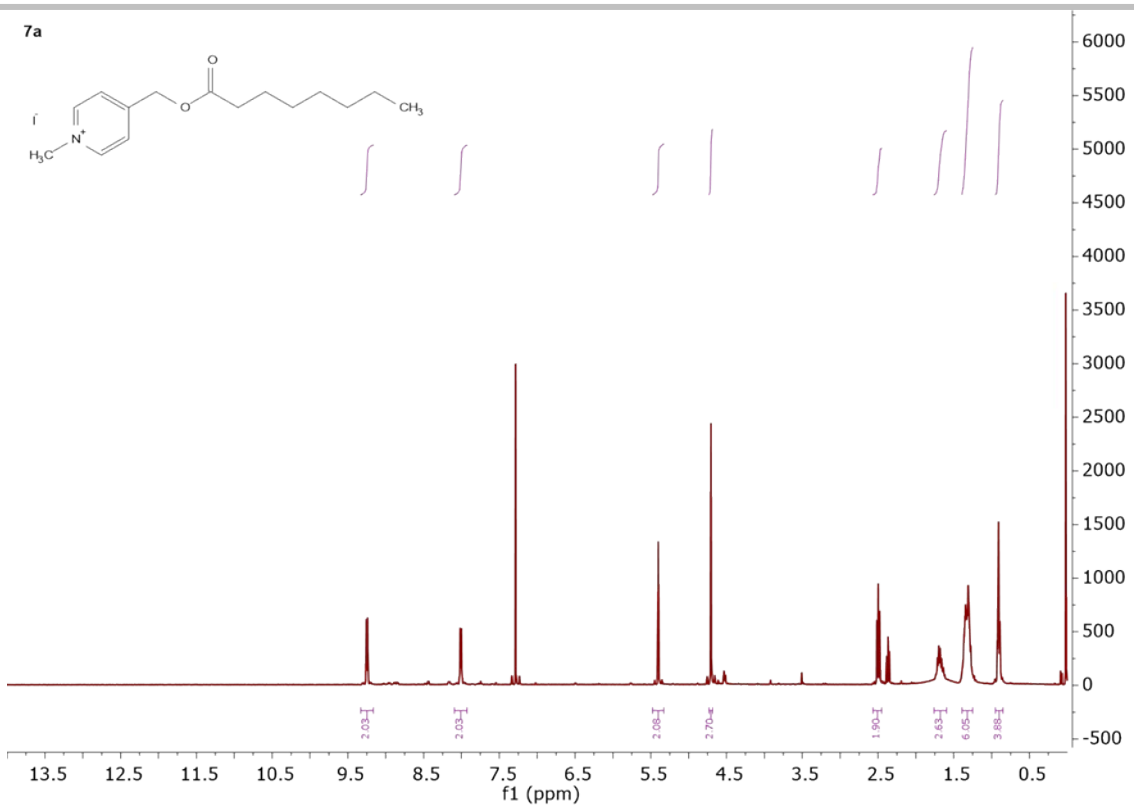

Figure S39. ^{1}HNMR spectra of compound **7a.**

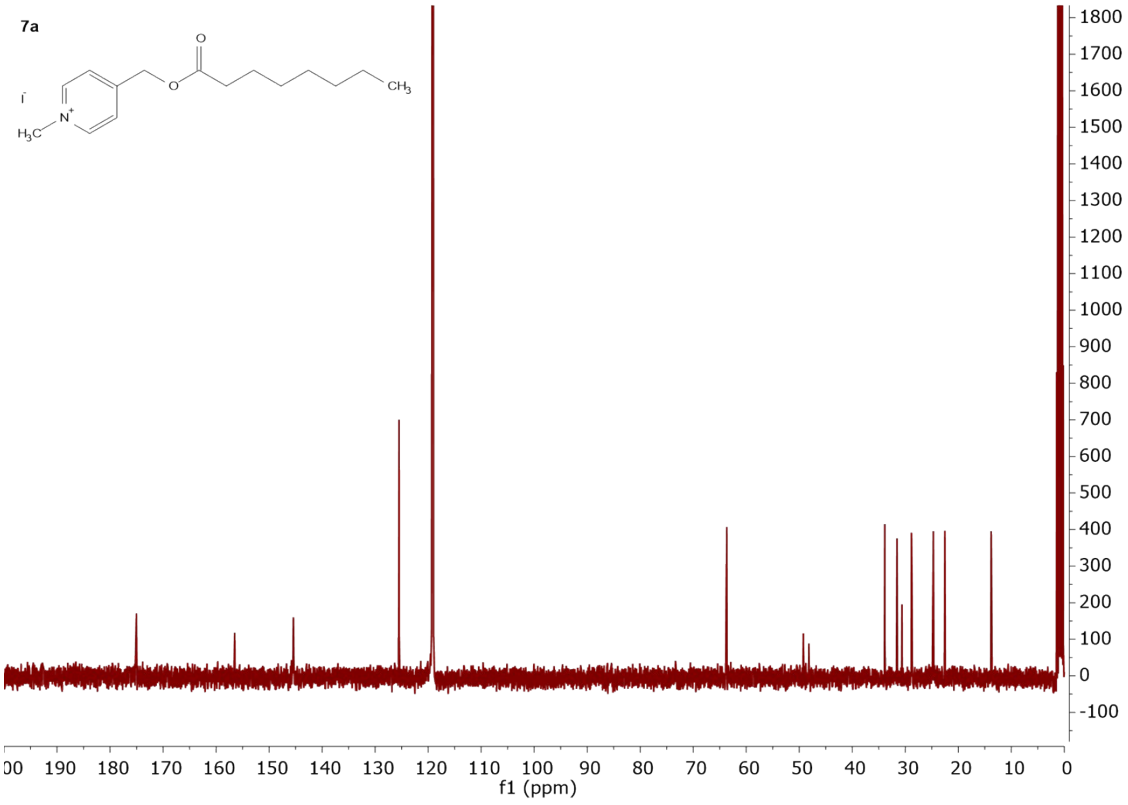

Figure S40. ^{13}C {^{1}H} NMR spectra of compound **7a**.

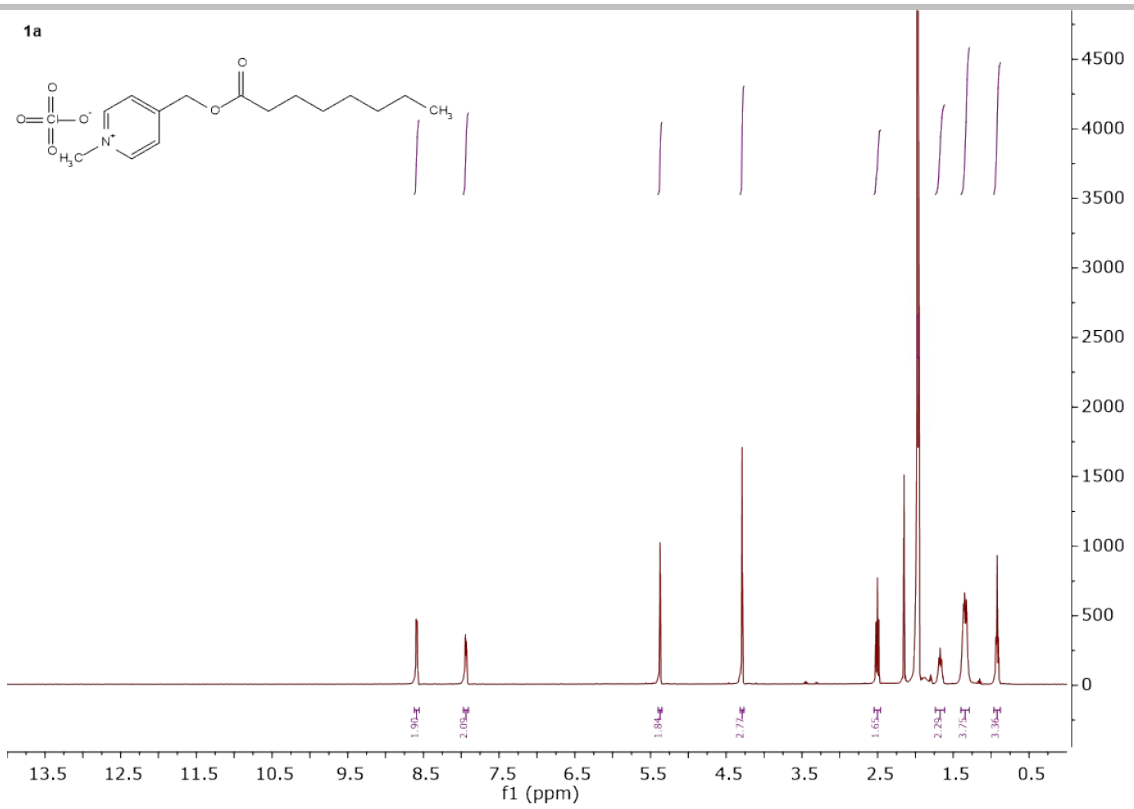

Figure S41. ^{1}HNMR spectra of compound **1a.**

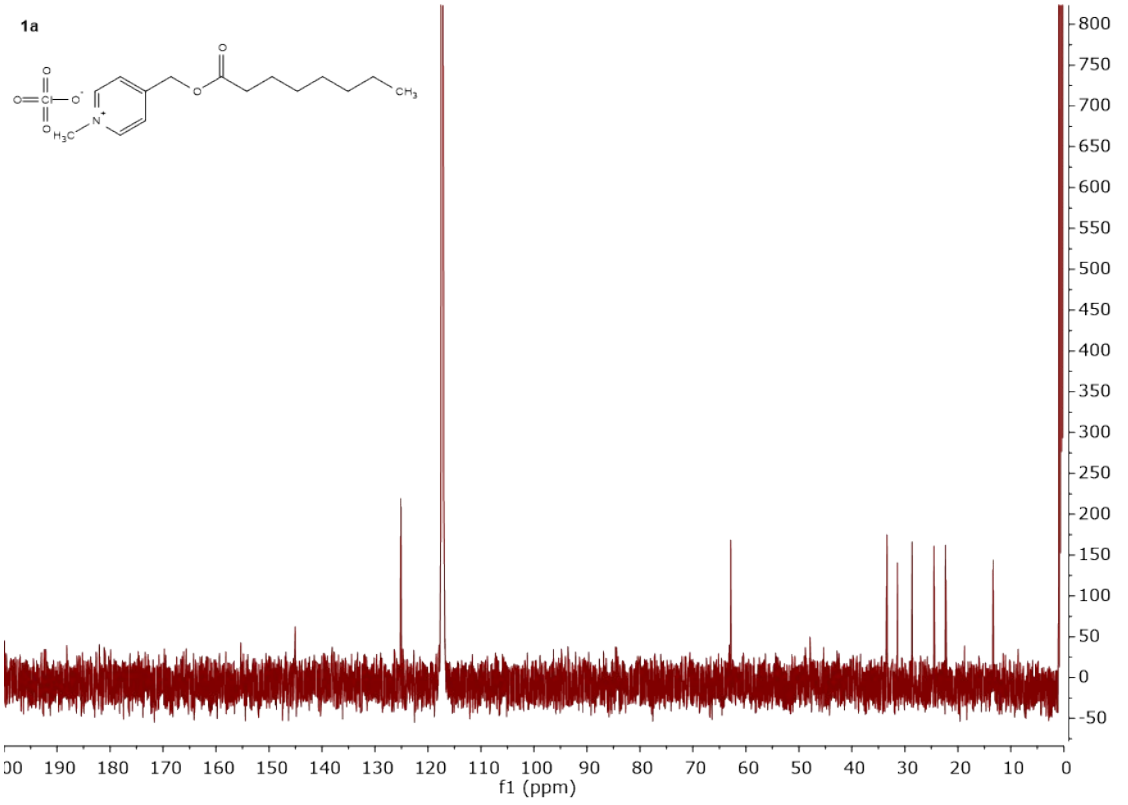

Figure S42. ^{13}C {^{1}H} NMR spectra of compound **1a**.

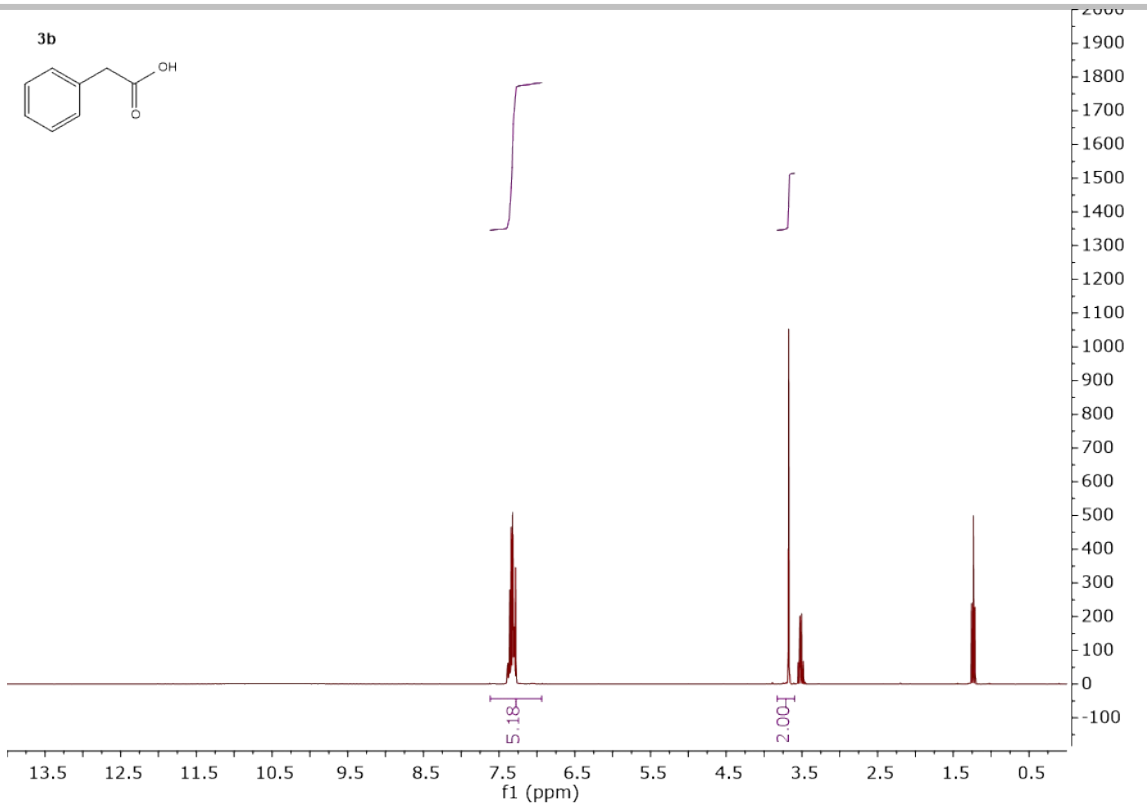

Figure S43. [1]HNMR spectra of compound **3b.**

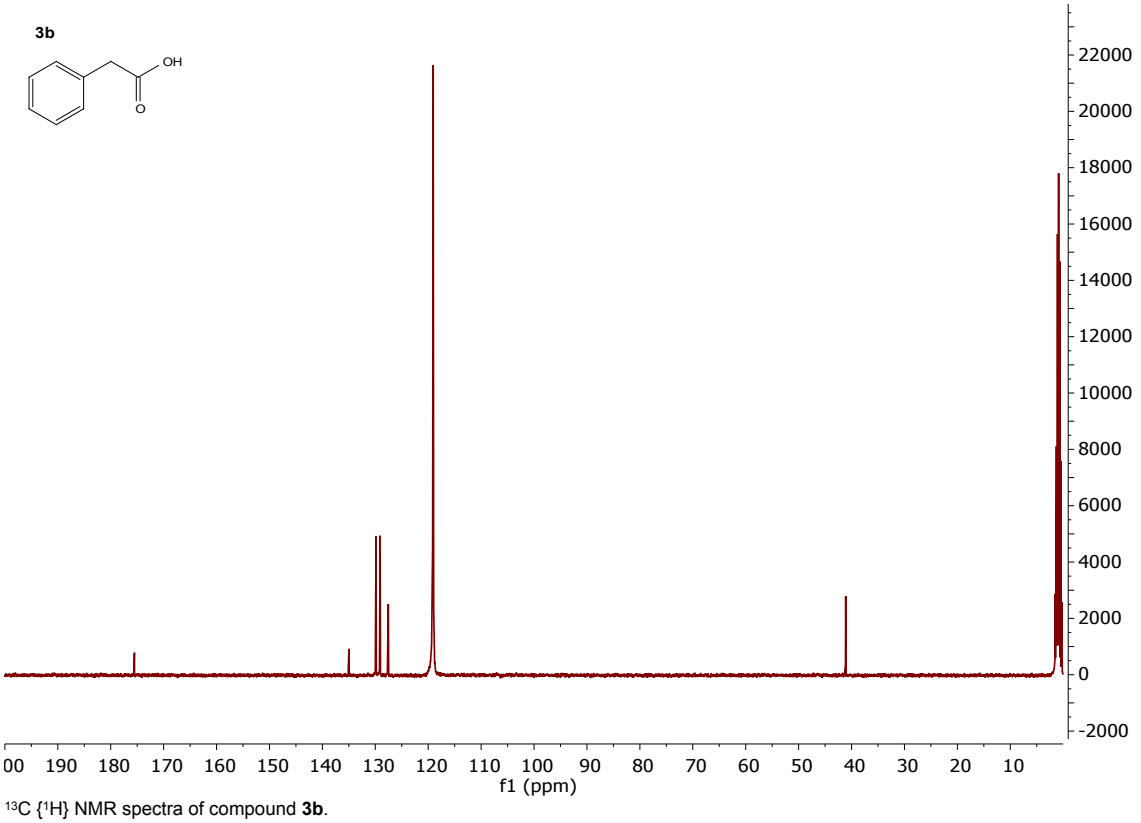

Figure S44. [13]C {[1]H} NMR spectra of compound **3b**.

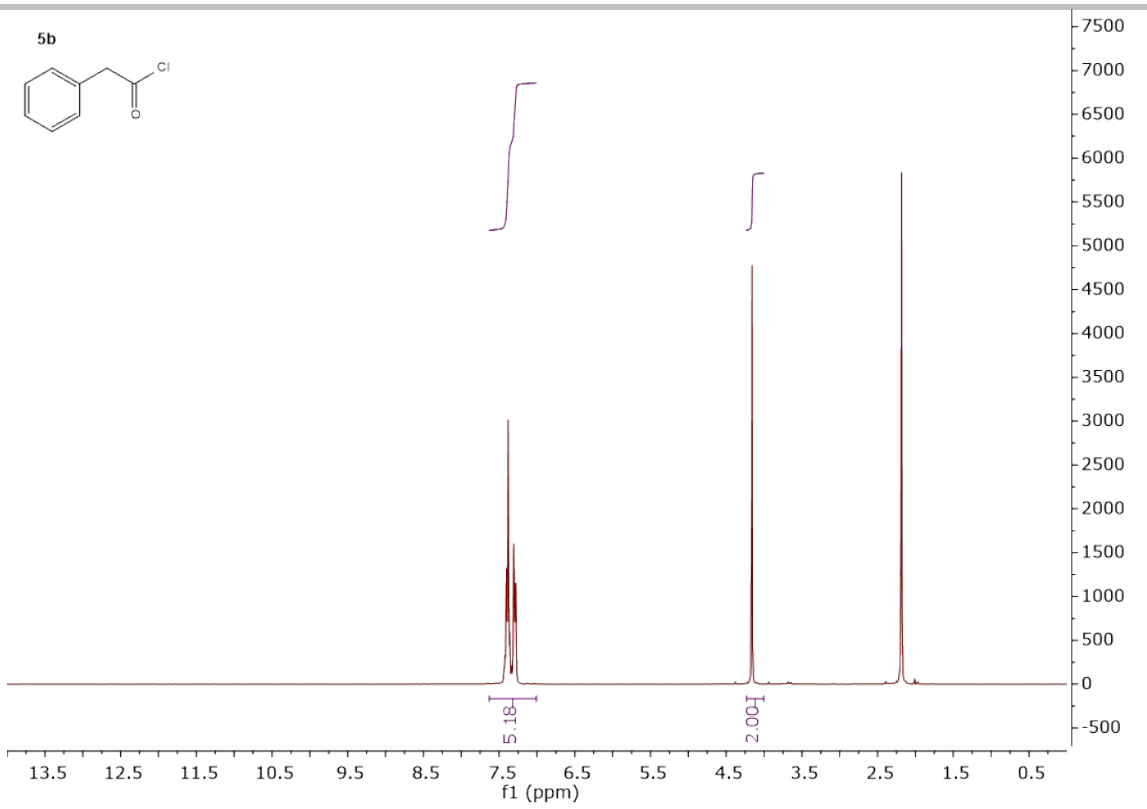

Figure S45. ^{1}HNMR spectra of compound **5b.**

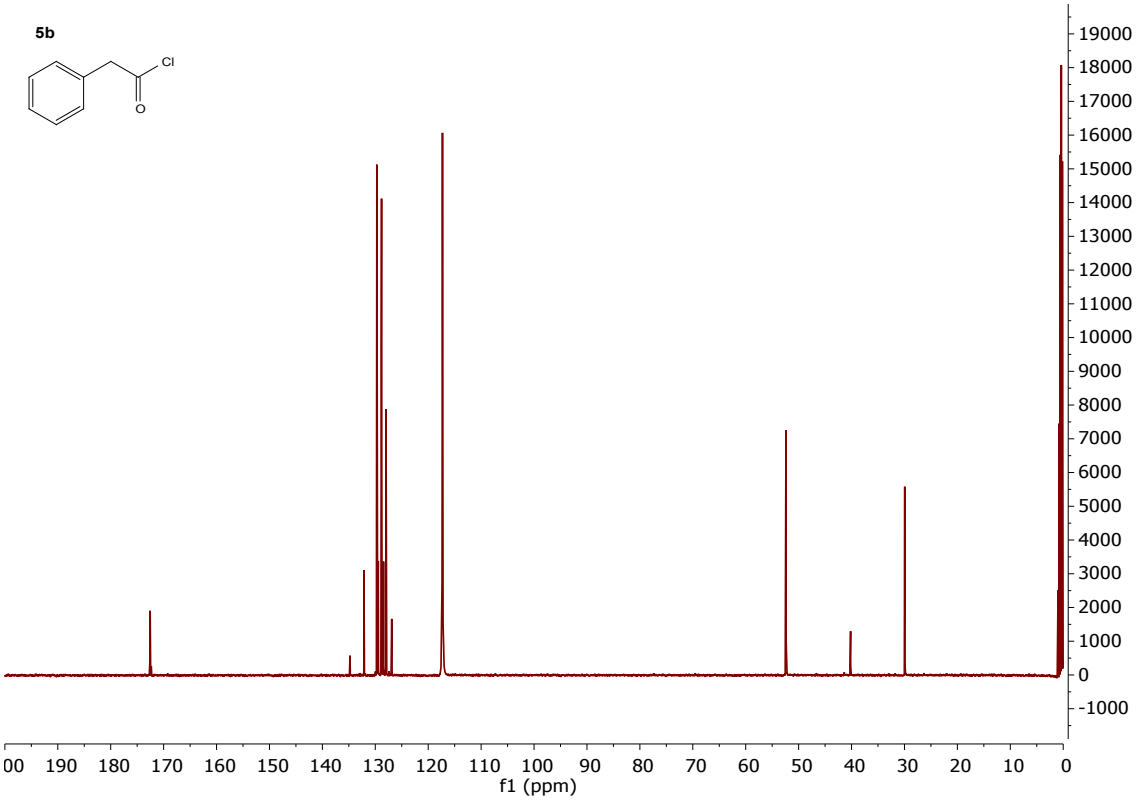

Figure S46. ^{13}C {^{1}H} NMR spectra of compound **5b**.

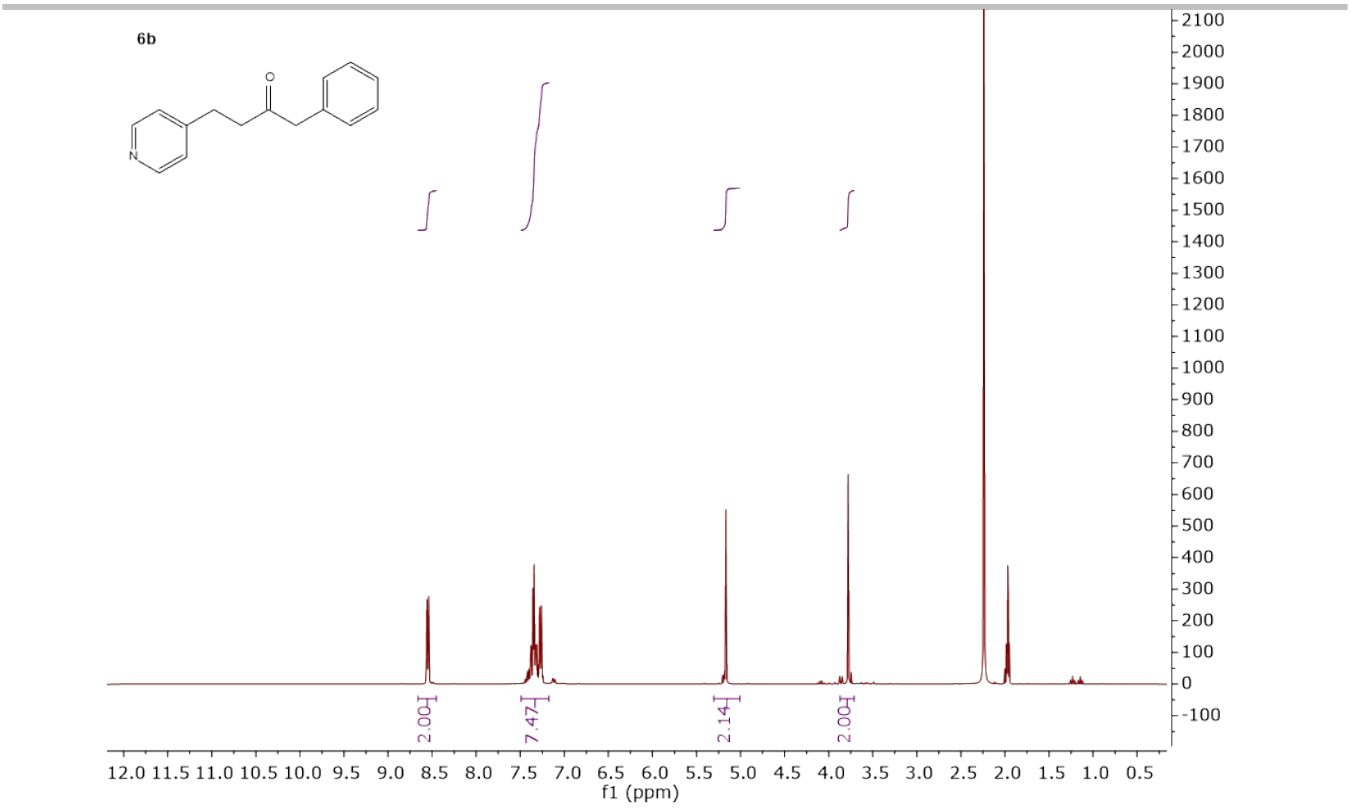

Figure S47. ^{1}HNMR spectra of compound **6b.**

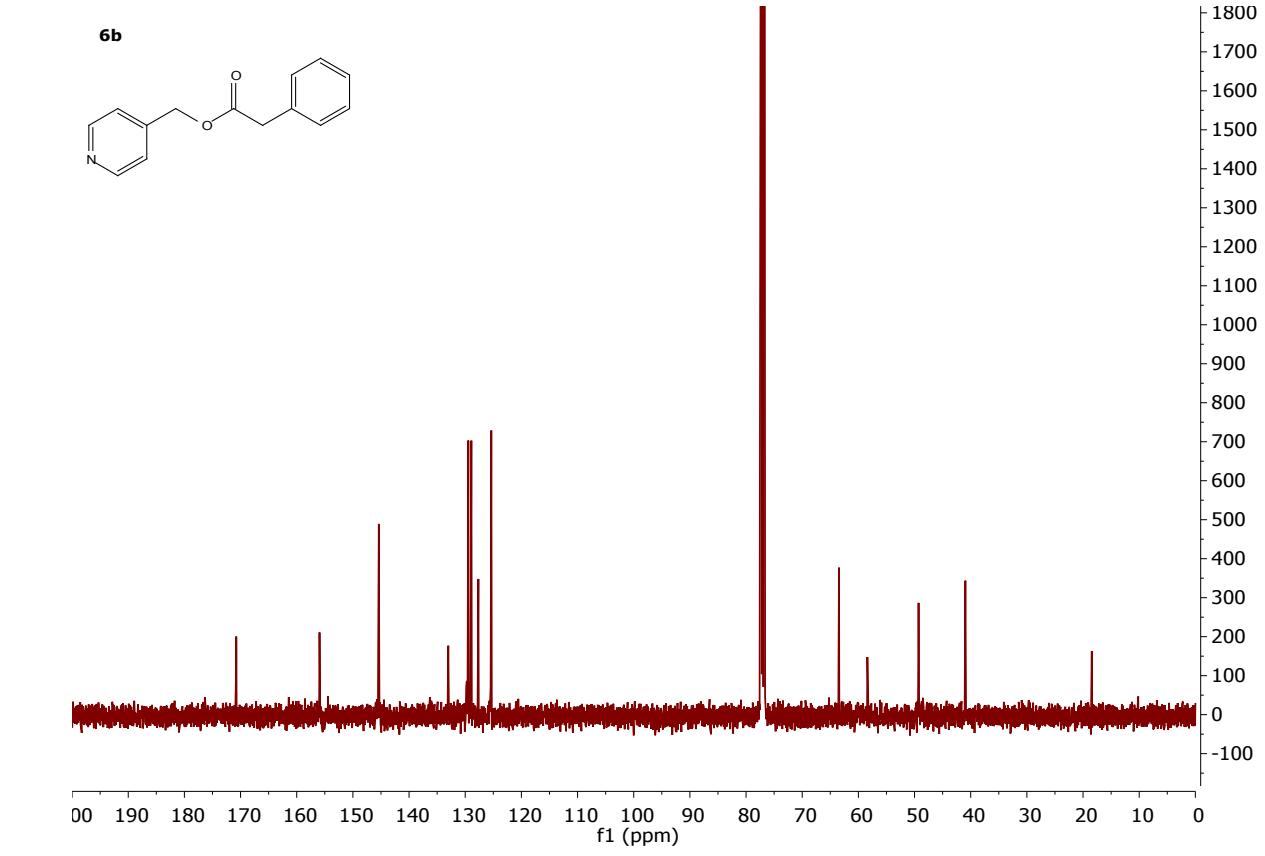

Figure S48. ^{13}C {^{1}H} NMR spectra of compound **6b**.

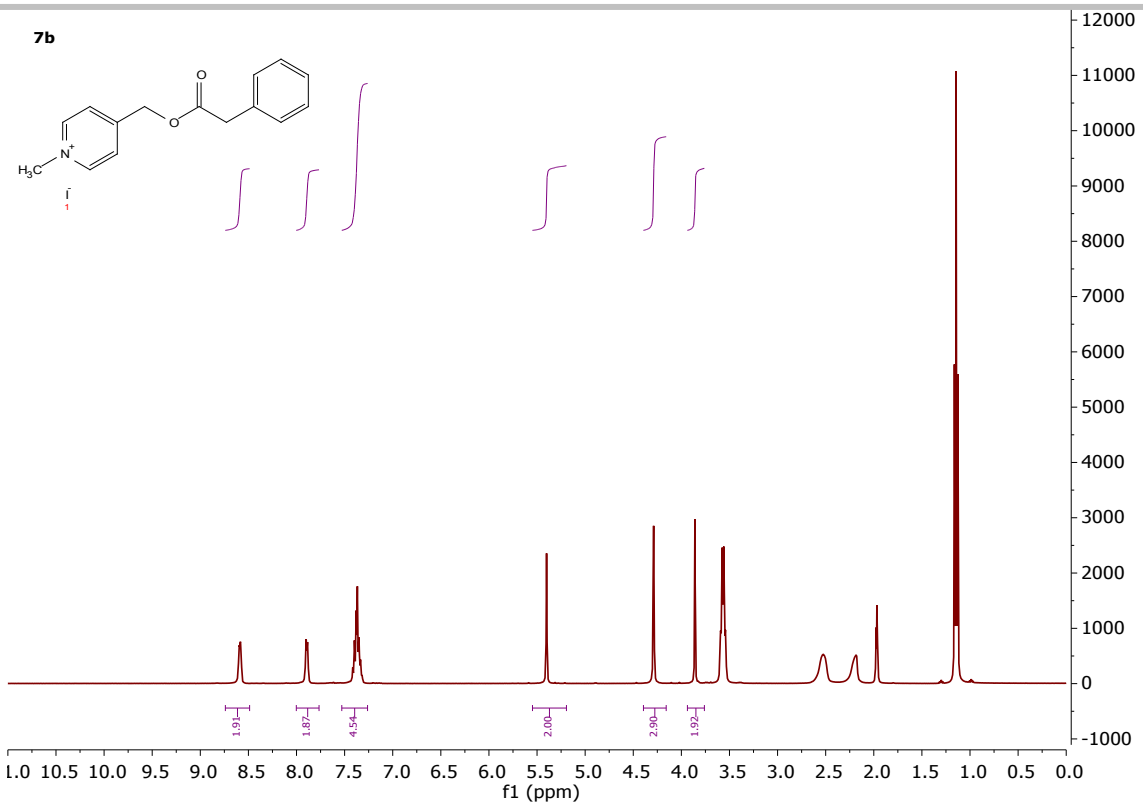

Figure S49. ^{1}HNMR spectra of compound **7b.**

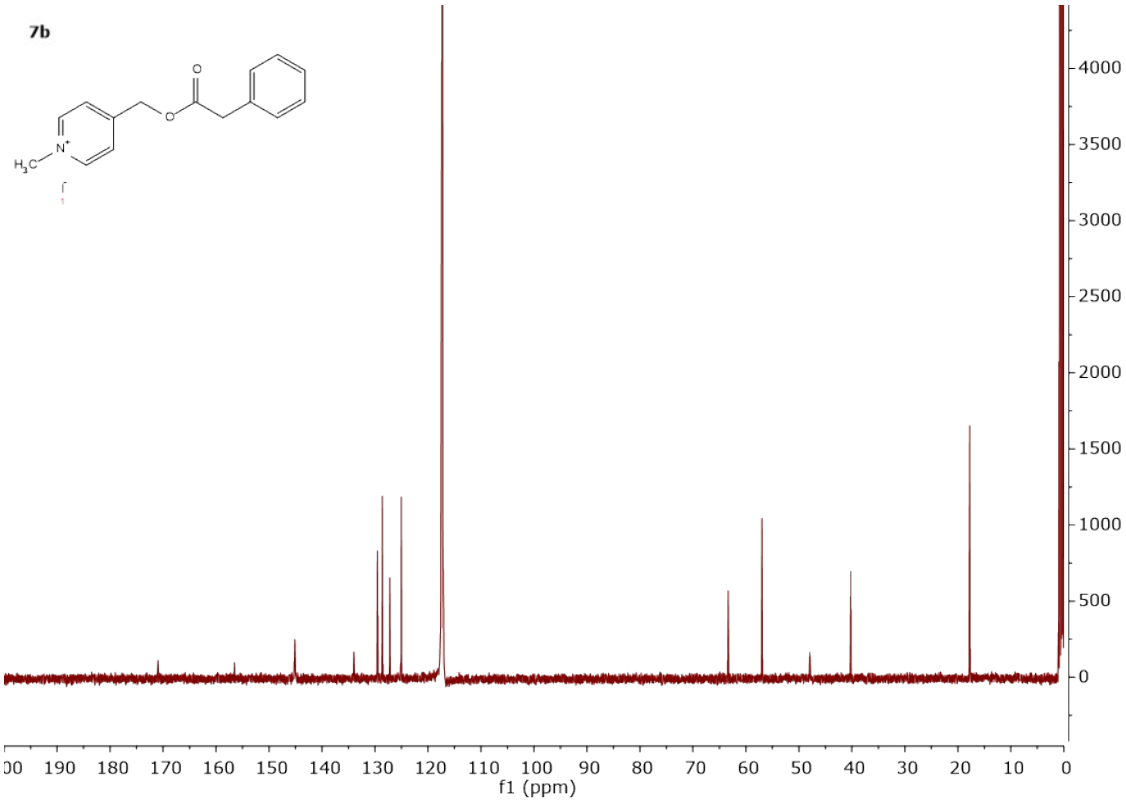

Figure S50. ^{13}C {^{1}H} NMR spectra of compound **7b**.

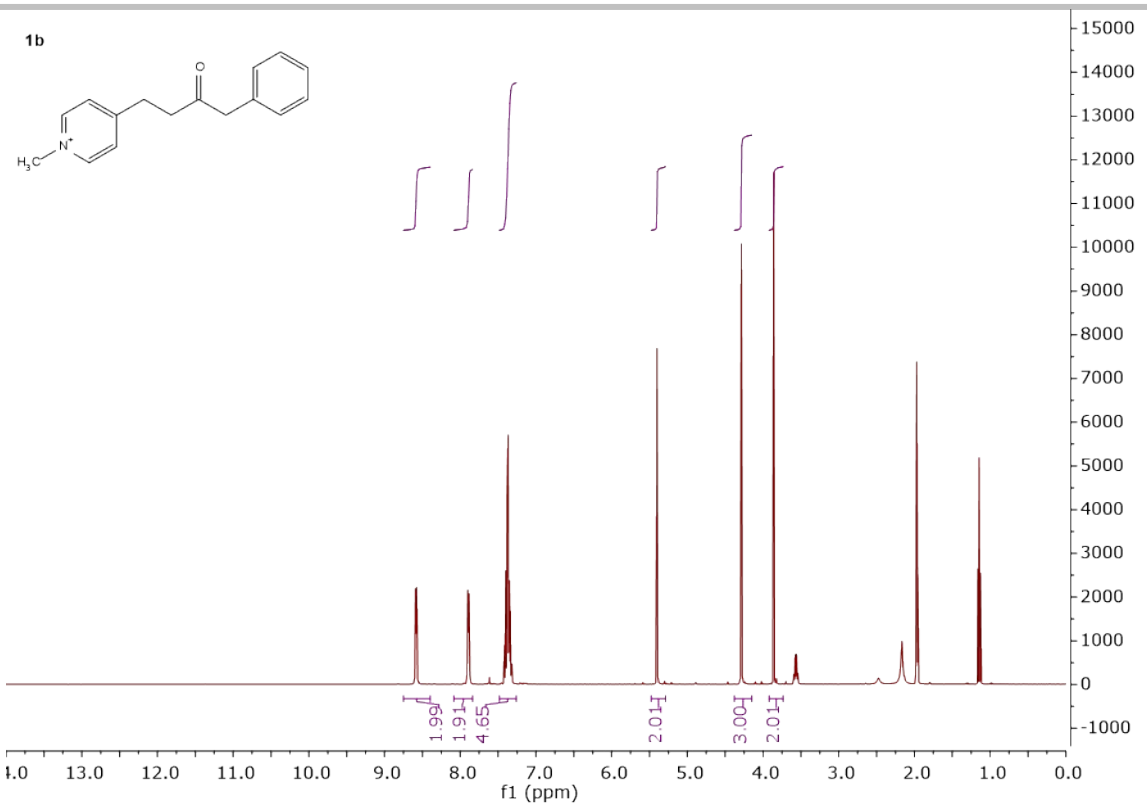

Figure S51. ^{1}HNMR spectra of compound **1b.**

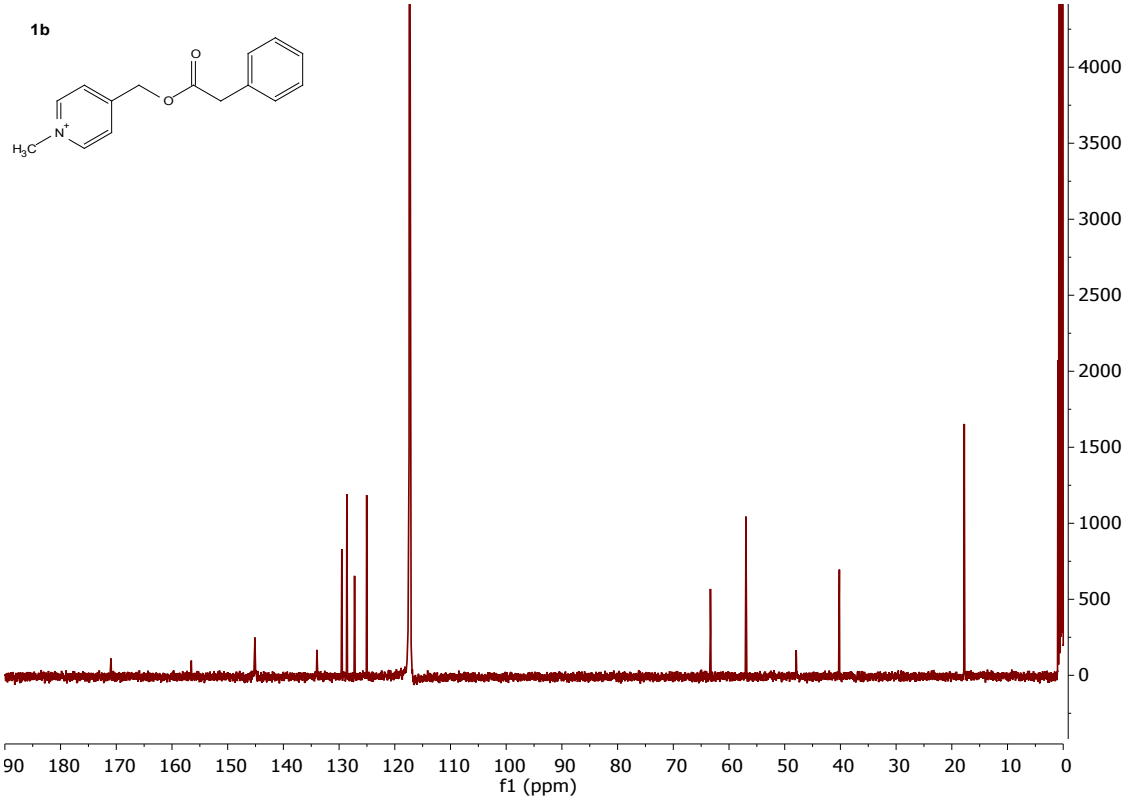

Figure S52. ^{13}C {^{1}H} NMR spectra of compound **1b**.

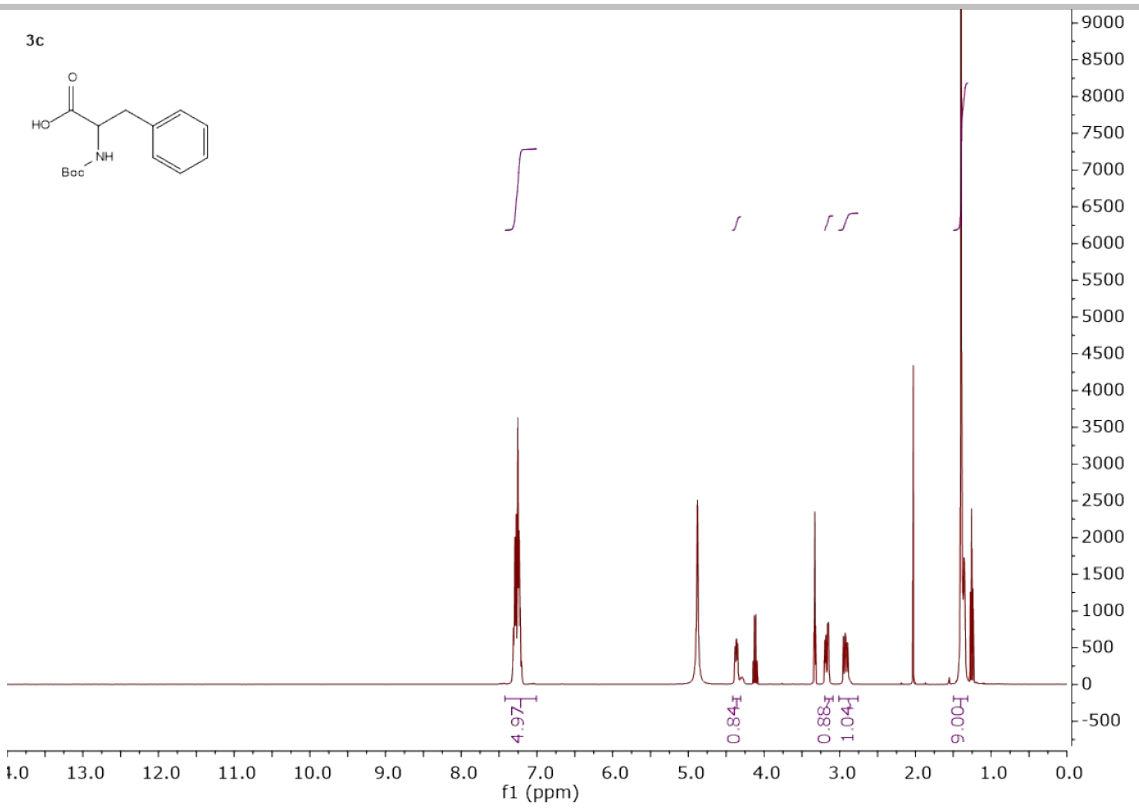

Figure S53. ^{1}HNMR spectra of compound **3c.**

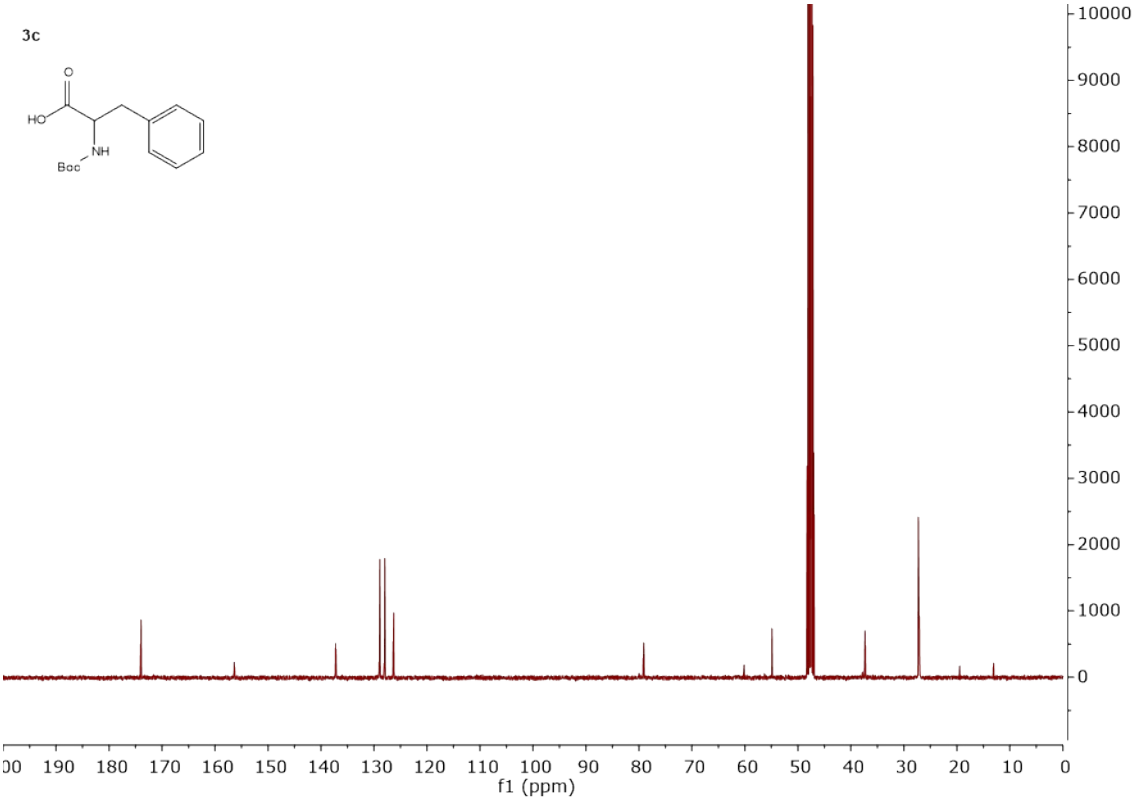

Figure S54. ^{13}C {^{1}H} NMR spectra of compound **3c**.

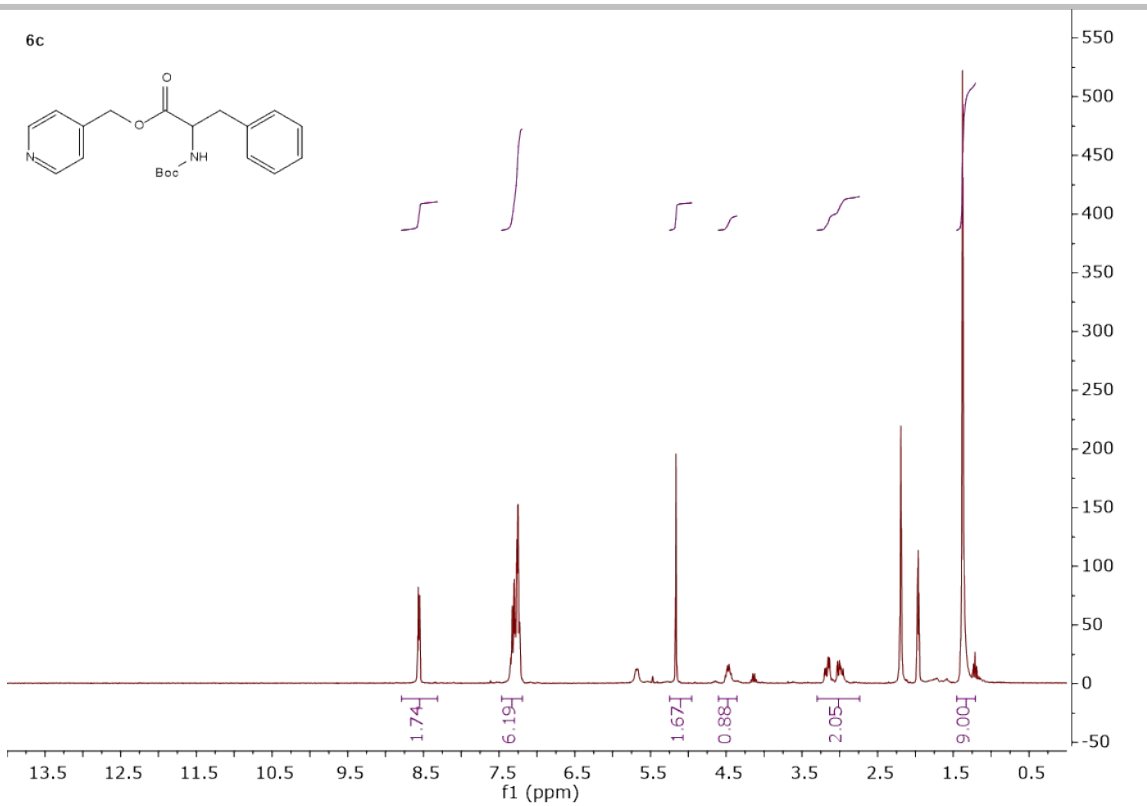

Figure S55. ^{1}HNMR spectra of compound **6c.**

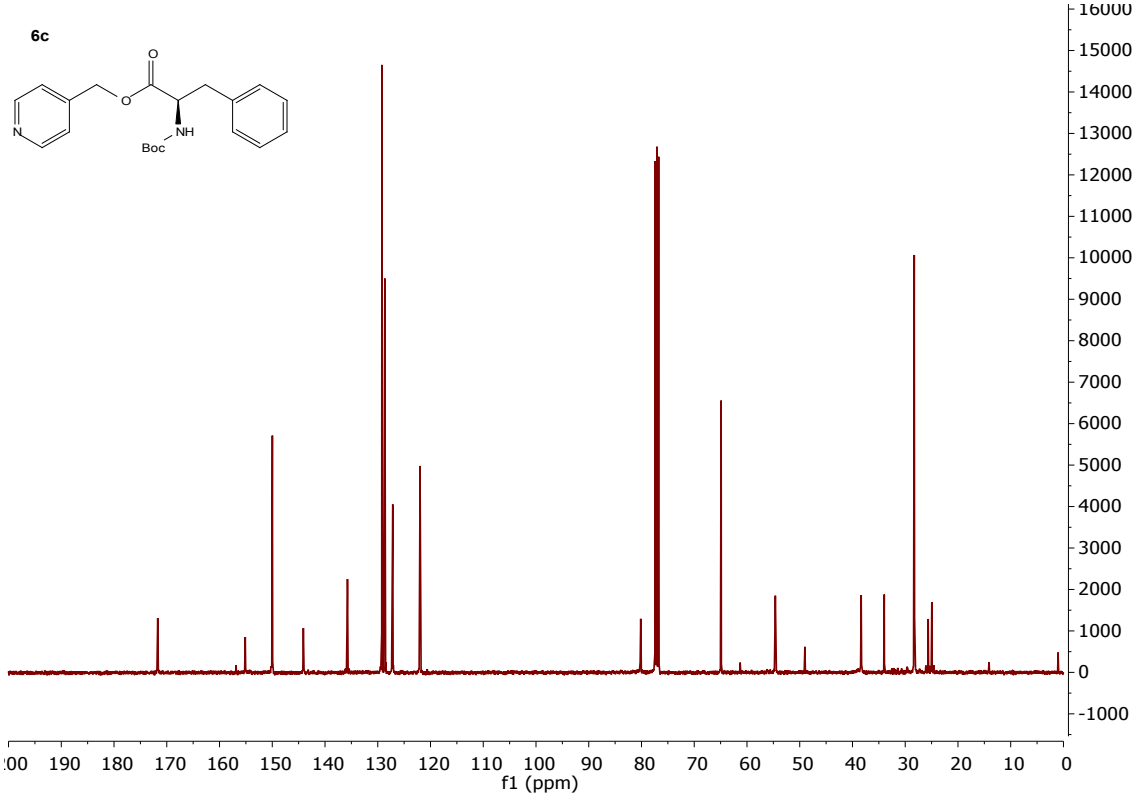

Figure S56. ^{13}C {^{1}H} NMR spectra of compound **6c**.

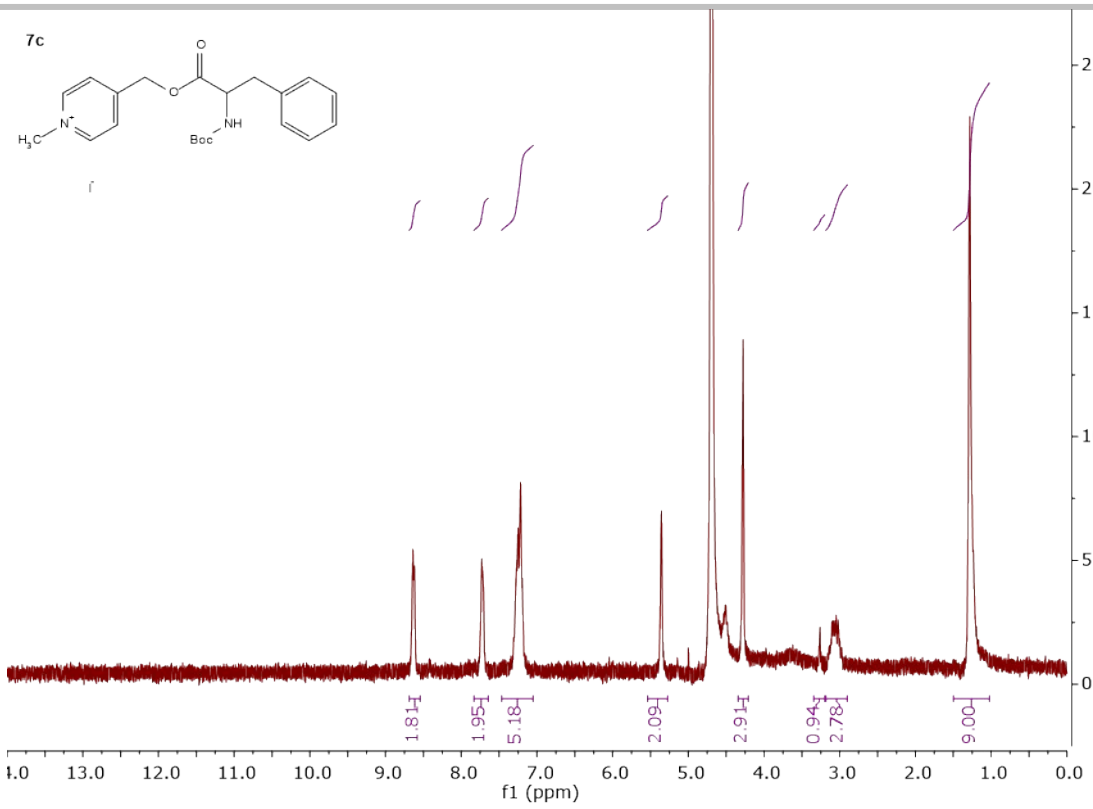

Figure S57. ^{1}HNMR spectra of compound **7c.**

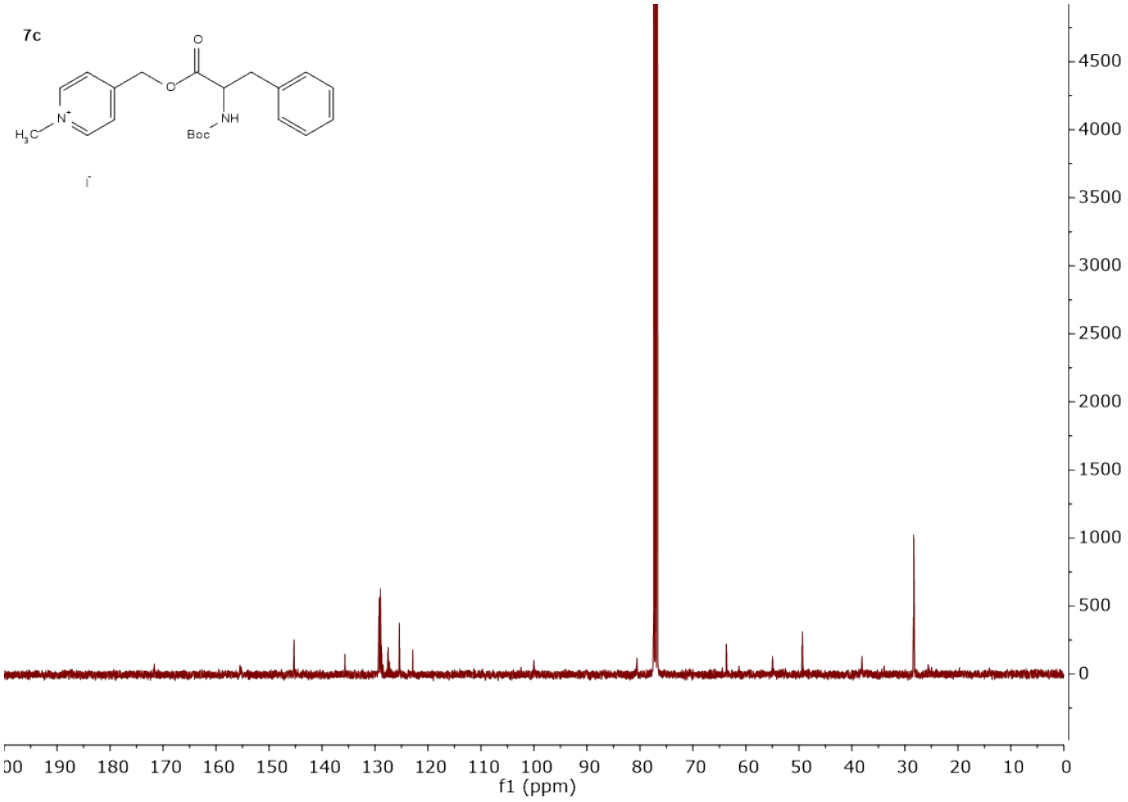

Figure S58. ^{13}C {^{1}H} NMR spectra of compound **7c**.

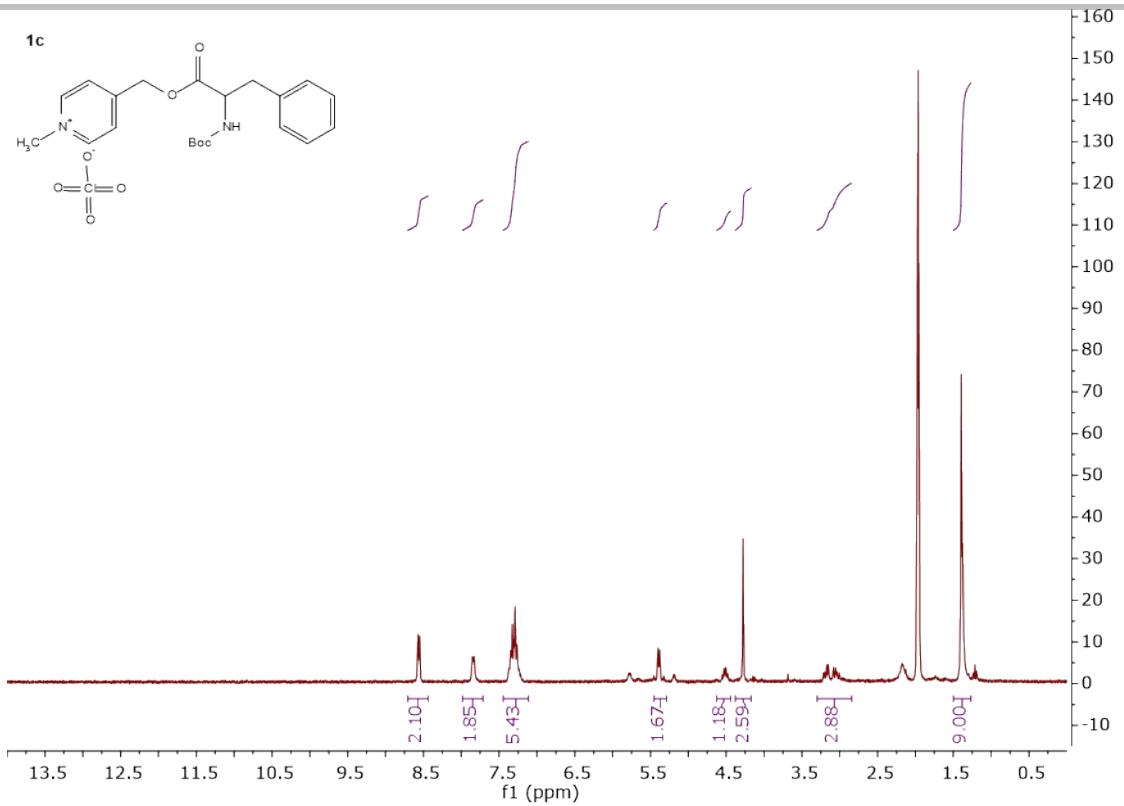

Figure S59. ^{1}HNMR spectra of compound **1c.**

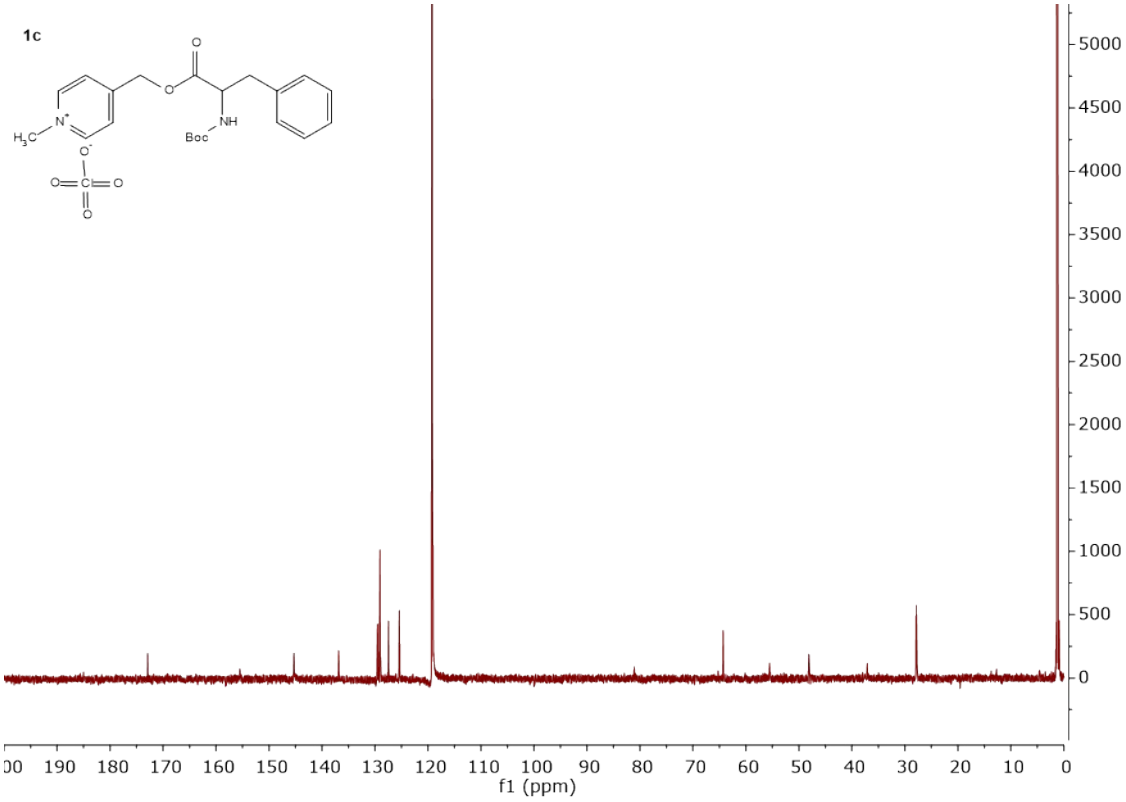

Figure S60. ^{13}C {^{1}H} NMR spectra of compound **1c**.

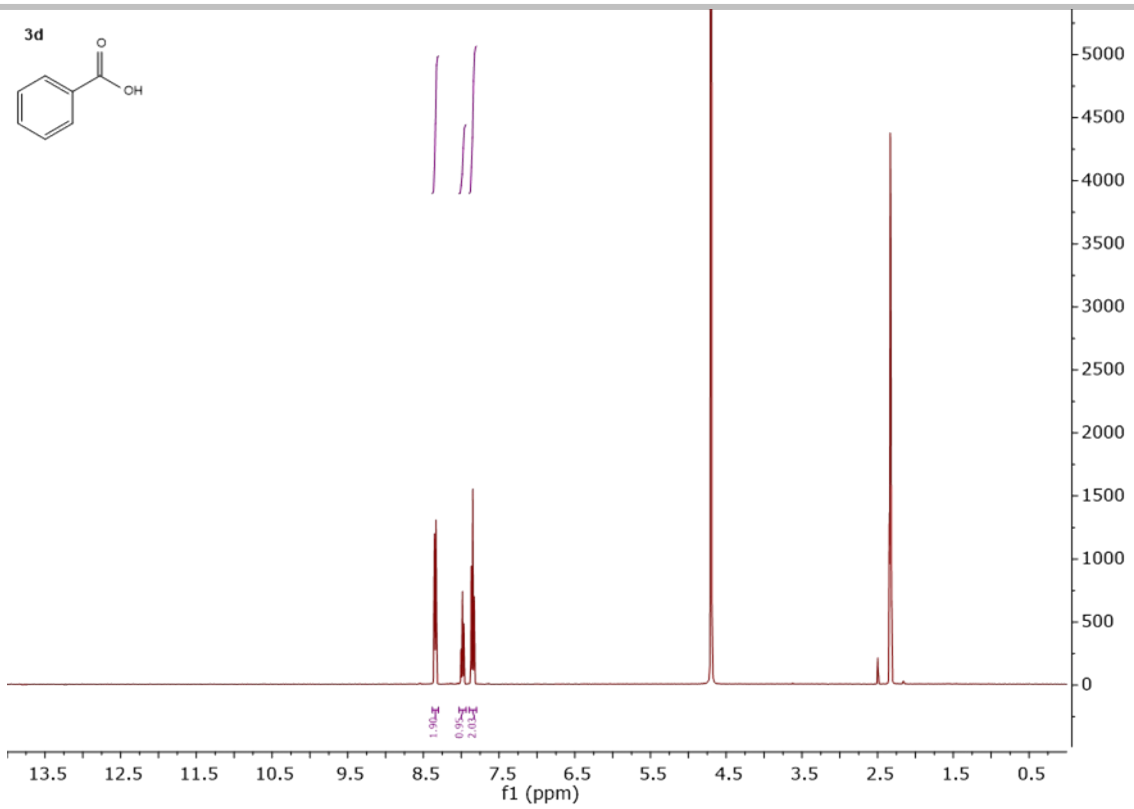

Figure S61. ^{1}HNMR spectra of compound **3d.**

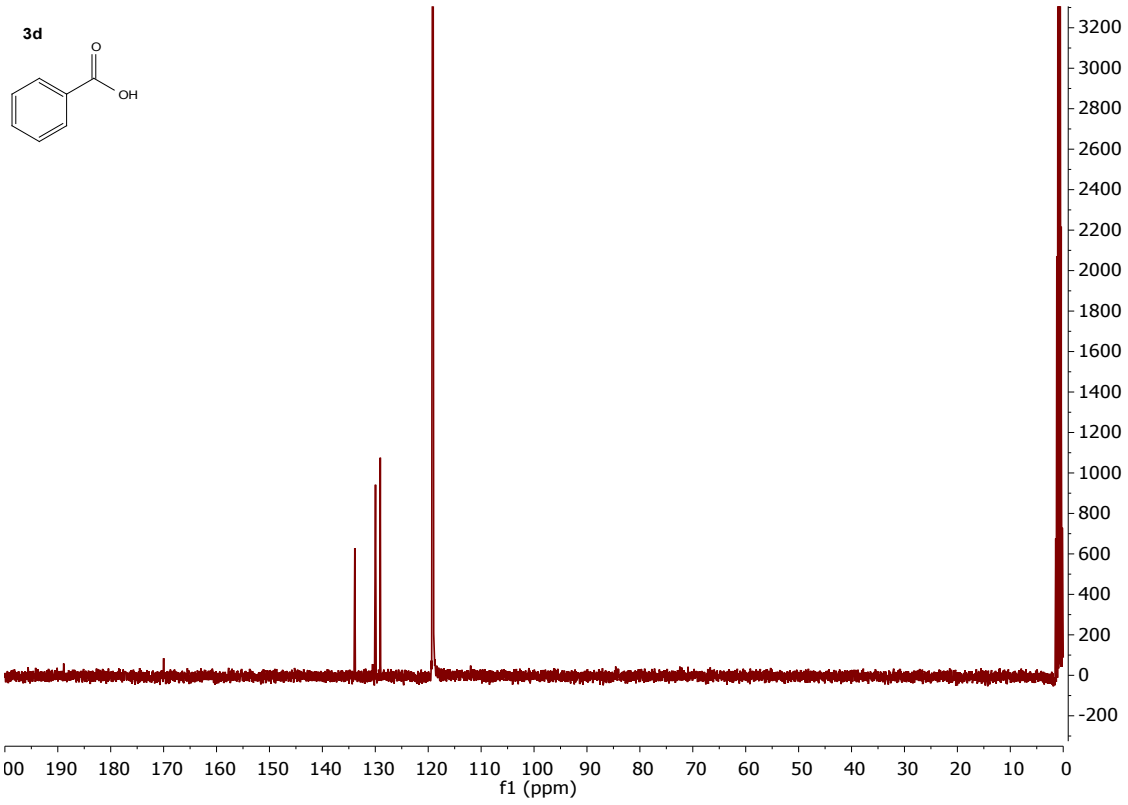

Figure S62. ^{13}C {^{1}H} NMR spectra of compound **3d**.

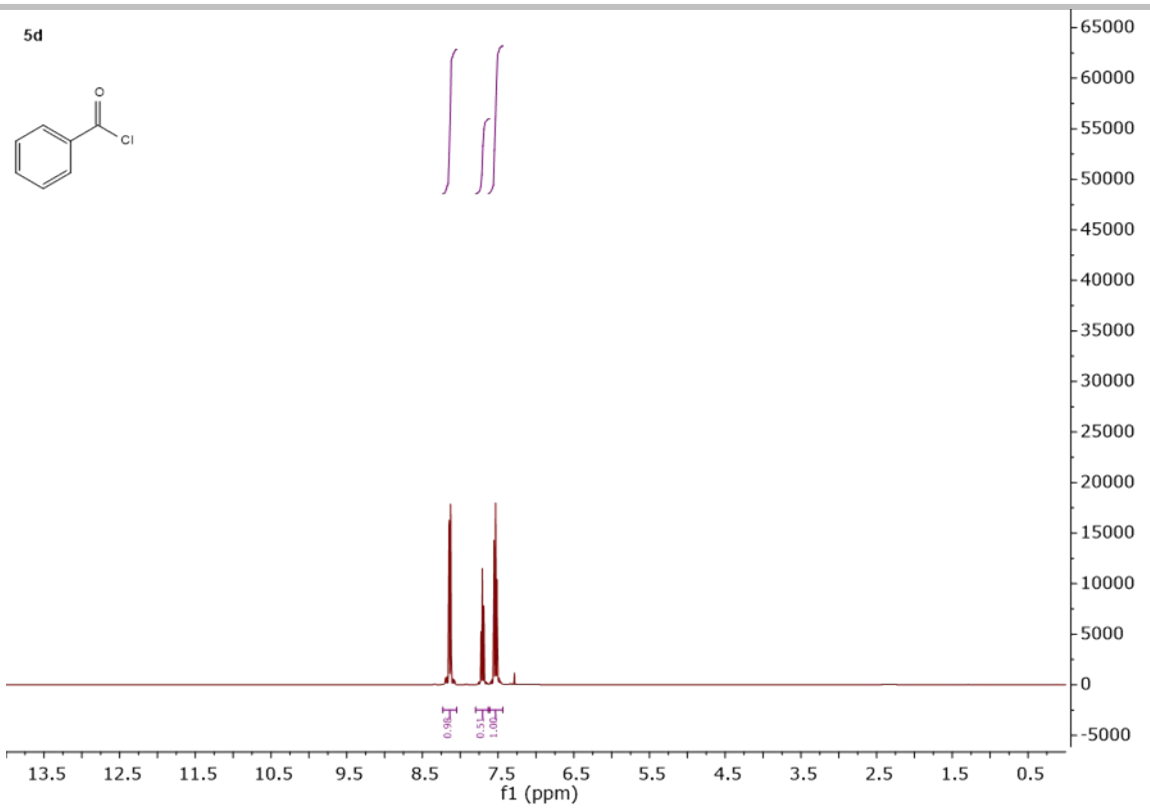

Figure S63. ^{1}HNMR spectra of compound **5d.**

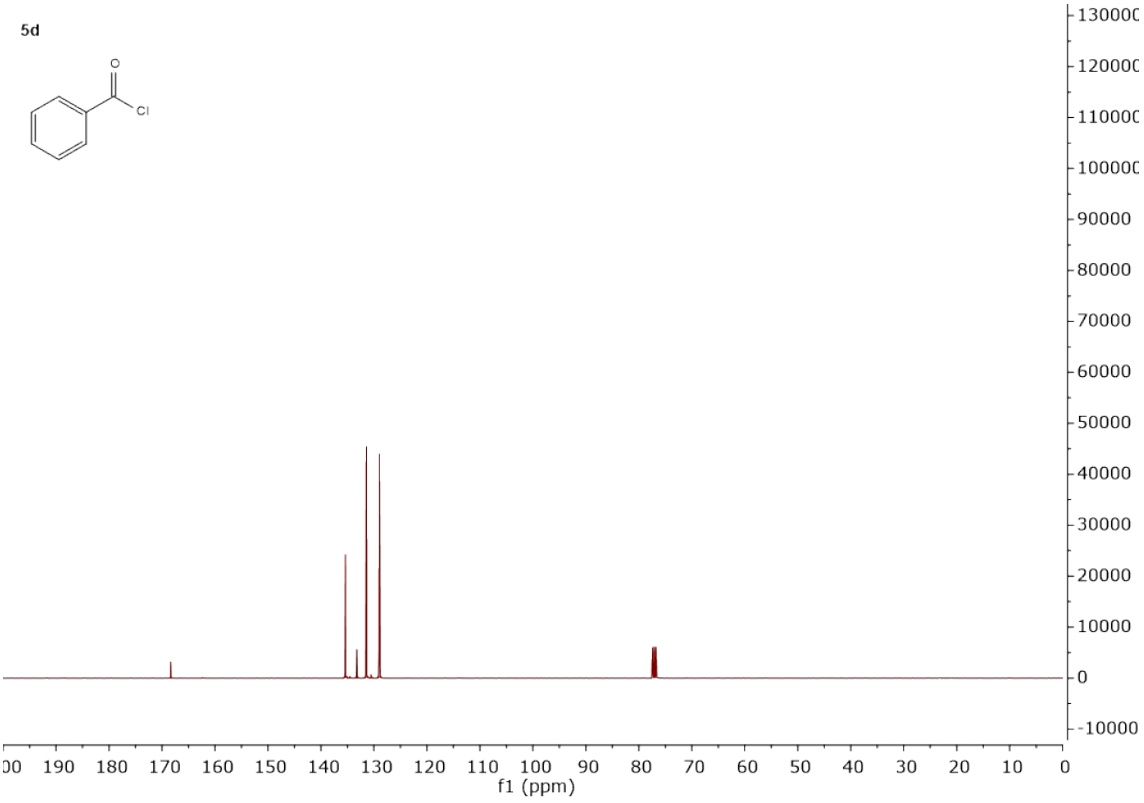

Figure S64. ^{13}C {^{1}H} NMR spectra of compound **5d**.

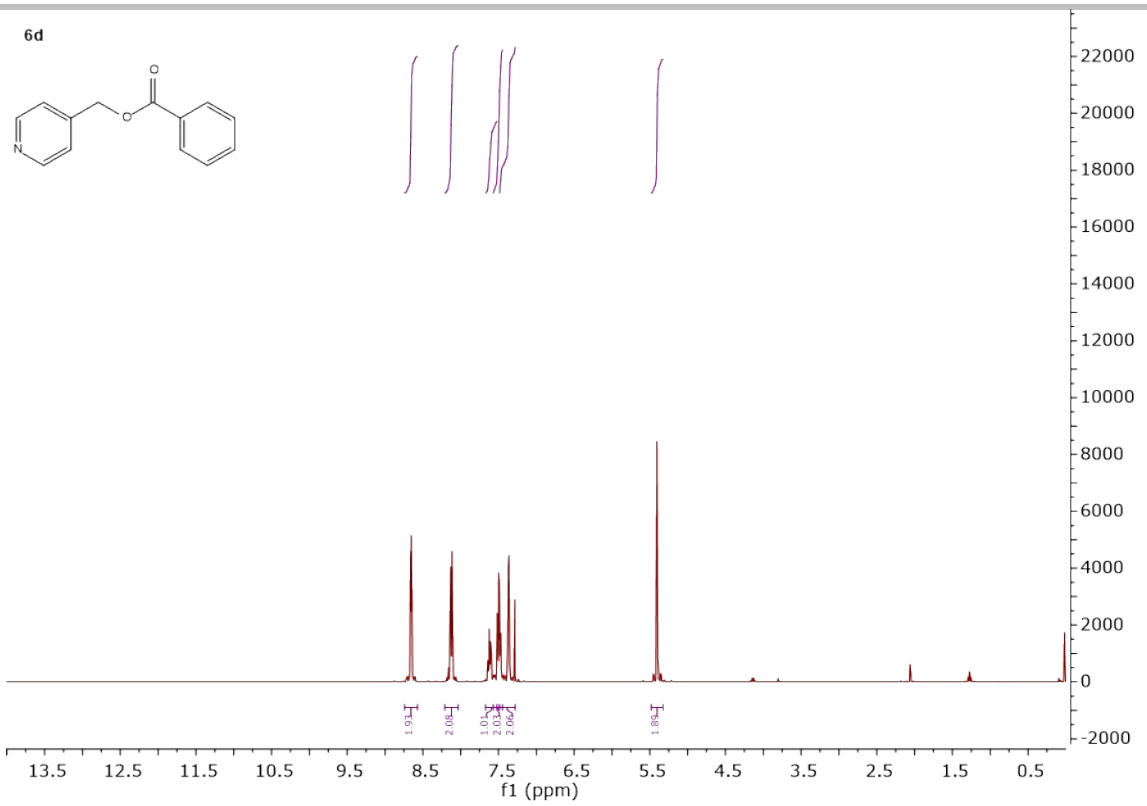

Figure S65. ^{1}HNMR spectra of compound **6d.**

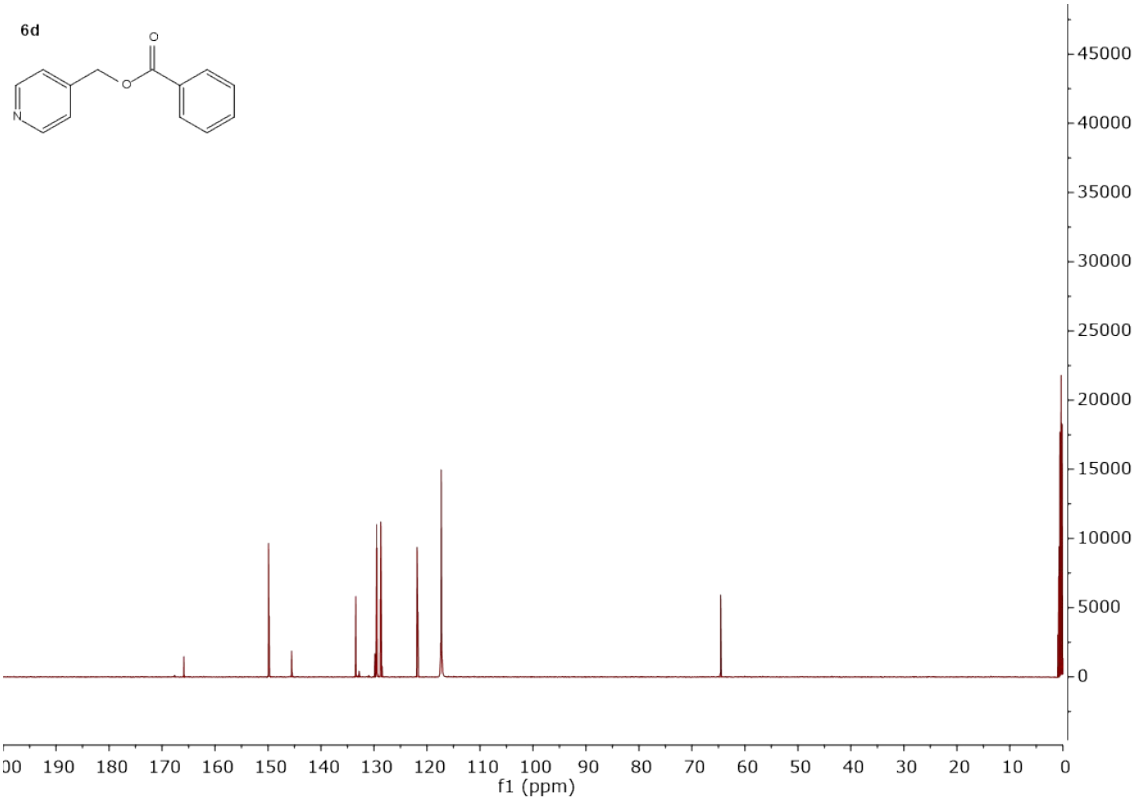

Figure S66. ^{13}C {^{1}H} NMR spectra of compound **6d**.

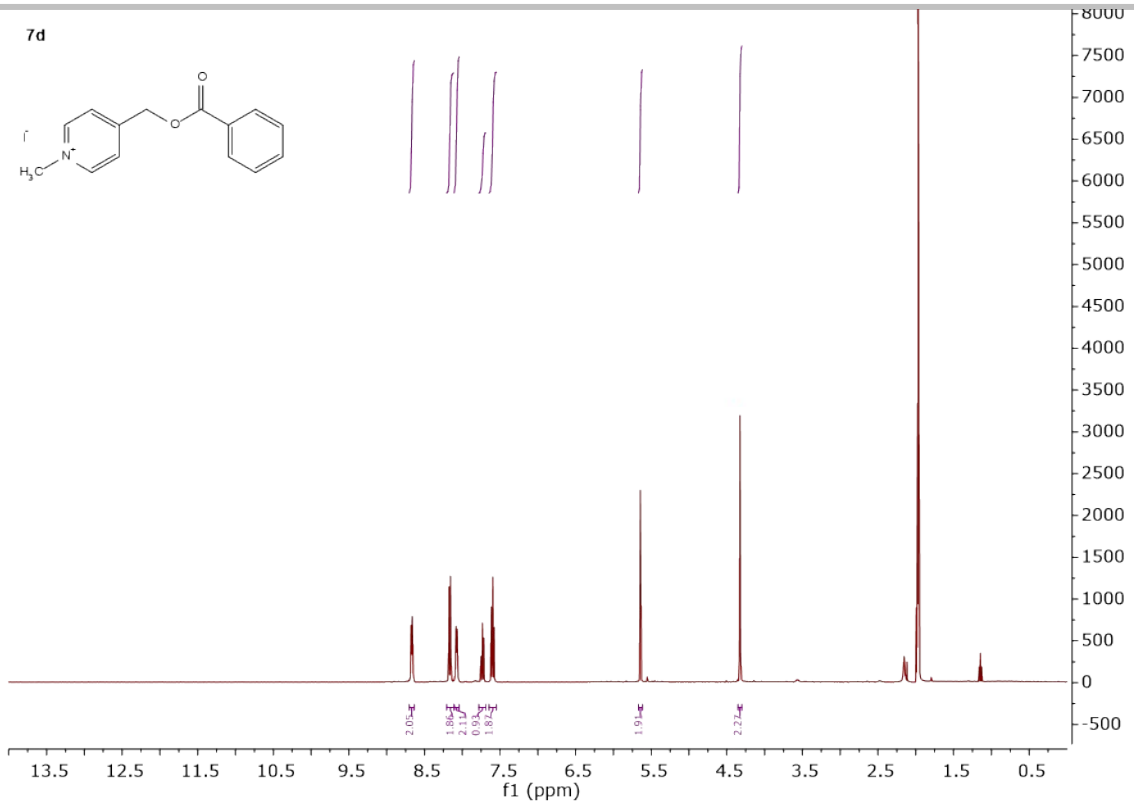

Figure S67. ^{1}HNMR spectra of compound **7d.**

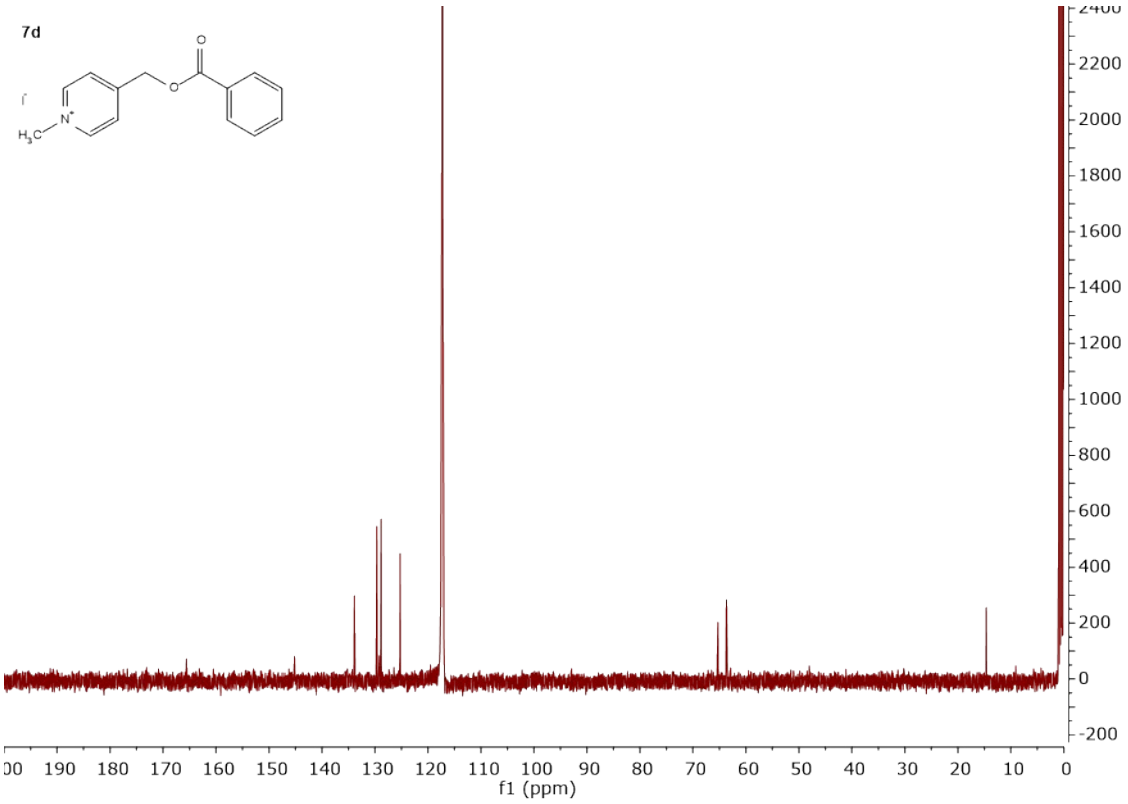

Figure S68. ^{13}C {^{1}H} NMR spectra of compound **7d**.

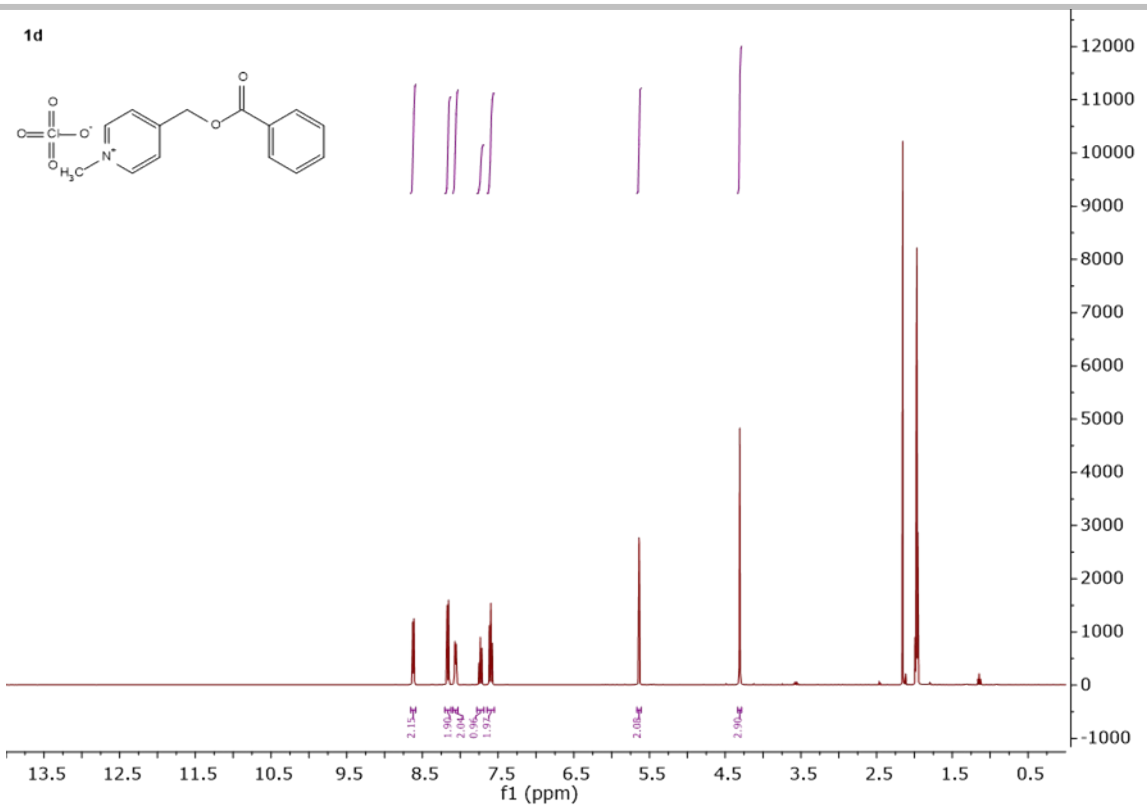

Figure S69. ^{1}HNMR spectra of compound **1d.**

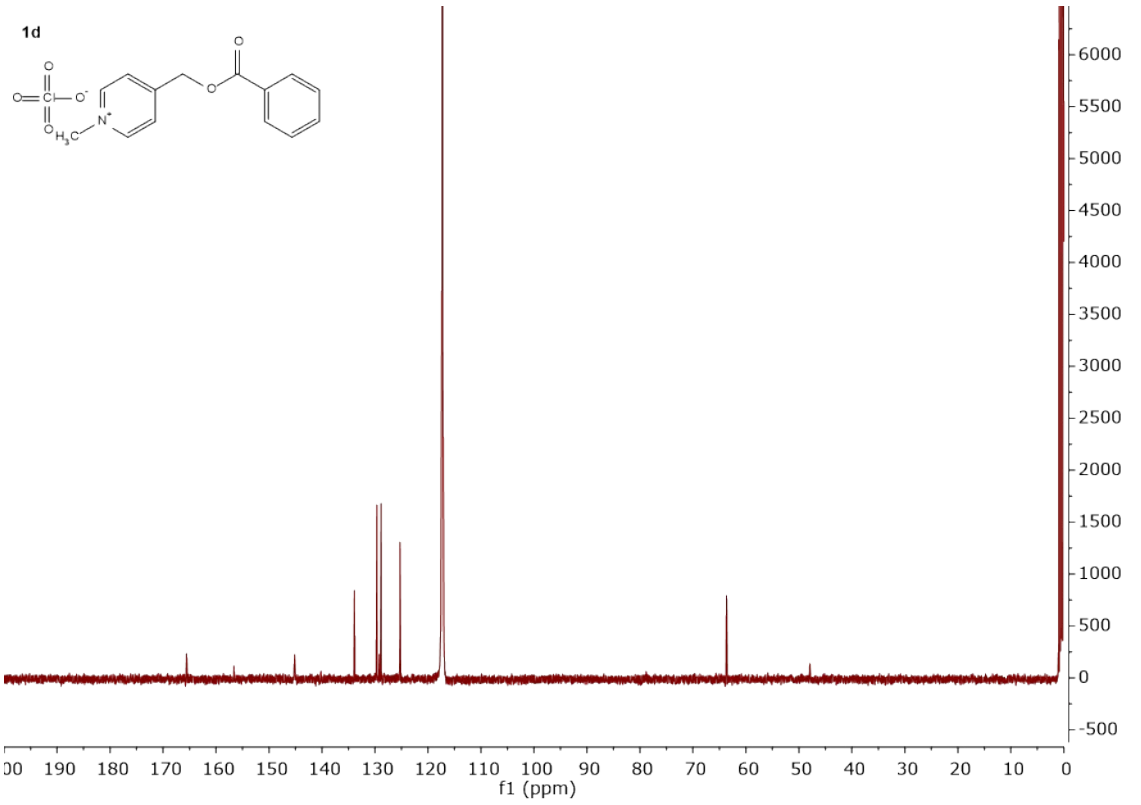

Figure S70. ^{13}C {^{1}H} NMR spectra of compound **1d**.

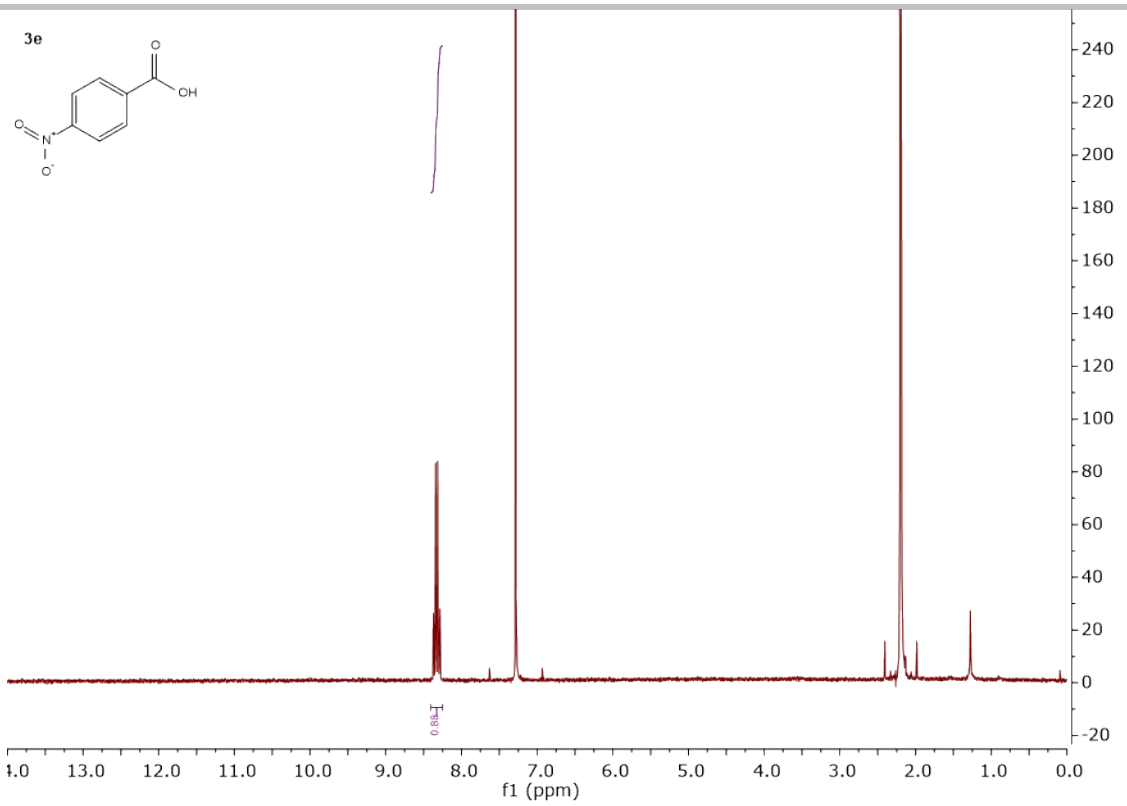

Figure S71. ^{1}HNMR spectra of compound **3e.**

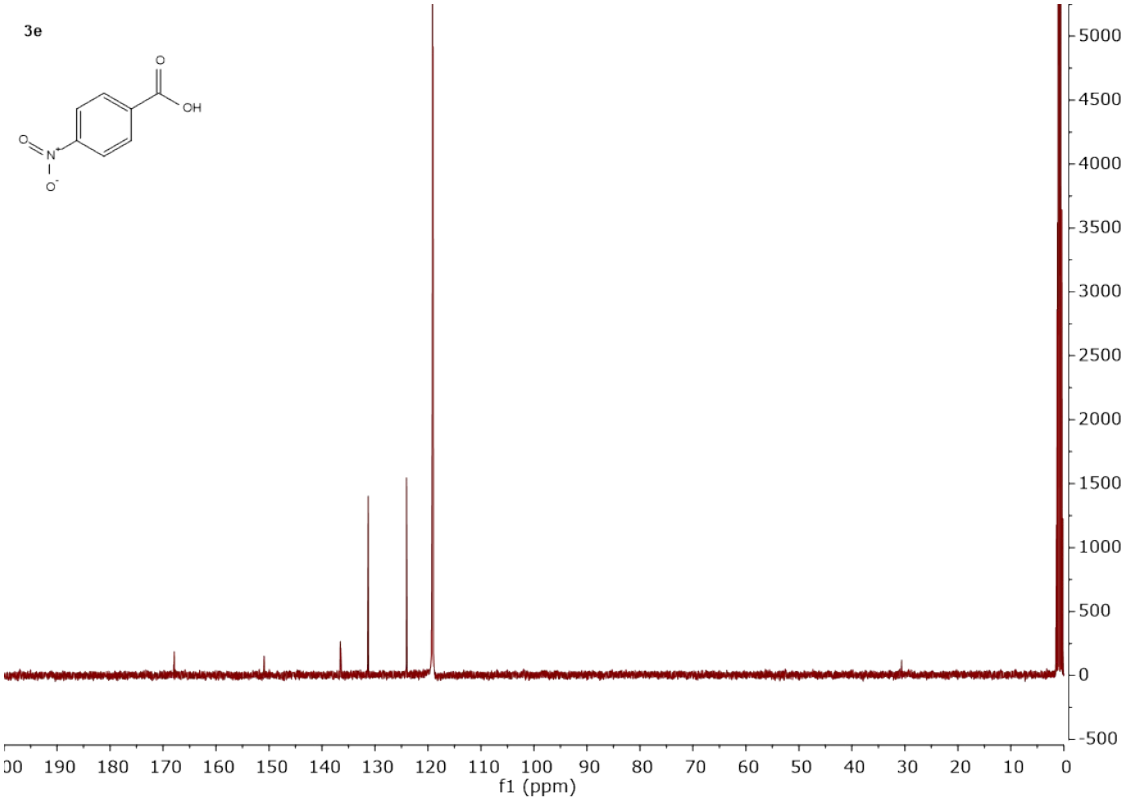

Figure S72. ^{13}C {^{1}H} NMR spectra of compound **3e**.

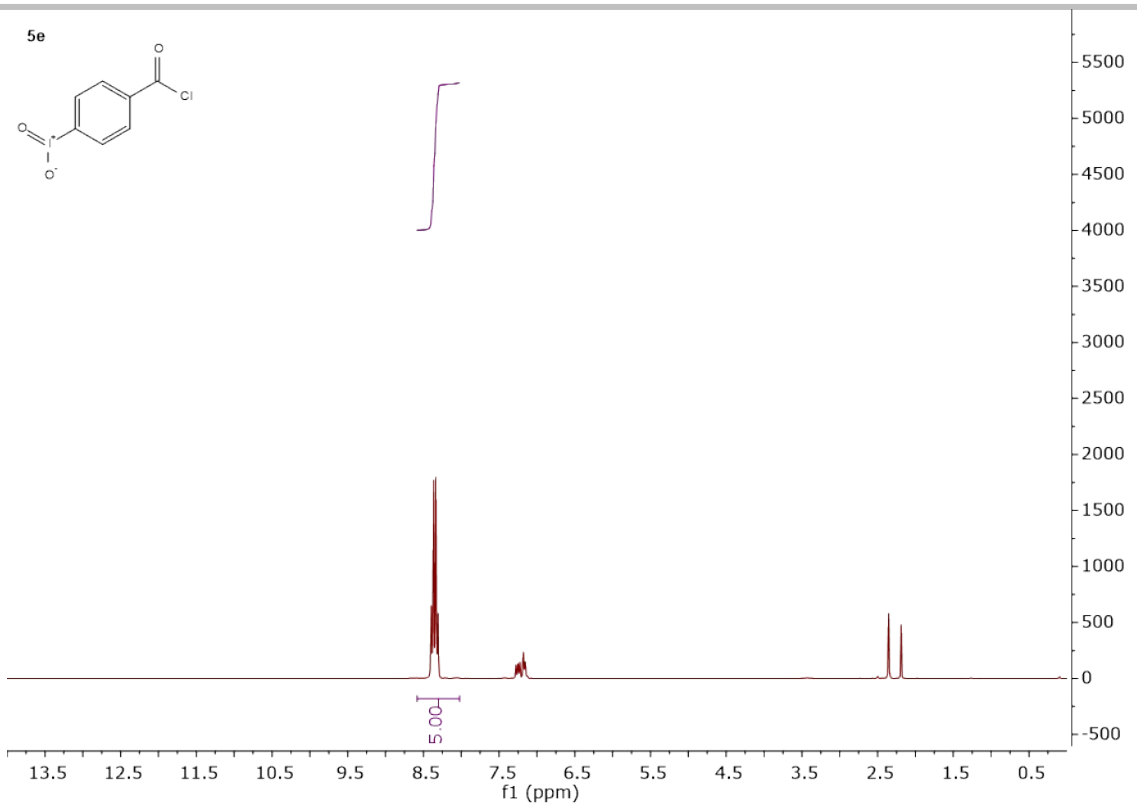

Figure S73. ^{1}HNMR spectra of compound **5e.**

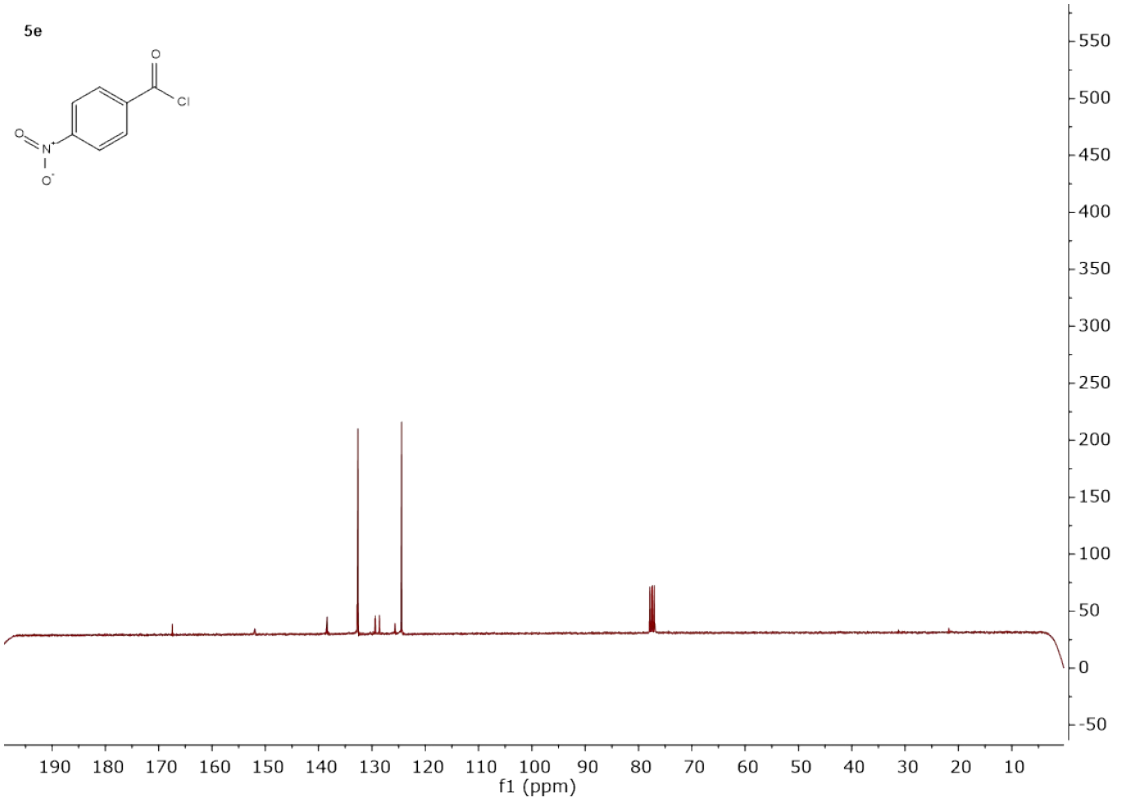

Figure S74. ^{13}C {^{1}H} NMR spectra of compound **5e**.

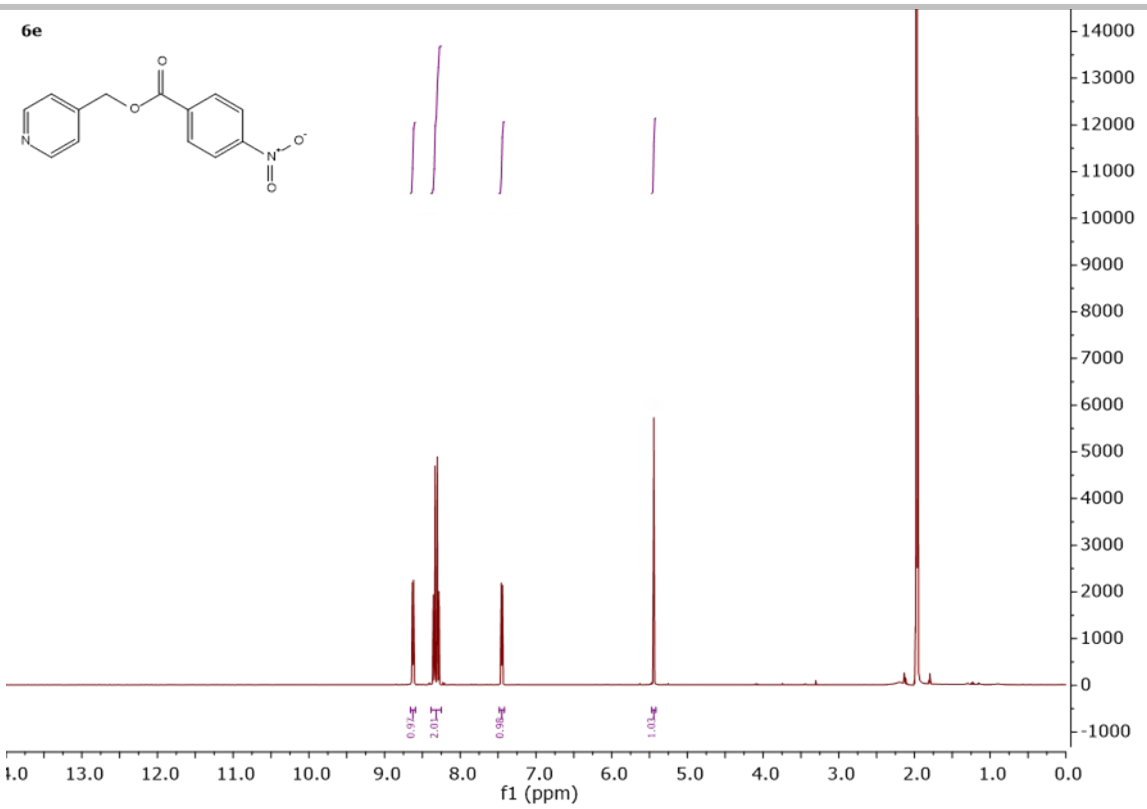

Figure S75. ^{1}HNMR spectra of compound **6e.**

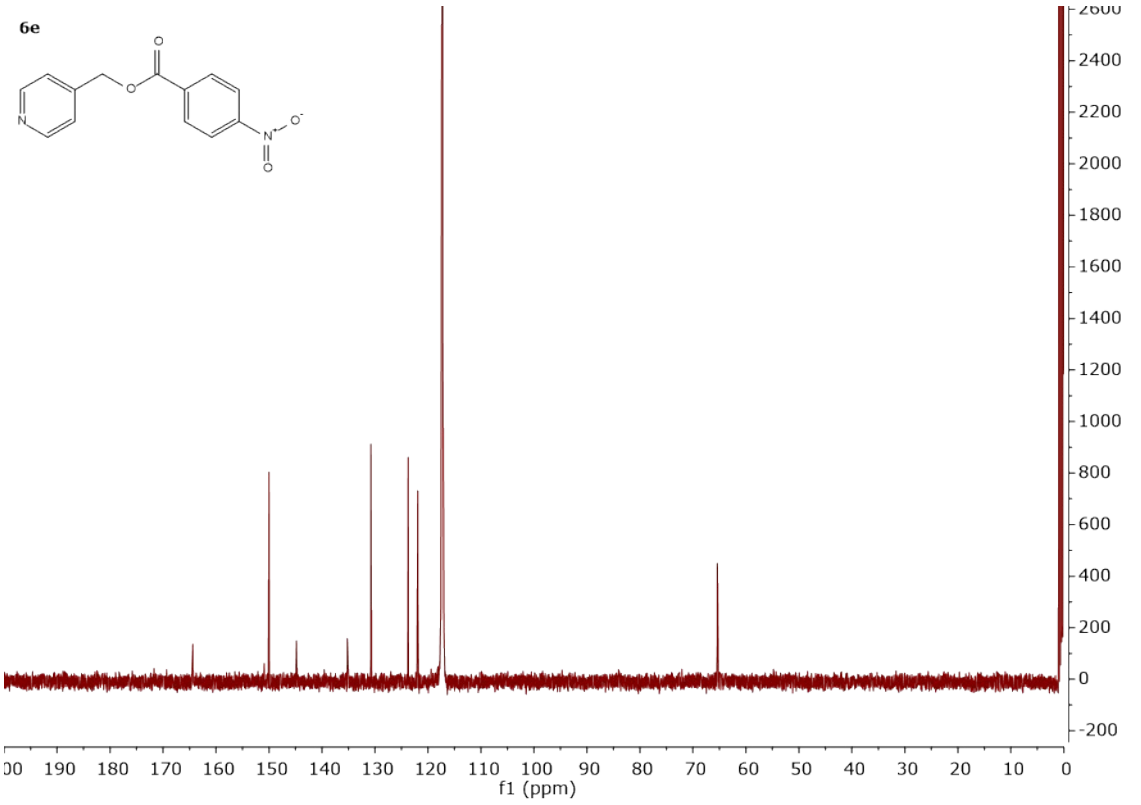

Figure S76. ^{13}C {^{1}H} NMR spectra of compound **6e**.

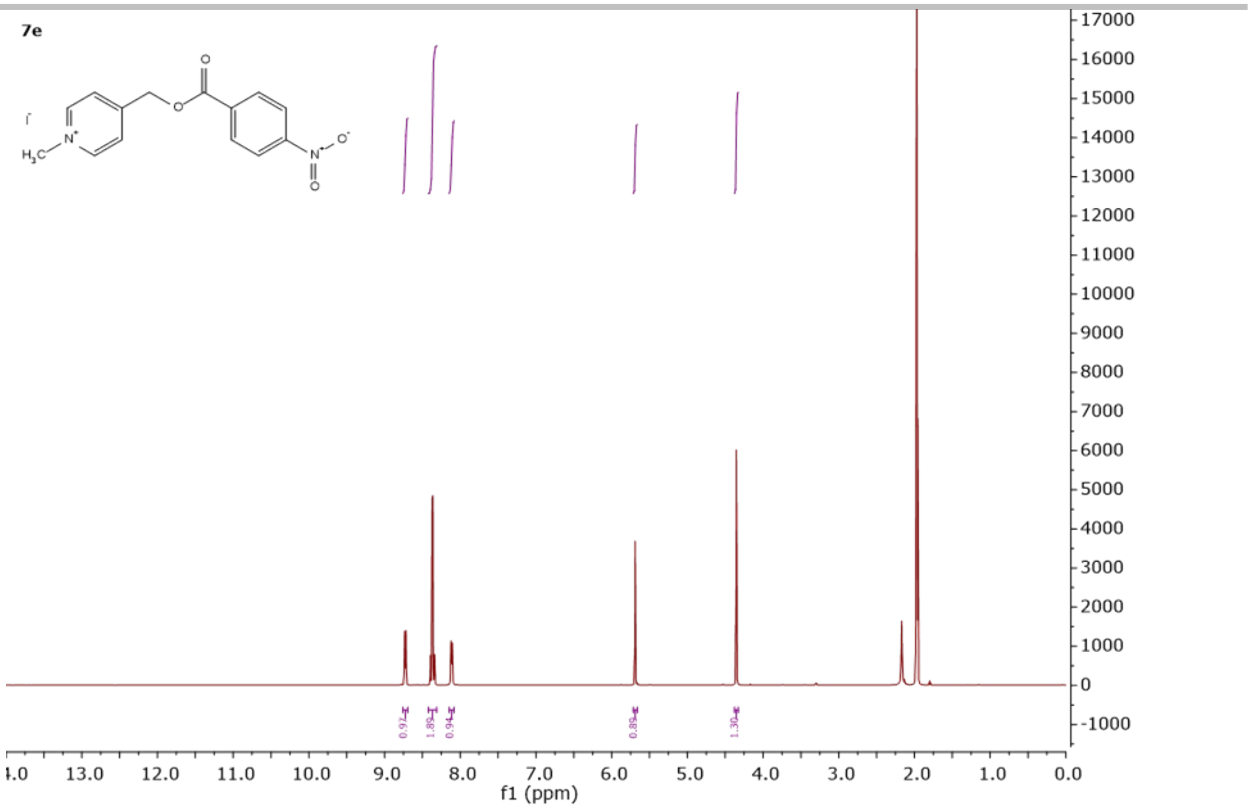

Figure S77. ^{1}HNMR spectra of compound **7e.**

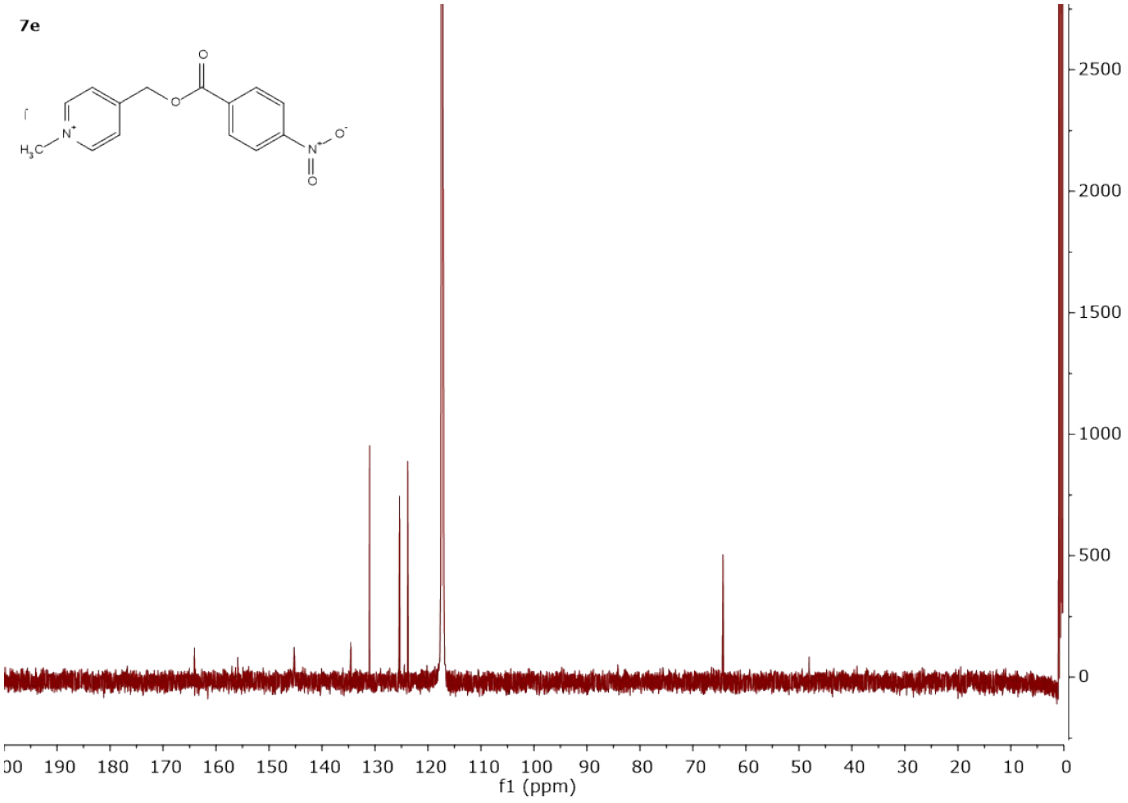

Figure S78. ^{13}C {^{1}H} NMR spectra of compound **7e**.

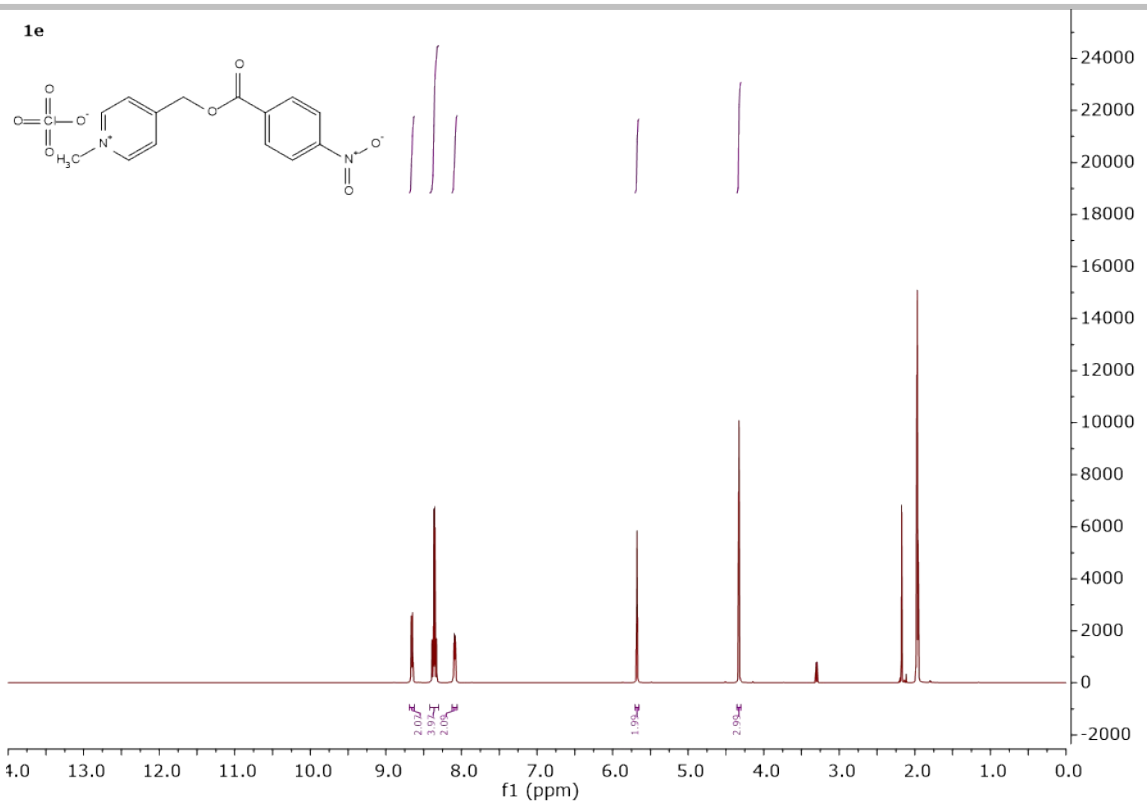

Figure S79. ^{1}HNMR spectra of compound **1e.**

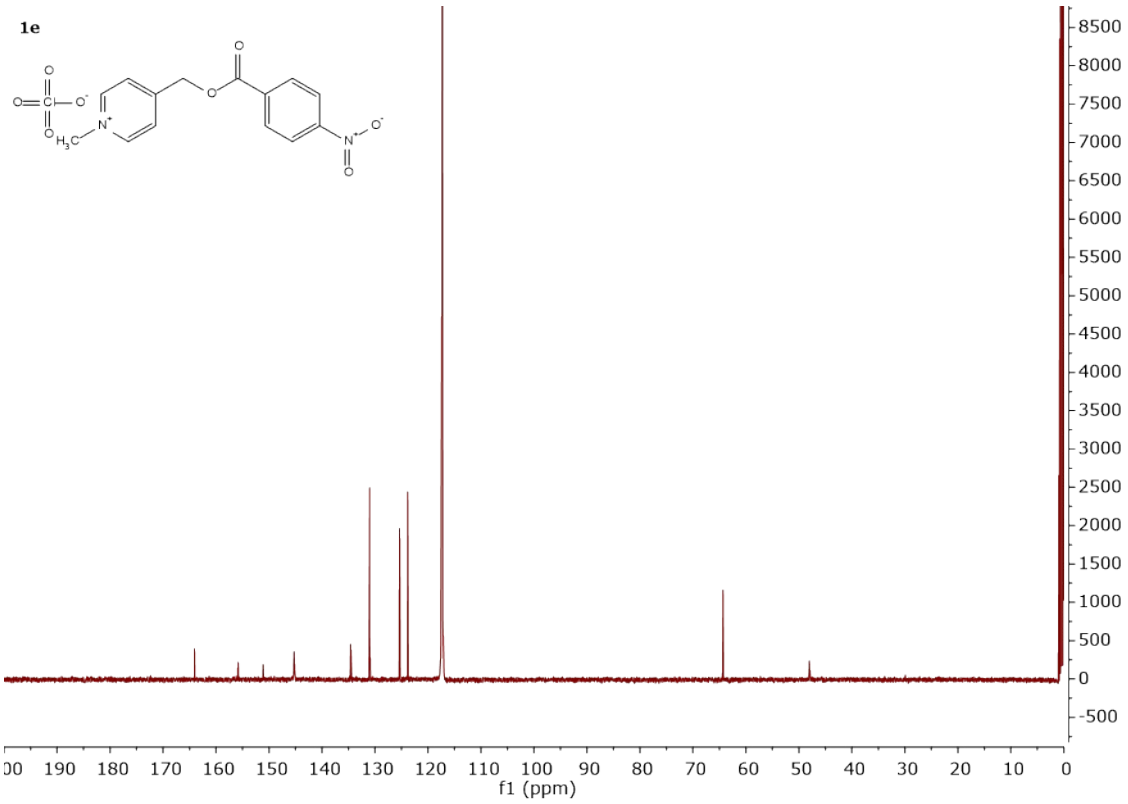

Figure S80. ^{13}C {^{1}H} NMR spectra of compound **1e**.

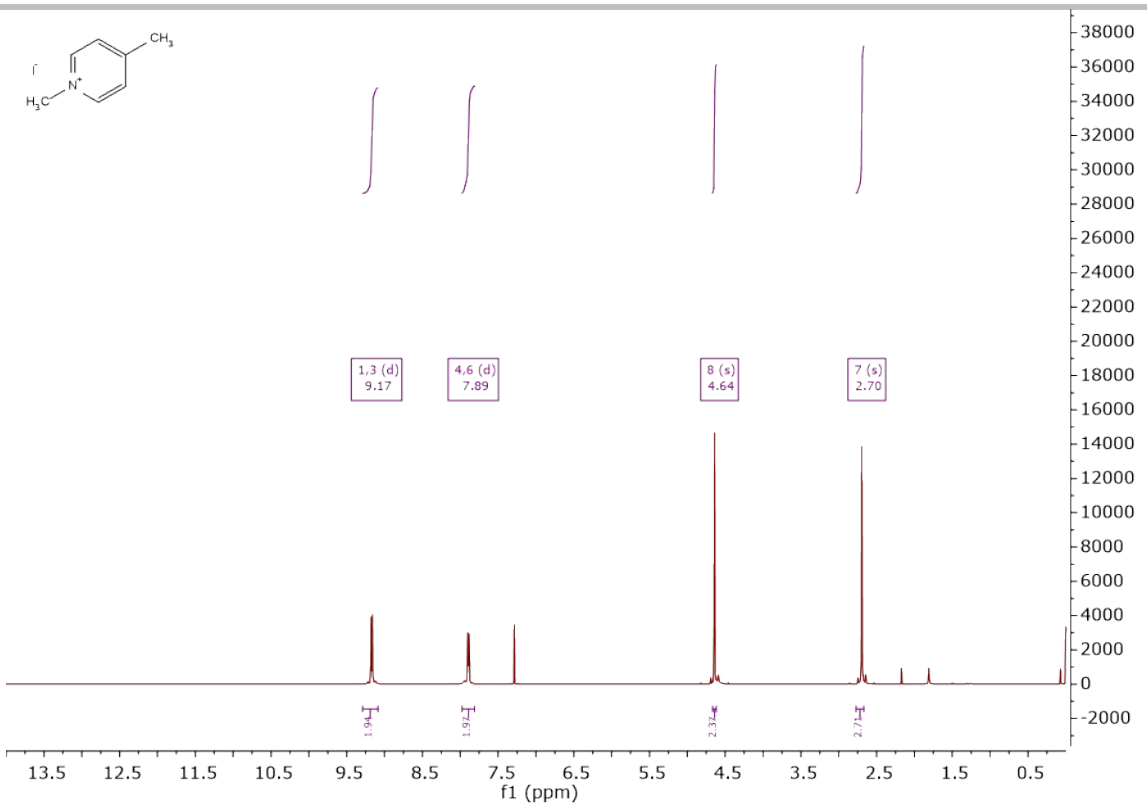

Figure S81. [1]HNMR spectra of N-Methyl 4 methyl pyridinium iodide.

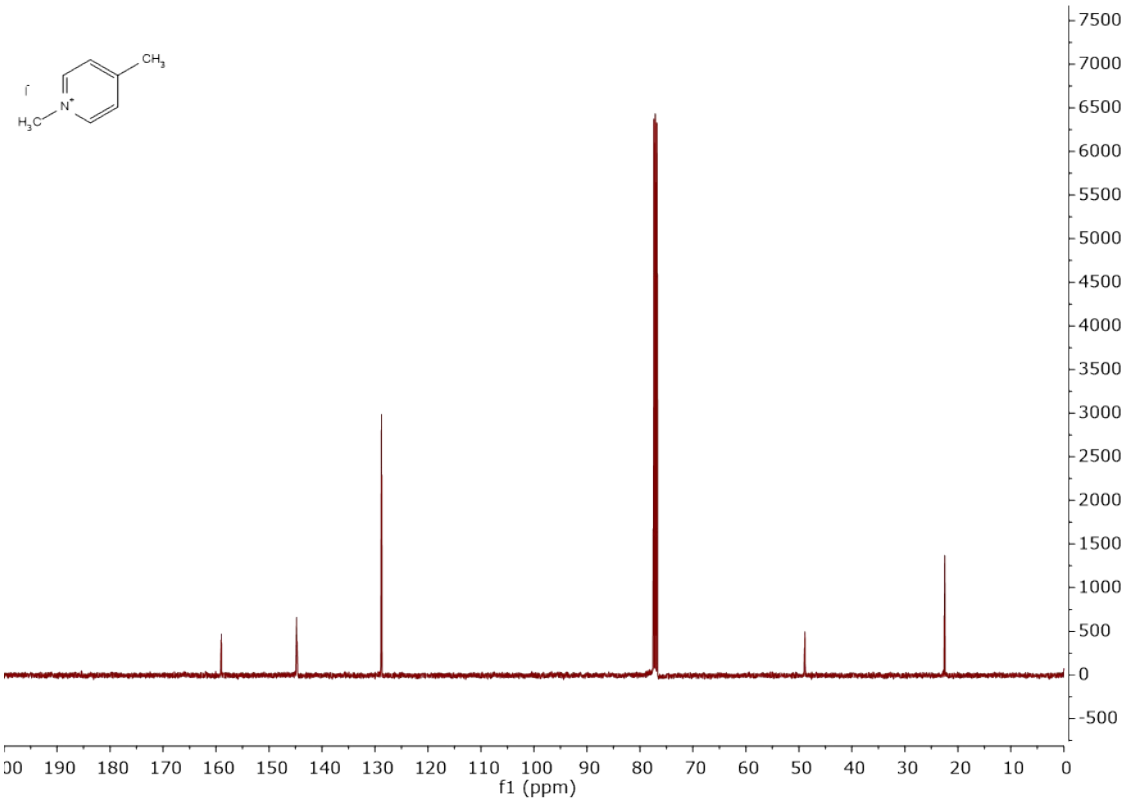

Figure S82. [13]C {[1]H} NMR spectra of N-Methyl 4 methyl pyridinium iodide..

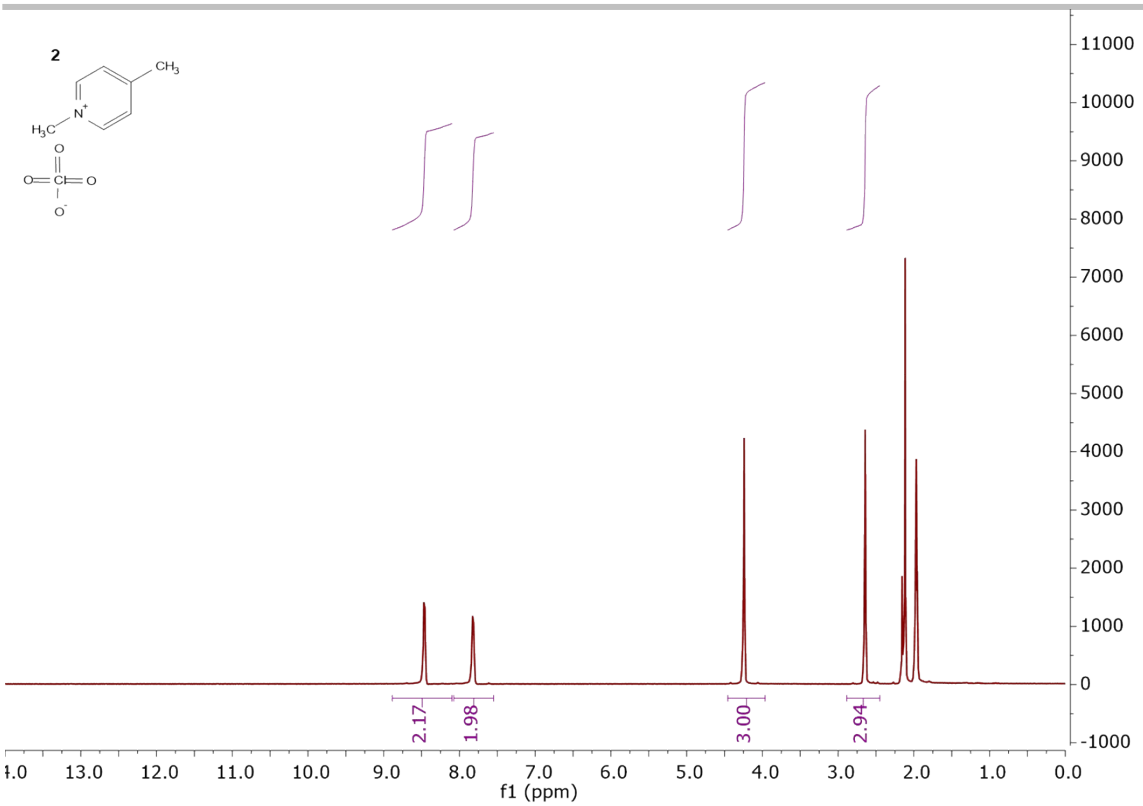

Figure S83. ^{1}HNMR spectra of compound **2.**

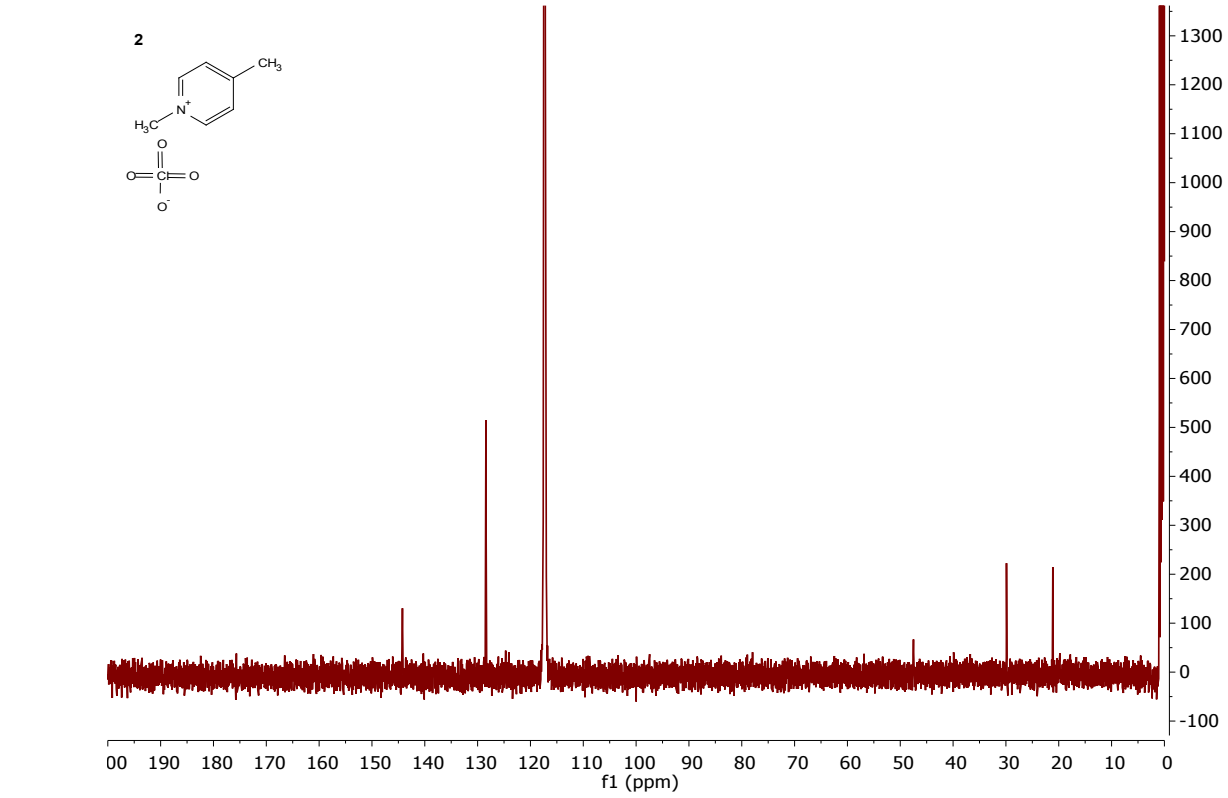

Figure S84. ^{13}C {^{1}H} NMR spectra of **2**.

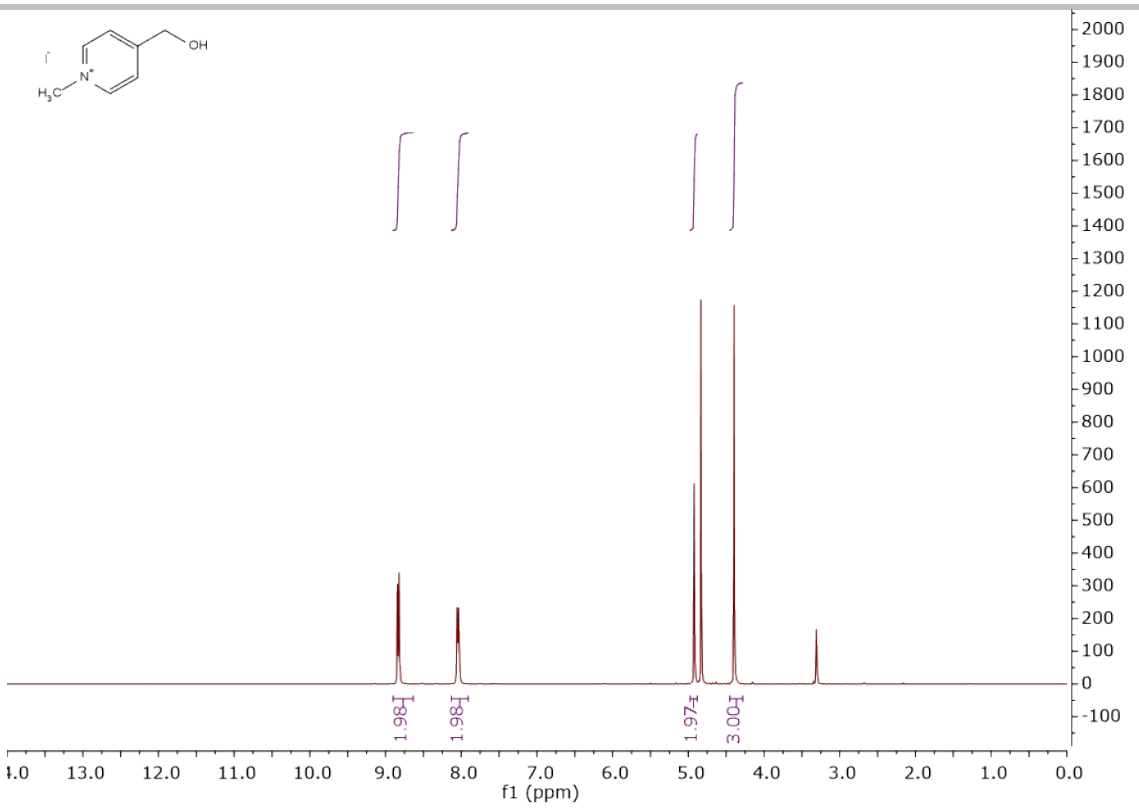

Figure S85. ^{1}HNMR spectra of N-Methyl carbinol iodide.

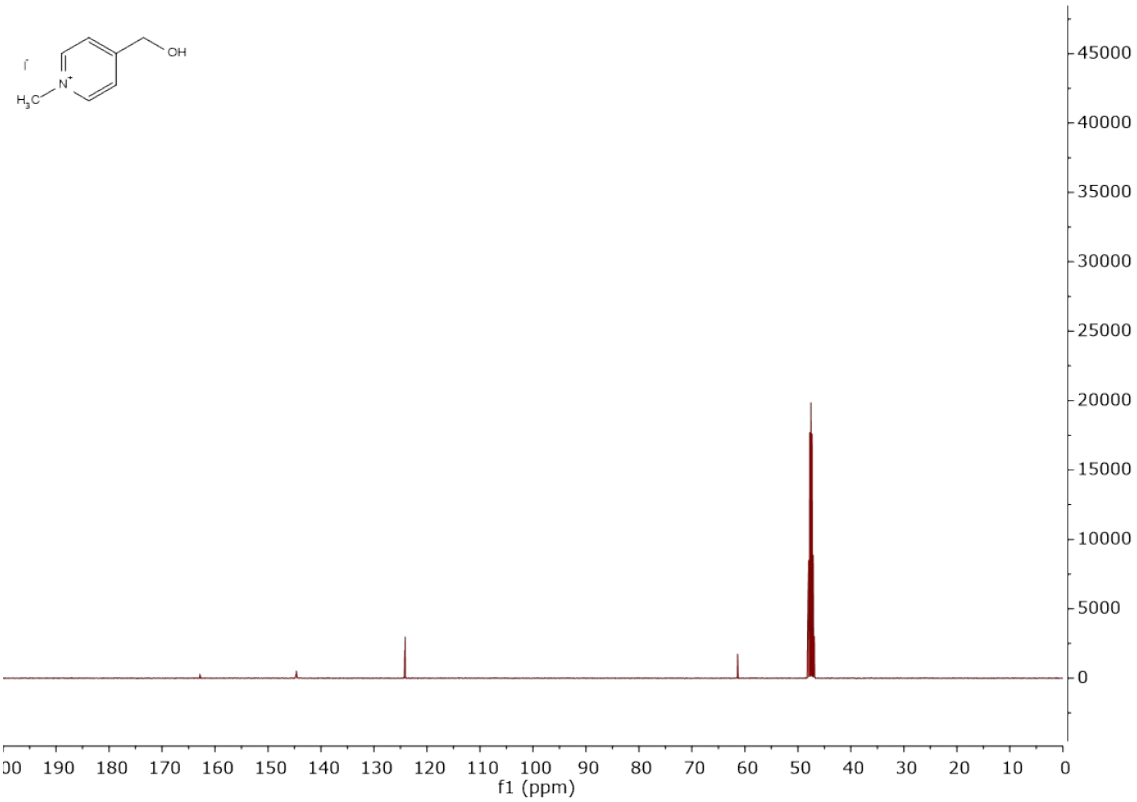

Figure S86. ^{13}C {^{1}H} NMR spectra of compound N-Methyl carbinol iodide.

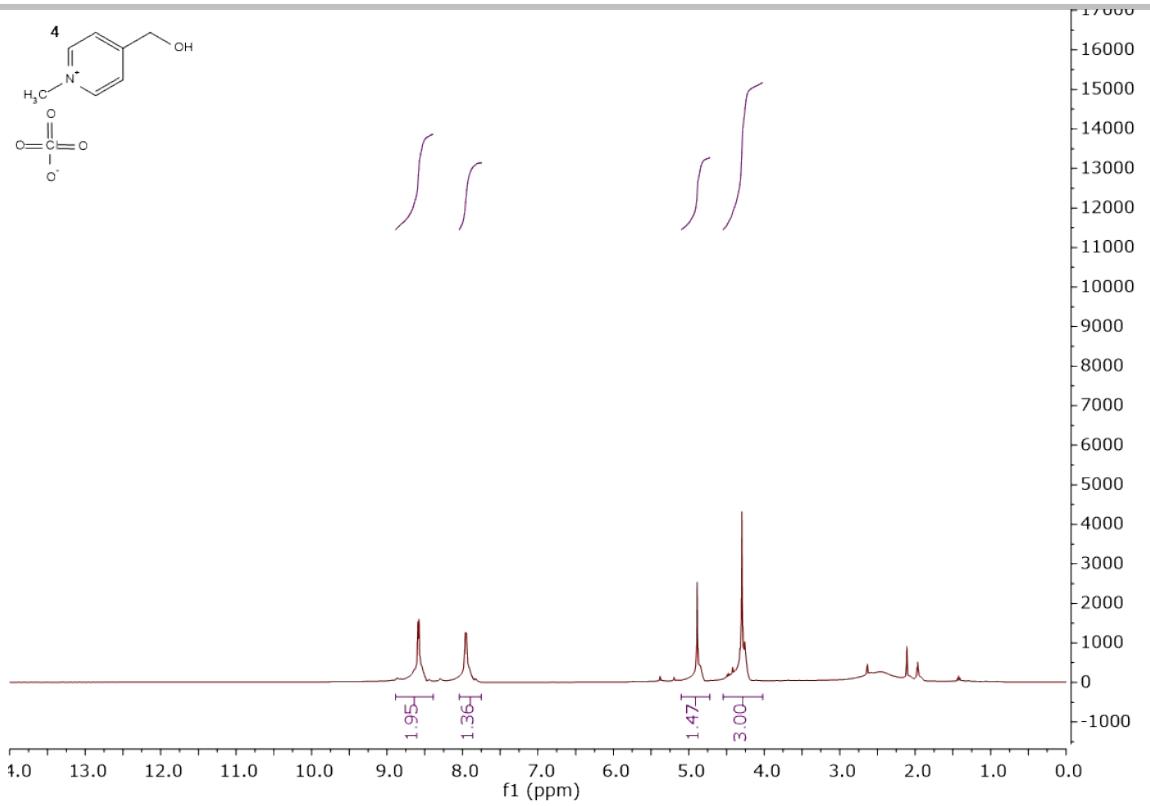

Figure S87. ^{1}HNMR spectra of compound **4.**

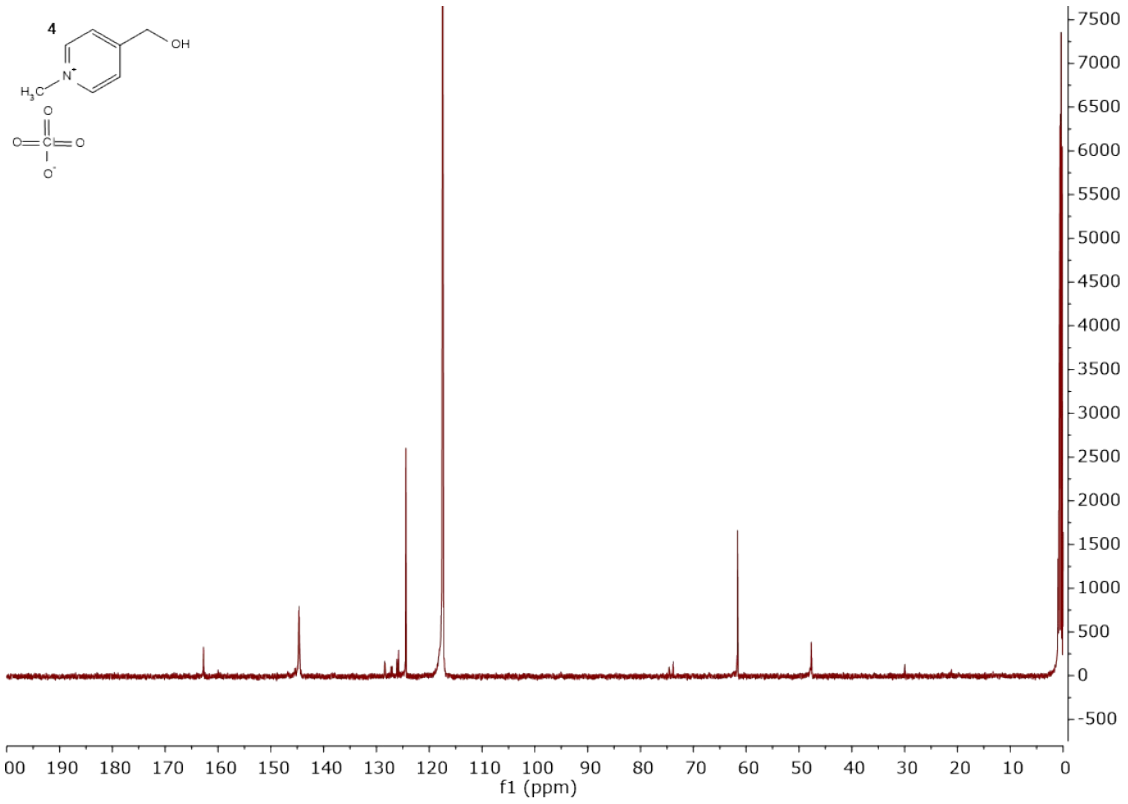

Figure S88. ^{13}C {^{1}H} NMR spectra of compound **4**.

References

[1] S. Cailotto, R. Mazzaro, F. Enrichi, A. Vomiero, M. Selva, E. Cattaruzza, D. Cristofori, E. Amadio, A. Perosa, *ACS Appl. Mater. Interfaces* **2018**, *10*, 40560-40567.

[2] C. Sundararajan, D. E. Falvey, *Photochem. Photobiol. Sci.* **2006**, *5*, 116-121.

[3] D. B. Grotjahn, L. S. B. Collins, M. Wolpert, G. A. Bikzhanova, H. C. Lo, D. Combs, J. L. Hubbard, *J. Am. Chem. Soc.* **2001**, *123*, 8260-8270.

[4] D. Bai, S. Yu, S. Zhong, B. Zhao, S. Qiu, J. Chen, J. Lunagariya, X. Liao, S. Xu, Int. J. Mol. Sci. 2017, 18, 544.

[5] F. Rigodanza, L. Đorđević, F. Arcudi, M. Prato, Angew. Chem. Int. Ed. **2018**, *57*, 5062–5067.

[6] R. R. Gagne, C. A. Koval, G. C. Lisensky, *Inorg. Chem.* **1980**, *19*, 2854-2855.

[7] A. J. Bard, L. R. Faulkner, Electrochemical Methods. Fundamental and Applications, Wiley, New York **1980**

[8] C. M. Cardona, W. Li, A. E. Kaifer, D. Stockdale, G. C. Bazan, *Adv. Mater.* **2011**, *23*, 2367-2371.